Morphological development of the western Wadden Sea after human intervention near the Afsluitdijk

Delft, June 2004

M.Sc. Thesis of M.J. Ubbink

Committee: Prof.dr.ir. M.J.F. Stive (DUT)
Ir. T.J. Zitman (DUT)
Ir. E.P.L. Elias (DUT)
Ir. P.J.T. Dankers (DUT)
Ir. K. Boorsma (ingenieursbureau Boorsma)

Preface

This report describes the study done within the framework of my Master of Science thesis and forms the final part of my study Civil engineering at the Delft University of Technology, Faculty of Civil Engineering and Geosciences, Division Hydraulic and Offshore Engineering.

In this report the consequences, both hydrodynamic as morphodynamic, as a result of the construction of a reservoir in the western Wadden Sea are investigated. The study has been done at the Delft University of Technology.

I would like to thank the members of my graduation committee prof. dr. ir. M.J.F. Stive, Ir. Zitman, Ir. E.P.L. Elias, Ir. P.J.T. Dankers and Ir. K. Boorsma for their comments and support during the accomplishment of my thesis.

Furthermore I would like to thank my family and friends for their support during my study and the fantastic years I spent in Delft.

Marit Ubbink.
Delft, June 2004

Summary

Due to the expected climate change, specialists foresee that the weather will be more extreme. It is expected that rainfall will be more concentrated resulting in peak-loaded river discharges. Because it is not always possible to discharge on sea, a water retention facility, like a reservoir, could prevent a flood near the rivers. This reservoir can also be used to supply water to the rivers during dry summers, when river discharges are not sufficient to prevent salt intrusion.

The proposed location of the reservoir is in the Wadden Sea, against the north side of the Afsluitdijk (Boorsma, 2003)[1]. This location provides good accessibility to the river network, and placing the reservoir outside the Lake IJssel enlarges the total fresh water storage area. By constructing a reservoir, the hydrodynamic and morphodynamic properties of the Wadden Sea basin are altered. However, the Wadden Sea has proven capable to adapt itself to changes in external forcing, like human intervention (e.g. Closure of the Zuider Sea and Lauwers Sea). Although changes in hydrodynamics occur instantaneously, it is expected to take decades before basin adapts to a new morphological state.

This study focuses on the estimation of the hydrodynamic and morphodynamic effects of constructing such a reservoir. The hydrodynamic impact of the reservoir is investigated using the Delft3D modelling system. Changes in tidal prism are determined for the Marsdiep, Eierlandse Gat and Vlie basin. The changes in tidal prism, and alterations in flow patters through the main channels are used for an expert-judgement based prediction of tidal divide displacements. These tidal prism changes and tidal divide displacements are important factors for the morphologic, reservoir related, basin changes. The long-term morphological evolution of the basins is determined by applying the semi-empirical model ASMITA.

Besides the proposed reservoir against the Afsluitdijk (reservoir AD), two alternatives are studied: reservoir LW, located on the shoal area Lutjeswaard (between Afsluitdijk and Texelstroom), and reservoir KZ, situated on the tidal divide separating the Marsdiep and Vlie basin, near the Kornwerderzand. For each reservoir surface area sizes are varied between 90 and 180 km^2.

For each of the alternatives hydrodynamic simulations (Delft3D-FLOW) and morphodynamic simulations (ASMITA) are made. Delft3D-FLOW results show a tidal prism decrease in Marsdiep and Vlie inlet for design alternatives AD and LW, due the reduction of basin area. The above average ebb volume decrease in the Vlie inlet for the AD and KZ reservoir points to the disruption of the important through flow between the Vlie and Marsdiep basin. The LW alternative does not disrupt this through flow.

The tidal divide displacements, between Marsdiep and Vlie, are determined using the computed tidal prism changes, and the expected morphological development of the channels. The part of the tidal divide near the Inschot, displaces into the Vlie basin for all investigated alternatives, the part near the Kornwerderzand flat, displaces into the Marsdiep basin for alternative AD and LW.

[1] Onderloopboezem in de Waddenzee houdt Nederland droog, van ir. K. Boorsma van ingenieursbureau Boorsma B.V. Land + Water nr. 9, september 2003.

The ASMITA based results show that construction of the reservoirs has positive effects on the morphological development of the basins and the adjacent coasts. Basin area reduction results in shorter adaptation time towards an equilibrium state. Especially, alternatives AD and LW reduce the adaptation time to equilibrium for the Marsdiep basin, while the adaptation time of the Vlie basin reduces with the construction of the KZ reservoir.

One should be aware that this study was a first pilot in order to obtain indications of morphological effects of constructing reservoirs in the Wadden Sea. Therefore a number of simplifications and assumptions had to be made. For example, tidal range was assumed constant, empirical relations are used, and the flow computations were only made for the initial state, not taking into account morphological alterations of the Wadden Sea bathymetry resulting from the reservoir. It is doubtful that such alterations can be modelled accurately, due to the complex and highly-dynamic nature of the Wadden Sea. Possibly, the modelled tidal prism change and interpretations of tidal divide displacement are not fully representative. As these are used as an input for the ASMITA model, the prediction of the long-term development of the channel, flat and delta elements can deviate.

From this study follows, that the LW alternative is the best option. This alternative is completely constructed in the Marsdiep basin and has only limit influence on the through flow between Vlie and Marsdiep. Thus, effects on the Vlie basin are small. The reduction of the Marsdiep basin is beneficial. After closure of the Zuider Sea the tidal prism increased considerably, and the basin had not yet reached equilibrium. After construction of the reservoir, equilibrium is reached in a shorter period.

Samenvatting

Als gevolg van voorspelde klimaatveranderingen verwachten specialisten dat het weer in de toekomst extremer zal worden. Verwacht wordt dat de neerslag geconcentreerder zal zijn per regenbui, terwijl de jaarlijkse hoeveelheid neerslag gelijk zal blijven. Deze hogere neerslag concentratie zal grotere piekbelastingen in de rivierafvoeren als gevolg hebben. Doordat afwatering op zee niet altijd mogelijk is zou een onderloopboezem, een reservoir, mogelijke overstromingen van rivieren kunnen voorkomen. Een dergelijk reservoir zou mede gebruikt kunnen worden om verzilting van de kustgebieden te voorkomen op het moment dat de (zoetwater) afvoer van rivieren tijdens langdurige droge en warme perioden niet voldoende is.

De voorgestelde locatie voor dit reservoir is in de Waddenzee, tegen de noordzijde van de Afsluitdijk (Boorsma, 2003)[2]. Deze locatie is gunstig gelegen ten opzichte van de verbinding met het rivieren netwerk en bovendien heeft plaatsing van het reservoir buiten het IJsselmeer een vergroting van de totale zoetwater opslag capaciteit tot gevolg. Door de bouw van een reservoir veranderen de hydrodynamische en morfodynamische eigenschappen van de Waddenzee. In het verleden heeft de Waddenzee bewezen in staat te zijn zich aan externe krachten, zoals menselijk ingrepen (afsluiting Waddenzee en Lauwerszee) aan te kunnen passen. De verwachting is echter dat het bekken tientallen jaren nodig zal hebben om zich aan de nieuwe morfologische situatie aan te passen terwijl de hydrodynamische veranderingen direct optreden.

Deze studie richt zich op de schatting van de hydrodynamische en morfodynamische gevolgen die worden veroorzaakt door de bouw van een dergelijk reservoir. Deze hydrodynamische gevolgen zijn onderzocht met behulp van het Delft3D model systeem. De aanpassing van het getijde prisma zijn bepaald voor het Marsdiep, Eierlandse Gat en het Vlie bekken. De veranderingen in getijde prisma en de veranderingen in de stroompatronen door de hoofdgeulen zijn gebruikt voor de voorspelling van de verplaatsing van de wantijen. De verandering van het getijde prisma en de verplaatsing van het wantij zijn belangrijke factoren voor de reservoir gerelateerde morfologische gevolgen. De lange termijn morfologische evolutie van de bekkens is bepaald door toepassing van het semi-empirische model ASMITA.

Naast het voorgestelde reservoir tegen de Afsluitdijk (reservoir AD), zijn twee andere alternatieven bestudeerd: reservoir LW, gelegen op het ondiepe gebied Lutjeswaard (tussen de Afsluitdijk en de Texelstroom) en reservoir KZ, gelegen op het wantij dat het Marsdiep met het Vlie bekken scheidt, nabij de Kornwerderzand. Voor ieder reservoir alternatief varieert het oppervlakte tussen de 90 en 180 km^2.

Voor alle alternatieven zijn hydrodynamische (Delft3D-FLOW) en morfodynamische (ASMITA) simulaties uitgevoerd. De Delft3D-FLOW resultaten laten een afname van het getijde prisma zien voor zowel het Marsdiep als het Vlie zeegat voor de alternatieven AD en LW, deze afname wordt veroorzaakt door een afname van het bekken oppervlak. De bovengemiddelde afname van het eb volume, dat door het zeegat van het Vlie stroomt, voor zowel het AD als het KZ reservoir impliceert een verstoring van de belangrijke doorstroom tussen het Vlie en het Marsdiep. Het LW reservoir verstoort deze doorstroom niet.

[2] Onderloopboezem in de Waddenzee houdt Nederland droog, van ir. K. Boorsma van ingenieursbureau Boorsma B.V. Land + Water nr. 9, september 2003.

De verplaatsingen van het wantij, tussen het Marsdiep en het Vlie bekken, zijn bepaald met behulp van de gemodelleerde veranderingen in het getijde prisma en de verwachte morfologische ontwikkeling van de geulen. Het deel van het wantij naast de Inschot verplaatst richting het Vlie bekken voor alle onderzochte alternatieven. Het deel van het wantij nabij de Kornwerderzand plaat verplaatst richting het Marsdiep bekken voor alternatief AD en LW.

De ASMITA resultaten laten zien dat de bouw van de reservoirs positieve effecten hebben op de morfologische ontwikkeling van zowel de bekkens als de aanliggende kust. Door de aanleg van het reservoir verkleint het oppervlakte van het bekken en is een kortere aanpassingstijd nodig om tot de evenwicht situatie te komen. Bij alternatief AD en LW neemt met name de aanpassingstijd van het Marsdiep bekken af, terwijl de aanpassingstijd van het Vlie bekken afneemt voor alternatief KZ.

Bij de interpretatie van de onderzoeksresultaten moet men bewust zijn van het feit dat deze studie een eerste opzet is geweest om een indruk te krijgen van de morfologische effecten die veroorzaakt worden door het bouwen van reservoirs in de Waddenzee. Derhalve zijn een aantal vereenvoudigingen en aannamen gemaakt, zoals een constante getijde slag en het gebruik maken van empirische relaties. Daarnaast zijn de berekeningen alleen gedaan voor de initiële situatie, waarbij geen rekening is gehouden met de morfologische veranderingen van de bodem van de Waddenzee als gevolg van het plaatsen van een reservoir. Door de complexe en sterk dynamische aard van de Waddenzee, is het te betwijfelen of dergelijke veranderingen nauwkeurig te modelleren zijn. Mogelijkerwijs zijn de gemodelleerde getijde prisma's en de interpretatie van de verplaatsing van het wantij niet geheel representatief. Aangezien de gemodelleerde getijde prisma's gebruikt worden voor de invoergegevens van ASMITA, kunnen voorspellingen over de lange termijn ontwikkeling van de platen, geulen en delta elementen afwijken.

Uit deze studie blijkt dat het LW alternatief de best optie is. In dit alternatief bevindt het reservoir zich volledig in het Marsdiep bekken en heeft slechts een beperkte invloed op de doorstroming tussen het Vlie en Marsdiep bekken. De hieraan gerelateerde oppervlakte afname in oppervlak van het Marsdiep bekken is voordelig voor de aanpassingstijd om morfologisch evenwicht te bereiken. Na de afsluiting van de Zuiderzee nam het getijde prisma aanzienlijk toe. De bouw van het reservoir op deze locatie heeft als gevolg dat de evenwichtssituatie in dit bekken in een kortere periode bereikt zal worden.

Table of contents

List of figures

List of tables

1 Introduction

1.1 Background

Climate change is a considerable problem in current society. Climate specialists do not only expect higher temperatures, but also warn for extremes in weather. Predictions are that the average rainfall remains constant, but more concentrated in extreme events. However, during the summer season an increase in duration of warm and dry periods is expected. The above effects of climate change on the Dutch inland can be divided into two critical situations:

1. As the rain is concentrated in a shorter period, river discharges are more peak loaded. Peak discharges through the present river system induce difficulties, due to the canalisation during the previous centuries.
2. During long dry periods, the fresh water discharge of the rivers decreases. This leads to increased salt-water flow coming from sea. To prevent this salt intrusion, the river discharge has to increase in and around the coastal zones. To increase the river discharge fresh water from lakes can be used. However, the water level in these lakes controls the ground water level in the surrounding area. The extraction of fresh water is thus limited.

According to Boorsma (2003), the need to store water in the winter season and the need for fresh water in the summer season can be fulfilled by the construction of a water retention facility: 'reservoir'. It is not clear where this reservoir can be situated. Two important features have to be taken into account to determine a location for the reservoir: the accessibility of the river network and the lack of space in the Netherlands. Combining the accessibility with the lack of space asks for a creative solution. Boorsma (2003) suggests the construction of a water reservoir in the Western Wadden Sea adjacent to the Afsluitdijk. If the reservoir is located on the seaside (Wadden Sea) of the Afsluitdijk, a good accessibility of the discharged river water is possible via the lake IJssel.

The Wadden Sea is a very dynamic area with a unique ecosystem and consists of a system of barrier islands, coastal inlets and tidal basins. History teaches us that the Wadden Sea has some resilience and is, to a certain extent, able to adapt to external forcings, like sea level rise and human intervention. Important human interventions are the closure of the Zuider Sea (1932) and the Lauwers Sea (1969). These actions had a large effect on the hydrodynamic and morphological aspects and until now, the Western Wadden Sea is still adapting itself to these interventions. We are interested in the effects on the Western Wadden Sea caused by the construction of a large-scale retention facility and leads to the following problem definition.

A reservoir is a solution for the expected water problems, caused by the changing climate. The construction of such a reservoir inside the western Wadden Sea influences the long-term morphological development of the Wadden Sea.

1.2 Objective

To investigate the hydrodynamic and morphological consequences for the western Wadden Sea due to the construction of a reservoir, this study will not be restricted to the area against the Afsluitdijk as proposed by Boorsma (2003). It is expected that construction of the proposed reservoir against the Afsluitdijk largely affects the Wadden Sea's hydrodynamics and morphodynamics, as the reservoir closes off the Doove Balg (an important channel in the Marsdiep basin). Two supplementary alternatives are studied: the construction of a reservoir on the shallow area between the Afsluitdijk and Texelstroom, and construction of a reservoir on the tidal divide separating the Marsdiep and Vlie basin, near the Kornwerderzand.

The objectives of this study are:

- *To investigate, with Delft3D-FLOW, the hydrodynamic consequences of a reservoir for the western Wadden Sea basins.*
- *To investigate, with ASMITA, the long-term morphological development of the tidal basins in the western Wadden Sea due to the construction of a reservoir.*

The long-term morphological development of the western Wadden Sea after the construction of the reservoir is determined by applying the semi-empirical model ASMITA. For this model, input parameters like the surface area and volumes of the flats and the channels are needed. In the basin with reservoir these parameters change as a result of the reservoir as well as the displacement in tidal divides. In the adjacent basins the change in these parameters only depends on the movement of the tidal divide. To determine the displacement of the tidal divides we used the change in the basin's tidal prism and the behaviour of the channels before and after the intervention. The change in tidal prism is modelled with Delft3D-FLOW. With the quantity of tidal divide displacement, new surface areas for the different basins are estimated and used as input for the ASMITA model.

1.3 Reader

This report starts with a brief description of the formation of the Wadden Sea, starting at the beginning of the Holocene. After this chapter, relevant theoretical background of tidal inlet systems is given. It is important to note, that the theoretical background in this report is only a small part of the complete theory. In chapter 4 and 5 the physical-mathematical models, used in this study, are described. Using the results of the Delft3D-FLOW model, chapter 6 deals with the influence of the reservoir on the tidal prism and the tidal range, while chapter 7 deals with the influences of the reservoir on the location of the tidal divides. If tidal divides shift, the basins get different surface areas. The allocation of new surface areas to the basins is described in chapter 8. This chapter also describes the morphological development of the basin after the construction of the reservoir and compares the morphological development in the present situation with the development of the studied alternatives. The report ends with the conclusions and recommendations of this research.

2 Development of the Wadden Sea

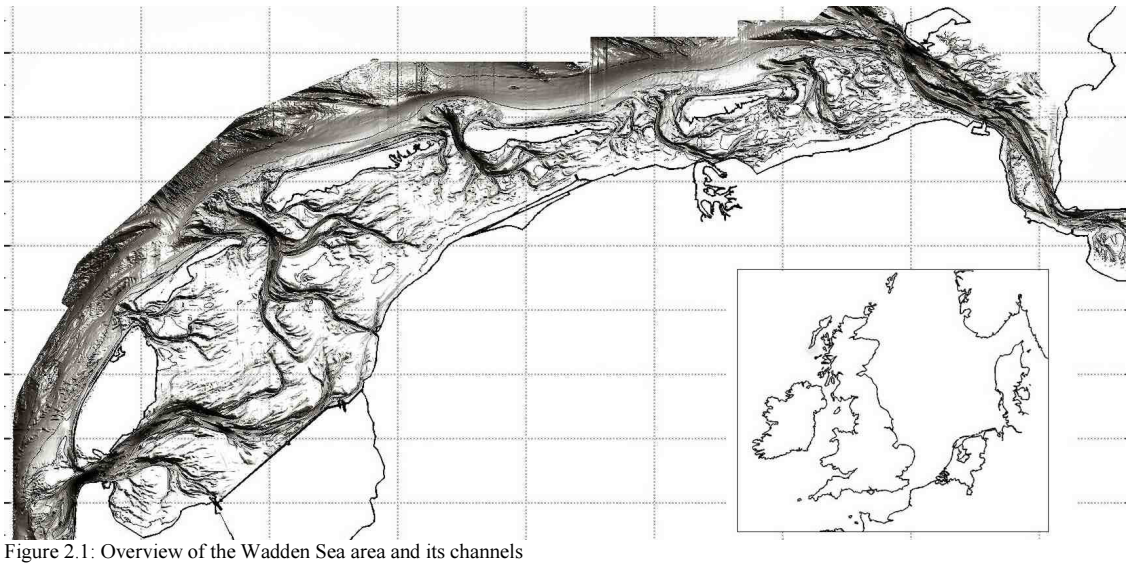

Figure 2.1: Overview of the Wadden Sea area and its channels

2.1 Introduction

The Dutch Wadden Sea consists of several barrier islands, coastal inlets and tidal basins. A tidal basin is subdivided in channels and flats, and separated by tidal divides: a theoretical line where the flow velocities are negligible, caused by tides from several directions coming together. The elements (channels and flats) of such a system interact with each other (and the outside world) by means of external forcings like tide, wind and waves. The interaction occurs by exchanging water and sediment between adjacent elements. History teaches us that this system is dynamic and that it is, to a certain extent, able to survive the rising sea level and human interventions. Furthermore, research has lead to better understanding and theoretical support of involved morphological phenomena.

The Wadden Sea is in a geological sense a very young landscape. It obtained its current shape around the beginning of the Holocene, some 10 000 years ago. The Holocene period is still going on and started when the last ice age stopped and the sea level started rising after a long period of retreat. In the following sections the formation of the Wadden Sea, subdivided in characteristic periods; and the influence of human intervention on the Wadden Sea will be described in more detail.

2.2 Formation Wadden Sea

The evolution of the earth has been divided in several geological periods, shown in Figure 2.2. The latest period is the quaternary, which is sub-divided in the Pleistocene and the Holocene. Currently we live in the Holocene, characterised by the end of the last ice age, caused by a continuous rise of temperature. Due to this rise in temperature the sea level started rising too. The topography formed during the Pleistocene has had a great influence on the structure and development of the current western Wadden Sea and barrier coast.

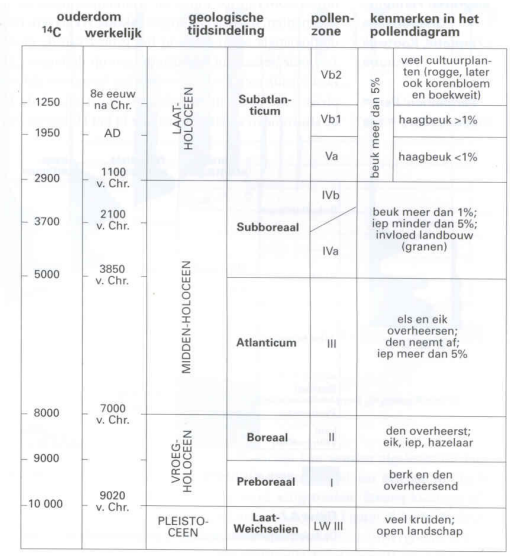

Figure 2.2: geological time table (Berendsen, 1997)

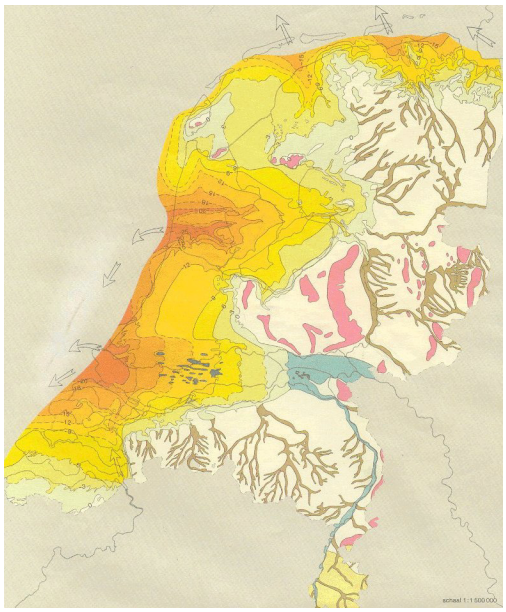

Figure 2.3: Preaboreal (Zagwijn, 1986)

2.2.1 End of Pleistocene

During the last ice age of the Pleistocene, the level of the sea was 100 to 135 m below the present sea level, the southern part of the present North Sea were dry and the United Kingdom and Ireland was connected with the rest of Western Europe. The ice layers from the different ice ages had resulted in a thick (fluvial Pleistocene) layer with a highly irregular surface, as can be seen in Figure 2.3. During the Holocene, these irregularities either have been filled up by fluvial sediment or have been used by rivers. The orientation of the later formed Texelstroom as well as where the Marsdiep came through are determined roughly by the lower parts of the Pleistocene layers.

The high parts of the Pleistocene and the deposits from the early Holocene resulted in a different development of the western and eastern Wadden Sea. In the higher western Wadden Sea, the barrier coast developed further away from the mainland than in the eastern Wadden Sea. The western barrier coast was almost closed and peat was formed behind it. From the Middle Ages on, the peat layer of the western Wadden Sea eroded gradually. The erosion of the peat layer, in combination with flooding, determined the current location of the Lake IJssel and the current dimension of the Western Wadden Sea.

2.2.2 Boreal

During the Boreal period the sea level rise was about 1m per century. Because of this rising sea level the shelf between the United Kingdom and Western Europe started flooding. At the end of the Boreal, approximately 8300 BP, the shelf was completely flooded.

2.2.3 Atlanticum

With the rising sea level, the coastline retreated and near the coastline, rivers changed in lagoons and estuaries. At the beginning of the Atlanticum, round 5800 BC the Dutch coastline was situated about 25 km west of the current position. Despite of the sea level rise, a sand bar was created at the West coast (see Figure 2.4), by the changed wave and tidal conditions in the North Sea. Behind this bar, a lagoon was enclosed between the higher Pleistocene mainland and the sea. In this lagoon large quantities of peat were formed, see Figure 2.4.

Figure 2.4: Early Atlanticum, 5500 BC (Zagwijn, 1986)

Figure 2.5: Late Atlanticum, 4100 BC (Zagwijn, 1986)

However, in the late Atlanticum, the rate of sea level rise increased again and the coast is not longer a closed coast and is probably subjected to a large tidal range. At the Pleistocene river valleys the sand bars were interrupted by inlets, see Figure 2.5. The lagoon became a tidal lagoon and had an area similar to the current Wadden Sea. Besides the described development, the Pleistocene high near Texel and Vlieland were also affected by the increasing sea level rise. The Texel high and Vlieland were affected by erosion due to the sand supply on the shore faces of the barrier islands along the coast in the West and the North of the Netherlands.

2.2.4 Sub-Boreal

The Sub-Boreal is characterized by a slower rate of sea level rise and enough sediment from the sea and from the rivers to cope with this sea level rise. The barrier coast in the West is closing again, turning the tidal lagoon into a fresh water environment, as can be seen in Figure 2.6. In the fresh water lake the formation of peat is facilitated. Despite of the peat formation in Friesland and Groningen, some tidal inlets remained and even became larger at the end of the Sub-Boreal.

2.2.5 Sub-Atlanticum

Till the period of the Sub-Atlanticum, developments in the formation of the Dutch coast and hinterland are influenced by nature. From about 1000 BC also human influences have to be taken into account. In the Sub-Atlanticum the rate of sea level rise stagnated. Maybe this stagnation caused the withdrawal of the coastline (Berendsen, 1997). In the area of the current Wadden Sea, the inlets are prevailing and new inlets are formed, especially at the Western part of the current Wadden Sea. Due to the newly formed inlets, the formation of peat ended and made place for marine sedimentation.

Figure 2.6: Middle Sub-Boreal, 2100 BC (Zagwijn, 1986)

Figure 2.7: Middle Sub-Atlanticum, 500 - 700 AD (Zagwijn, 1986)

At the roman time, the middle Atlanticum, the fresh water lake is called lake Flevo. The lake Flevo is located at approximately the same location as the current Lake IJssel. At this time the lake has no connections with the sea. Due to the continuing erosion, breakthroughs occurred and finally a connection became truth between the sea and the former lake Flevo, see Figure 2.7. The lake Flevo is from now on a sea and is called the Zuider Sea.

The first connection between the lake Flevo and the sea has been formed thru the current Vlie inlet. Another important breakthrough is the opening of the Marsdiep, which occurred supposedly between 800 and 1300 during the big storms of the 12th century. Now the western part of the Wadden Sea was created. The strong current entering the Marsdiep caused continuous erosion of the peat. As a result of this peat erosion the Marsdiep channel became deeper and the tidal volume of the Marsdiep inlet increased. The Zuider Sea reached its largest size around 1200 BC, since then the current Wadden Sea decreased in size, due to continuous sedimentation of the tidal flats in order to follow the relative sea level rise and its siltation along the Wadden shores (Stive, et al. 1990).

2.3 Human Intervention

From 1000 BC the developments in the Netherlands are not only influenced by nature only, but also by man. The influences of man increased with time. In the beginning of the 10th century the first dikes were raised, influencing the distribution of water over the various outlets of the main rivers. The purpose of these dikes varied, not only were they meant to prevent salt-water intrusion or flooding, they were also used to obtain navigation levees and to facilitate land traffic. With the change in the hydraulic conditions, the sediment distribution changed and much of the sediment did not reach the Dutch coast anymore. The coast couldn't follow the sea level rise and retreated again.

Under the pressure of an increasing population, extensive cultivation of peat areas started in the 9th century. From the 11th century artificial drainage, first by gravity and later by windmills, was used. Due to the cultivation works, the land subsided and more break-throughs of the dunes appeared. The formation of the Wadden Sea is partly caused by these break-throughs (Zitman, 1990). Another consequence of the subsiding land was major flood disasters, characterising the first half of the 13th century. With the introduction of the steam engines during the industrial revolution, new means were available against water inconvenience.

2.3.1 The Afsluitdijk

However, the steam engines could not prevent the vulnerability of large parts of the Netherlands to inundations. To protect these parts against the inundations, plans to construct a dam are made. The first plan originates from Hendrik Stevin in 1667. Since then several plans were designed pleading for different locations of the dike. Depending on the location, the Afsluitdijk should protect the provinces Utrecht, Noord-Holland and eventually Friesland and Groningen against the inundations. However, not until the flooding disaster of 1916, when large-scale inundations took place in the province of Noord-Holland and around the former Zuider Sea, the plans were taken serious. These inundations eventually led to the decision to close the Zuider Sea and to construct a number of large polders in the newly formed Lake IJssel. The polders were needed to solve the problems of the growing population: from 4 million in 1875 to 7 million in 1918. Not only was the land needed to accommodate the population, but also for agriculture, as appeared during the First World War. People had then realised that the Netherlands was dependent on foreign countries for the supply of food.

The construction of the Afsluitdijk, which finished in 1932, can be considered as the starting point of modern coastal engineering in the Netherlands. Not only was the construction of the dike itself an advanced work, also the engineering needed for the construction was advanced. Scientists expected that the closure of the Zuider Sea would change the tidal motion and would cause higher tides. Unfortunately hydraulic engineering was mainly an empirical science and

prediction of the disturbance of the tidal flow, caused by the Afsluitdijk, was beyond the then engineering practice. To investigate the consequences of the Afsluitdijk the Lorentz commission was appointed. The Lorentz Commission developed a technique for tidal computations to predict current velocities during closing operation and changes in the tides in the Wadden Sea after completion of the closure. This way, Lorentz determined a location for the Afsluitdijk that would hardly affect the tidal characteristics in the Wadden Sea and adjacent coastal areas.

2.3.2 Hydrodynamic consequences of the Afsluitdijk

Preceding the closure in 1932, the Texel and Vlie inlet tidal basin covered the southwestern part of the Wadden Sea and the former Zuider Sea (figure 2.8, left panel). In total, the basin covered a surface area over 4,000 km^2 with a basin length of 130 km. After the closure, the basin area reduced substantially to an area of 712 km^2 (figure 2.8, right panel) and a length of about 30 km. A tidal divide now separates the two basins, Texel and Vlie, with a residual transport between the two basins remaining.

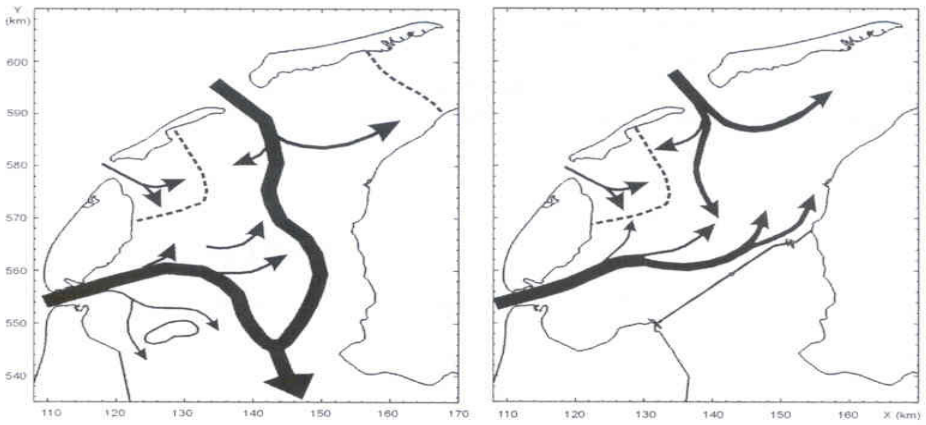

Figure 2.8: Tidal waves in Zuider Sea before closure (Thijsse, 1972)

The closure of the Zuider Sea has decreased the Texel Inlet basin area substantially, whereas the tidal prism increased about 20%. This apparent contradiction mainly results from the changed characteristics of the tidal wave in the basin. Preceding the closure, the tidal wave in the Zuider Sea consisted of the combined tidal waves of the Texel and Vlie Inlets. These two tidal waves propagated separately through the Wadden Sea and merged into one tidal wave in the Zuider Sea area (as illustrated in figure 2.8, left panel). The tidal wave reflected at the southern boundary of the Zuider Sea basin, about 130 km inland from the Texel inlet. The basin length (L) equals about half the tidal wave length (λ) and, in a hypothetical situation without bottom friction and the wave propagating at an oblique angle to the shore, a standing wave would form in the basin. In such case, at the location $L \approx 0.5\lambda$ from the southern boundary an anti-node in water level occurs at which discharges are zero and all exchange of water south of this boundary takes places in the basin.

In reality, the tidal wave propagating through the Zuider Sea, that is limited in depth, decreased and deformed by bottom friction. The reflected tidal wave is considerably smaller in amplitude than the incoming tidal wave. The interference of the two waves results in the formation of a damped tidal wave with a propagating character at the inlet and a standing character near the

southern boundary. A schematisation of the resulting tidal wave envelope is indicated by (I) in Figure 2.9 (after Kragtwijk, 2001).

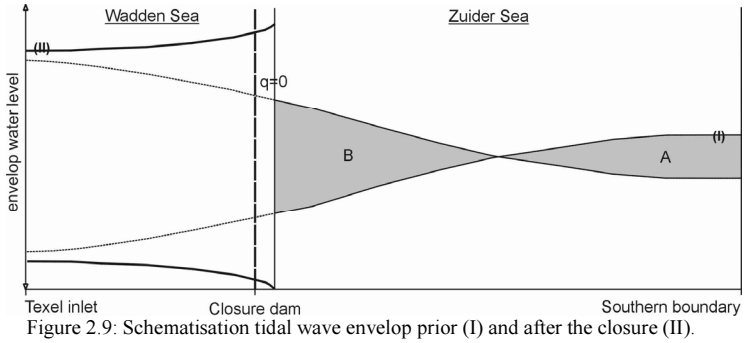

Figure 2.9: Schematisation tidal wave envelop prior (I) and after the closure (II).

The no-exchange boundary (indicated by q=0 in Figure 2.9) is no longer located at $L \approx 0.5\lambda$, but is formed at the location were the areas indicated by (A) and (B) balance. This location is closer to the southern boundary. The actual location of the closure dam is north of the no-exchange line because the tidal ranges in the basin were predicted to increase substantially. Due to the closure dam the basin length reduced to about 30 km (figure 2.8, right panel) that is small compared to the tidal wave length ($L \approx 0.2\lambda$), and a tidal wave is formed with a standing wave character. This strong decrease in basin length reduced the damping of the tidal wave due to friction and with more reflection at the closure dam, the tidal ranges increased drastically (tidal wave envelope after the closure indicated by (II) in figure 2.9). This is the reason that the location of the closure dam was chosen seaward of the no-exchange location, i.e. to minimize the changes in flow velocities through the inlets (Lorentz et al., 1926).

Figure 2.10: Increase of tidal range at Den Helder after closure

Alterations in tidal range and tidal volumes were predicted and have occurred. The increase in tidal range is clearly reflected in Figure 2.10 by the water level observations of the measuring station Den Helder, located in the Texel inlet gorge. The tidal ranges increased nearly instantaneous with approximately 15%. This corresponds reasonably with the 21% increase predicted by Lorentz et al. (1926). At the location of the Afsluitdijk in Den Oever, the increase in tidal range was even more dramatic as an increase of nearly 100% was observed and predicted (Thijsse, 1972).

In addition to this increase in tidal range, the changed flow patterns in the basin must have contributed to the large changes in hydro- and morphodynamics of the basin. The closure resulted in closing of the southward-directed flow channels. Consequently these channels lost their effective function, while flow through eastward-directed channels increased. This latter flow was further enhanced by the eastward deflection of the tidal wave at the closure dam (Figure 2.8, right panel). The two tidal waves originating from Texel and Vlie inlet now meet east of the original meeting point, at the location of Harlingen, forming a tidal divide. This eastward extension resulted in an actual drainage area that is slightly larger than the active part of the drainage area prior to the closure (Kolk and Schalkers, 1980).

The analysis shows that most of the former Zuider Sea did not actively take part in the water exchange with the Wadden Sea. The basin area after the closure is at least comparable with the active basin area prior to closure. Combined with the enlargement of the tidal range an increase in tidal prism of about 26% was observed (and predicted).

2.3.3 Morphological consequences of the Afsluitdijk

Prior to the closure, it is plausible that the basin was in an equilibrium state (Louters and Gerritsen, 1994). A relation existed between relative size of the intertidal shoals and drainage area (Eysink et al., 1992). With the closure, the back part of the basin (Zuider Sea) that contained a relative large portion of shoals was separated from the basin. The remaining shoal area was too small relative to the area of the channels; therefore, a morphologic adjustment of the basin was to be expected during the stage of non-equilibrium after the closure.

The analysis of the basin hydrodynamics indicates an increase in tidal prism and change in flow patterns after the closure, which resulted in drastic changes in basin and ebb-tidal delta morphology (Elias et al., 2003). Large sedimentation areas were observed in the terminal parts of channels (see, e.g., the Vlieter, Vliestroom and Texelstroom) where tidal currents reduced to almost zero and the loss of discharge caused the channels to accrete rapidly (Berger et al., 1987).

Large changes were also observed in the upper part of the Texelstroom (Elias et al., 2003). The alterations in flow patterns resulted in an increasing importance of this channel. A prominent feature is the lateral channel migration (Oost, 1995) indicated by the alternating pattern of sedimentation and erosion areas. In addition, the Texelstroom migrated northward aligning along the Texel island back barrier shoreline. The inertia of the increased discharge and resulting increased flow through the channel extended the upper part of the channel in eastward direction. Such an eastward extension and increasing channel depth also occurred at the Doove Balg channel due to the eastward deflection of the flow at the closure dam.

As the Texelstroom connects to the inlet gorge Marsdiep, the orientation of the inlet gorge and the ebb-tidal delta is related to the orientation of the Texelstroom as they have a tendency to align due to inertia of flow. The observed south-western rotation of the Texelstroom by alignment along the Texel coastline after the closure most likely has contributed to the, already occurring, southward rotation of the ebb-tidal delta (Elias et al., 2003).

3 Processes in the Wadden Sea

3.1 Introduction

To acquire a better understanding of the morphological evolution of the Wadden Sea, some of the presumed dominant underlying processes are explained in this chapter. In the various sections different processes are explained separately. However, it is important to realise, that some processes influence each other and cannot be considered separately.

3.2 Propagation vertical tidal wave

The vertical tidal motion in the Dutch North Sea and the Wadden Sea is generated by the tidal wave from the Atlantic Ocean. In fact two tidal waves are entering the North Sea. One of them enters the North Sea through the Dover Strait; the other tidal wave comes from the north and turns around Scotland. The merge of those two tidal waves together with reflection and the coriolis effect result in a difficult tidal motion in the North Sea. The tidal wave moves in anti-clockwise direction and has two amphidromal points, one in the middle of the southern North Sea and one in the northern North Sea (figure 3.1). The vertical tidal movement is more or less zero in the amphidromal point and increases with the distance form the amphidromal point.

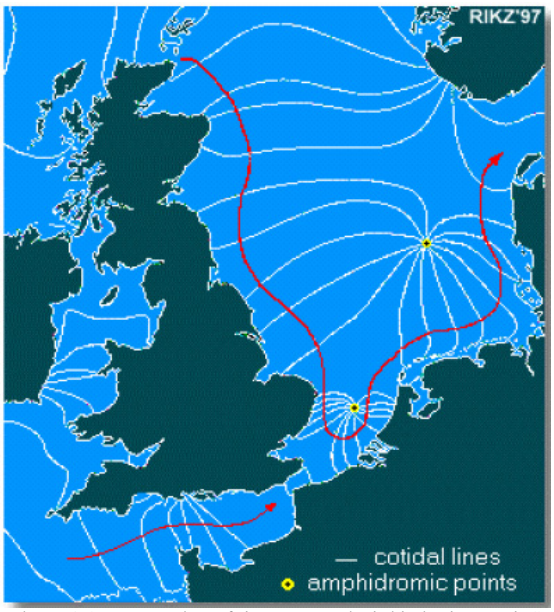

Figure 3.1: Propagation of the astronomical tide in the North Sea (www.getij.nl)

If we consider the tidal movement along the Dutch coast, the tide moves from the South to the North and meets the second tidal wave at Texel. The merged tidal wave moves to the east along the Dutch and German islands. The amplitude of the tidal wave decreases form the South of Holland till it reaches its minimum at Den Helder (figure 3.2) after which the tidal wave increases. Besides, the shape of the tidal wave changes from a regular, sinusoidal, shape at Vlissingen to a more complicated shape (several sinusoidal waves) at Den Helder, where the two tidal waves meet. Eastward of Den Helder, the shape of the tidal wave gets more sinusoidal again. The tidal wave, propagating in eastward direction along the North Sea coast, penetrates the Wadden Sea through the various tidal inlets. Due to the limited depth and the large storage capacity of the Wadden Sea, the propagation of the tidal wave is reduced. Inside the basins the tidal range is variable, due to the energy loss of the tidal wave caused by bottom shear stress and reflections on the mainland shoreline (Eysink, 1993).

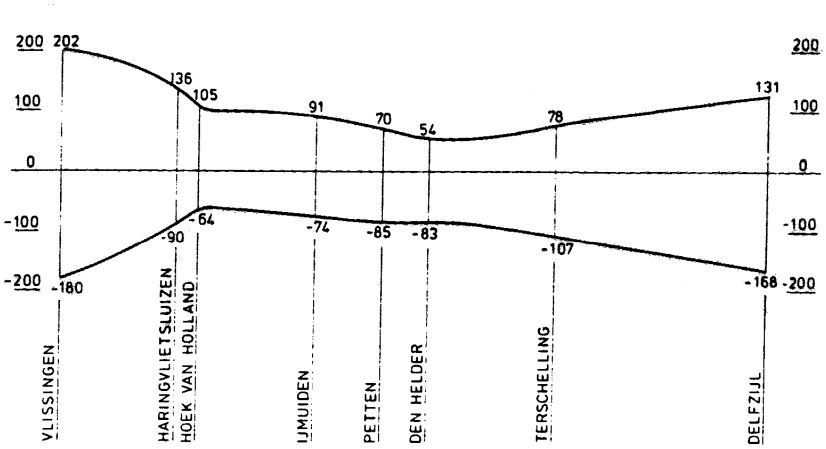

Figure 3.2: Development of tidal range along the Dutch coast (Van der Spek and Noorbergen, 1992)

Astronomical tide

The development of the tidal wave can be described by the astronomical tide. The astronomical tide consists of a rest component a0 and several harmonic components, from which the semi-diurnal lunar component (M_2) and the semi-diurnal solar component (S_2) are the most important. In addition there are other components, like the K_1 and O_1, which refer to the daily inequality due to the declination of the moon and the sun. Other important parameters of the astronomical tide are the overtides. The overtides are due to non-linear interactions of the tidal components and lead to sub-harmonic and super-harmonic tides. For the M_2 component the overtides are the M_4, M_6, etc.

3.3 Tidal divides

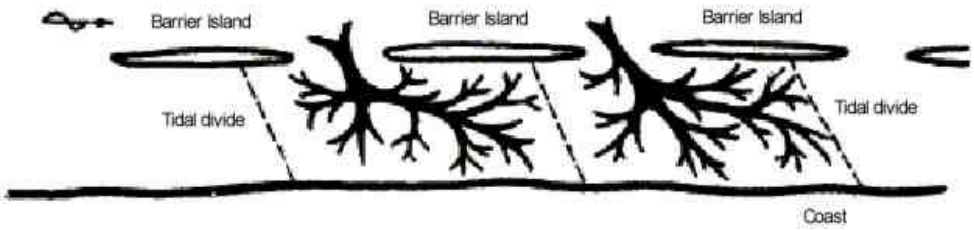

Figure 3.3: Tidal divide (Van Veen, 1950)

Tidal waves, entering two successive inlets, meet behind the enclosed island. The tidal divide is the location where both tidal waves meet, resulting in negligible flow velocities. If we consider the vertical tide however, the waves amplify each other. The closer to the tidal divides, the higher the vertical tide. As the tidal divide moves in flow direction, the tidal divide is not a strict line. However, the average position of the tidal divide can be found due to the high sedimentation rate, caused by the low flow velocities. Tidal divides are thus characterised by higher bed level. Only under conditions with strong wind, drift currents will pass the tidal divides during high water. Due to the tidal divides the Wadden Sea can be considered as a system consisting of different

individual tidal systems, whereby each tidal system is constituted of an outer delta and a tidal basin.

The western part of the Wadden Sea has a more complicated structure. Due to a through flow from the Vlie to the Marsdiep basin (Ridderinkhof, 1988), a location with negligible flow velocities is not present. The location with lowest flow velocities is defined as tidal divide. The Eierlandse Gat has well defined tidal divides.

3.4 Development of a barrier coast

About 32 000 km (13,1 %) of the worlds total coastline is classified as a barrier coastline (Donselaar, 1996). The Wadden Sea of the Netherlands, Germany and Denmark is the largest associated barrier coast in the world (Reijngoud, 1998).

Some factors determining the development and the preservation of a barrier coast are:

- Tidal range
- Waves and wind
- Sea level rise

In the following sections the influence of these factors on the development of the tidal inlet system is explained.

3.4.1 Tidal range

The development of the tidal wave along the Dutch coast is explained in section 3.2. In summary, the amplitude of the tidal wave changes along the Dutch coast. Due to the variation in tidal range along the Dutch coast, a longshore water surface gradient is generated, resulting in a tide-driven longshore current. This tide-driven longshore current is called the horizontal tide.

The tidal wave, propagating in eastward direction along the North Sea coast, penetrates the Wadden Sea through the various tidal inlets. Due to the large sediment transport capacity of the tidal flow, the interaction between the tidal current along the North Sea and in the inlet determines the geometry of the ebb-tidal delta. Another factor determining the ebb-tidal delta geometry is wave action. Hayes (1979) distinguished several types of tidal inlets by combining the relative effects of tidal range and wave action:

- Wave dominated inlets;
  Are characterized by long continuous barriers, with only few tidal inlets and a lot of washovers.

- Mixed energy-wave dominated;
  Are characterised by a large number of inlets and a smaller number of washovers. The size of the ebb-tidal delta will become somewhat larger.

- Mixed energy-tide dominated;
  Are characterised by abundant tidal inlets, relative large ebb-tidal deltas and usually drumstick barriers.
  The Dutch Wadden Sea is a mixed energy-tide dominate tidal inlet system

- Low-tide dominated;
  Occasionally show wave built bars.

- High-tide dominated;
  Are characterised by predominant tidal current ridges, extensive salt marshes and tidal flats. Inlets of this type often have large ebb-tidal deltas and very deep inlet gorges.

3.4.2 Waves and Wind

Sediment transport by waves takes place due to non-broken waves and due to broken waves. The sediment transport generated by non-broken waves is a result of wave asymmetry, meaning that the waves do not have a perfect circular pattern. As a result net sediment transport coastwards occurs. The other transport mechanism occurs when waves are breaking and stir up a lot of sediment. The stirred-up sediment is transported by the longshore current in the breakerzone, induced by waves approaching the coast under an angle. Waves at the Dutch coast generally approach the coast from west / southwest direction, resulting in an east / northeast directed longshore current.

The above-described process is important for the sediment supply for North Sea side of the barrier islands and for the ebb-tidal delta. The Wadden Sea basin is subjected to a very limited amount of wave energy. Waves generally break in water with a depth of about twice the wave height, admitting only a limited amount of wave energy to pass the shoals of the ebb-tidal delta and enter the Wadden Sea (Eysink and Biegel, 1992). Waves in the Wadden Sea are mainly generated by local winds. Only during a high storm flood, part of the sea waves and swell will penetrate the Wadden Sea and break on the first tidal flats in the basin.

Wind has an important effect on the water motion in the Wadden Sea. Wind generates shear stresses at the water surface, which causes drift currents and wind waves. If the wind blows perpendicular to the coast, the drift currents lead to an increasing surface level elevation in the wind direction (wind set-up). The opposite phenomenon, when the wind is blowing perpendicular of the coast, is called wind set-down.

In the limited geometry of a tidal basin, with differences in water depths, the combination of tide and wind induced currents and waves leads to a complicated sediment transport pattern. In general however, the tidal flow will dominate, but on the tidal flats and at the tidal divides, the opposite may occur during conditions with strong wind (Eysink, 1993).

3.4.3 Sea level rise

Since the end of the latest ice age, some 10 000 years ago, the sea level has been rising. The increase in temperature, which resulted in melting ice caps and expansion of water, induced a sea level rise of 120 to 140 meters. The rise in sea level was very rapid at first, but later the rate gradually decreased. In general, the sea level has gradually risen in the past thousand years. Only during the Middle Ages, also called the 'little' Ice Age, the sea level dropped. However, as from 1850 the temperature increased again and the sea level along the Dutch coast rose by some 20 to 30 centimeters, regaining the level of the Early Middle Ages.

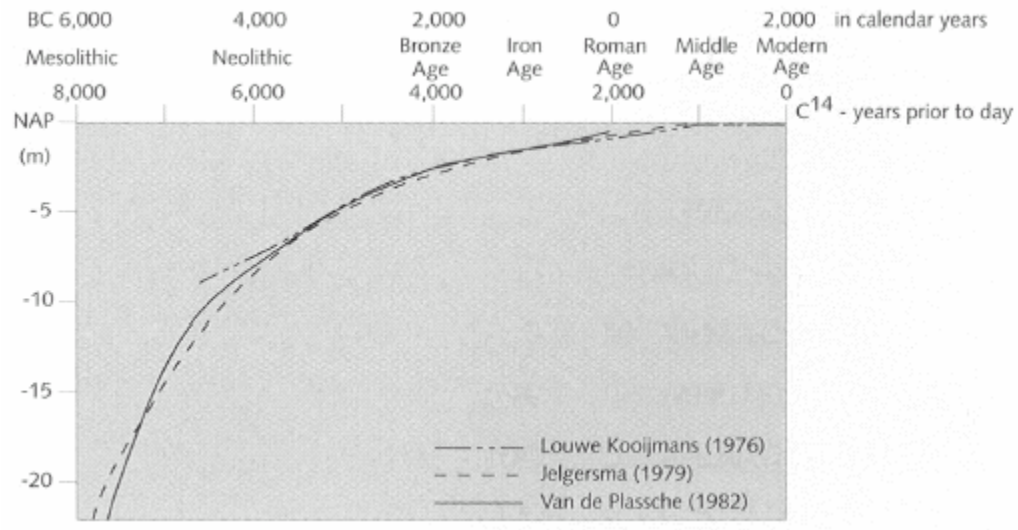

Figure 3.4: Sea level rise curve

Measurements from the past 150 years show a fairly constant sea level rise of approximately 20 centimeters per century. However, probable due to the increase in CO_2 emission and other 'greenhouse gases' the increase of the global mean temperature could intensify. For the Dutch coast, the worse case could be a rise by 85-105 centimeters per century. Empirical proof, however, for the projected acceleration in the rate at which the sea level rises is lacking till now (Louters & Gerritsen, 1994).

Besides the rising of the sea level, also the sea floor subsidence determines the sea level rise. The combined effect of sea level rise and sea floor subsidence is called relative sea level rise. A recent study carried out in connection with the Normal Amsterdam Level (NAP) proved that the level of the deep stratum of the coast changes. A natural process of sea floor subsidence has been discovered, which varies between 4 to 8 centimeters per century along the Dutch coast. Since this is a result of large-scale geological processes, it is very likely that comparable ground shift will occur in the future centuries (Louters & Gerritsen, 1994).

In addition to the natural subsidence, human induced subsidence has to taken into account too. Human activities like sand and shell mining and gas extraction are acceleration the sea floor subsidence in the Wadden Sea.

3.5 Components of a tidal inlet system

A tidal inlet system consists of a tidal inlet and a tidal basin. The tidal inlet consists of ebb-tidal delta and the adjacent coasts. Their morphological development is related to the hydrodynamic forcing of tidal prism and offshore waves. The tidal basin consists of two elements: flats and channels. The morphological development of the tidal basin is related to the tidal range and the basins surface area.

The sediment distribution between the components of the tidal inlet system is an important factor in the morphological development. Short-term (years) behaviour and development of a tidal inlet system is determined by the internal distribution of sediment. The exchange of sediment between adjacent elements, thus flat-channel and channel-delta and delta-adjacent coast occurs on the

medium-term (decades). The exchange of sediment with the outside world / adjacent coast is important for the long-term (centuries) behaviour of the system.

3.5.1 Ebb-tidal delta and adjacent coast

Ebb-tidal deltas are sediment accumulations on the seaward side of, and both morphologically and dynamically connected to, tidal inlets. They form important morphological elements along the barrier islands (Sha, 1990). Ebb-tidal deltas are important as permanent and temporary sediment reservoirs. When the tidal inlet demands sediment, this is usually first provided by the ebb-tidal delta. If there is not enough sediment 'available', this sediment will be delivered by the adjacent coast.

According to Hayes (1970) several components can be recognised in an ebb-tidal delta, such as a main ebb-channel, margin linear bars, a terminal lobe, swash platforms and bars, and marginal flood channels (figure 3.5).

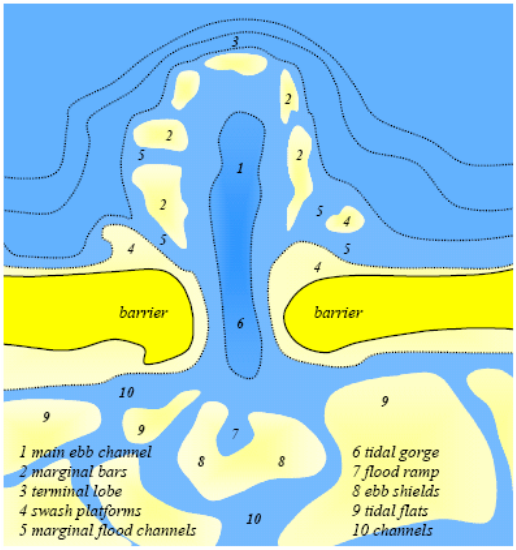

Figure 3.5: Layout of a typical ebb-tidal delta

The main ebb channel (element 1 in figure 3.5), usually situated in the central part of the ebb-tidal delta, is surrounded by swash platforms (4), which are broadsheet of sand, and by linear bars (2), depositions build up by the interaction between flood- and ebb tidal currents with wave-generated currents. The terminal lobe (3) is a steep seaward-sloping body of sand, which forms the outer end of the ebb-tidal delta. The marginal flood channels (5) usually occur between the barrier islands coast and the swash platforms.

Dean and Walton (1975) defined the volume of the ebb-tidal delta by means of the no-inlet bathymetry. In their definition they suppose that the inlet does not disturb the no-inlet bathymetry of the coastal slope. Therefore, the bathymetry is assumed to be equal to the bathymetry of the adjacent coasts. The difference in volume between the no-inlet bathymetry and the bathymetry of the ebb-tidal delta is the volume of the ebb-tidal delta (shown in figure 3.6).

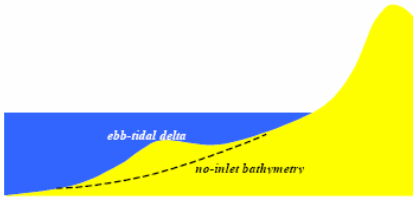

Figure 3.6: Volume ebb-tidal delta

Ebb-tidal delta morphology

The morphology of the ebb-tidal delta depends on the interaction of tidal currents and waves. The ebb-tidal delta sediment transport can be explained as follows: the longshore wave induced current and the tidal current transport sediment to the ebb-tidal delta system. During flood sediment is transported through the inlet into the Wadden Sea, while during ebb sediment leaves the Wadden Sea.

As the cross-section of an inlet is small, flow velocities are high and so is the sediment transport capacity. On the ebb-tidal delta, due to bottom friction, flow-velocities decrease very quickly with increasing distance from the inlet. The decrease in flow-velocity results in ever-higher sedimentation rates. By this mechanism the ebb-tidal delta can develop and preserve itself.

In a study by Walton and Adams (1976) it was concluded that a relation exists between the volume of sand stored in the ebb shoals of an inlet and the tidal prism (relation 3.5). Dean (1988) further demonstrated that the volume of the ebb-tidal delta would be larger in case of low onshore-directed wave energy and large tidal forces. Under these circumstances the ebb-tidal delta can extend far seaward, without a clear terminal lobe. However, if the onshore-directed wave energy would be larger, the ebb-tidal delta volume would become smaller.

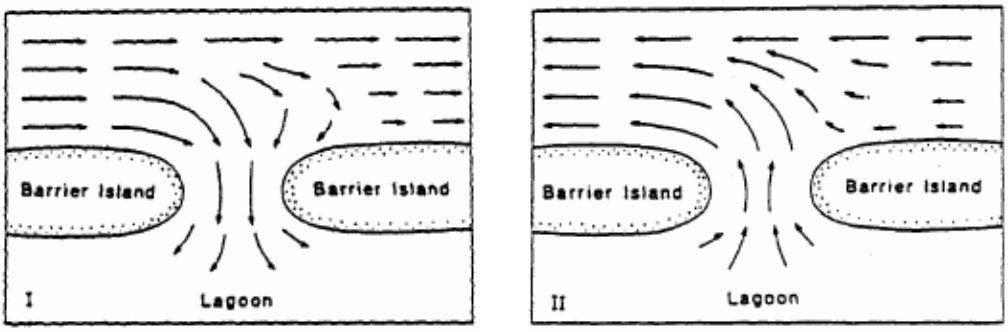

Figure 3.7: Flow pattern at mid-flood (I) and mid-ebb (II) (Sha and Van den Berg, 1993)

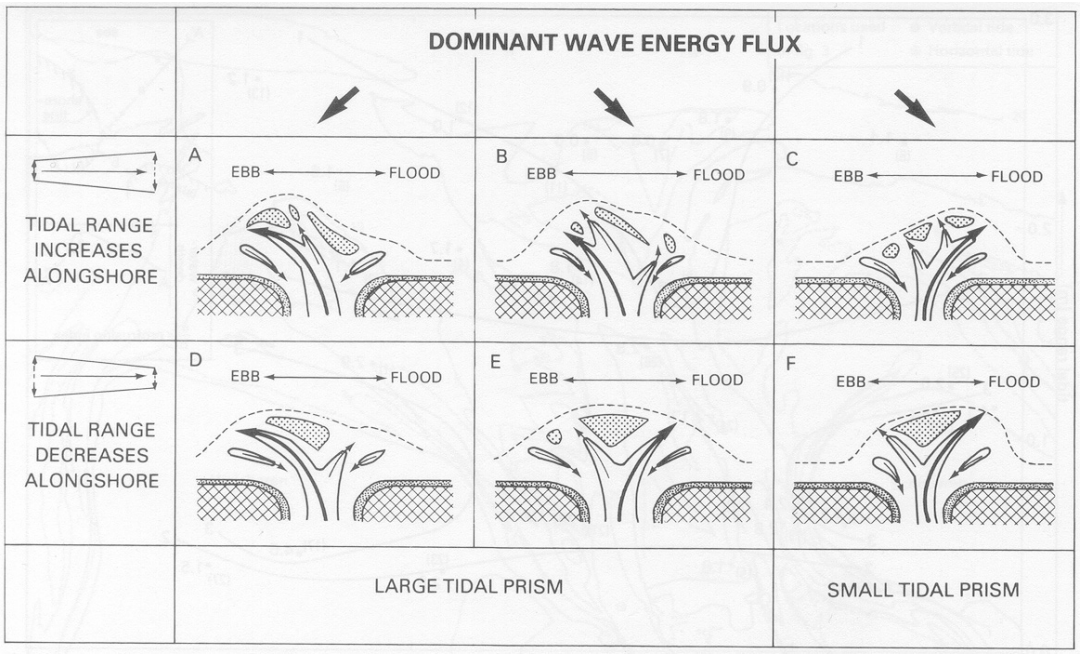

Figure 3.8: Development of outer delta with different prism and tidal range (Sha and Van den Berg, 1993)

For the shape of the ebb-tidal delta not only the tidal longshore current is of concern; more important is the relation between the tidal range and the wave energy flux. Sha and Van den Berg (1993) determined that an increase in tidal range in the same direction as the tidal wave propagation gives a stronger ebb-tidal delta asymmetry. Likewise, the waves try to push the main ebb channel in the direction of the main wave at deep water. According to Sha (1990), the variation of the ebb-tidal deltas of the Wadden Sea is mainly determined by the magnitude of the tidal prism. Inlets with a large tidal prism show up-drift asymmetrical ebb-deltas, while inlets with a small tidal prism show down-drift asymmetrical ebb-tidal deltas. The actual geometry of the ebb-tidal delta is determined by a combination of the effects as shown in figure 3.8.

Sediment bypassing

As mentioned above, the main processes concerning sediment transport in the ebb-tidal delta depend on tidal currents and waves. In the section above the influence of waves and tidal currents on the shape of the ebb-tidal delta are explained. In this section, the sediment bypassing will be discussed.

Sediment bypassing is defined as the process that allows material, after a short interruption caused by an inlet, channel, jetty or other type of littoral barrier, to become part again of the normal littoral drift zone a short distance down drift from the littoral barrier. Bruun & Gerritsen (1959) described two principles of sediment bypassing by natural action. One of them concerns a bypassing mechanism, which only occurs in situations with considerable wave action: bypassing via offshore bars. In this case, a submerged offshore bar is formed in front of the tidal inlet. The wave generated littoral drift flows over the bar in the direction of the down drift island. As the total longshore current drift capacity remains the same for the submerged bar and the normal beach, the dimensions of the submerged bar can be estimated. The depth of the submerged bar is restricted by the breaker depth of the waves. If the littoral drift will increase, due to higher waves offshore, the submerged bar will decrease in depth and increase in width.

The other bypassing mechanism concerns tidal flow action and can be divided in migration of bars and channels and sediment transport by tidal flow in the channels. Generally, tidal channels migrate in down-drift direction. One of the reasons for this may be that littoral material is deposited on the up drift banks of the channels forcing the down drift. Another occurring process is the meandering capacity causing channel migration of curved channels. The bars in between the channels may follow this migration and once join the down drift barrier coast.

FitzGerald (1988) subdivided the sediment bypassing along mixed-energy coasts in three different and independent models (see figure 3.9): inlet migration and split breaching, stable inlet processes and ebb-tidal delta breaching. FitzGerald (1988) mentions that in real tidal inlets, all three types can occur simultaneously or may dominate alternately. The movement of sand along the terminal lobe by wave action is almost always present at mixed energy coast.

In the first model of FitzGerald (1988), inlet migration and spit breaching is the main issue of the model. This model is applicable when littoral transport is a dominant process. Littoral material transported to the tidal inlet can cause constriction of the inlet throat. The decrease in cross-sectional area will result in greater scouring capacities, which will cause erosion of the down-drift barrier beaches. Due to the above process the inlet will migrate in down-drift direction. The rate of migration is dependent on sediment supply, wave energy, tidal currents and the composition of the channel bank. Due to the down-drift migration, the inlet channel is elongated, which results in lower discharge efficiency. After a storm, generally a shortcut has been created, replacing the old

inlet channel. Once the old inlet has attached to the down drift coast, a large quantity of sand has bypassed the inlet.

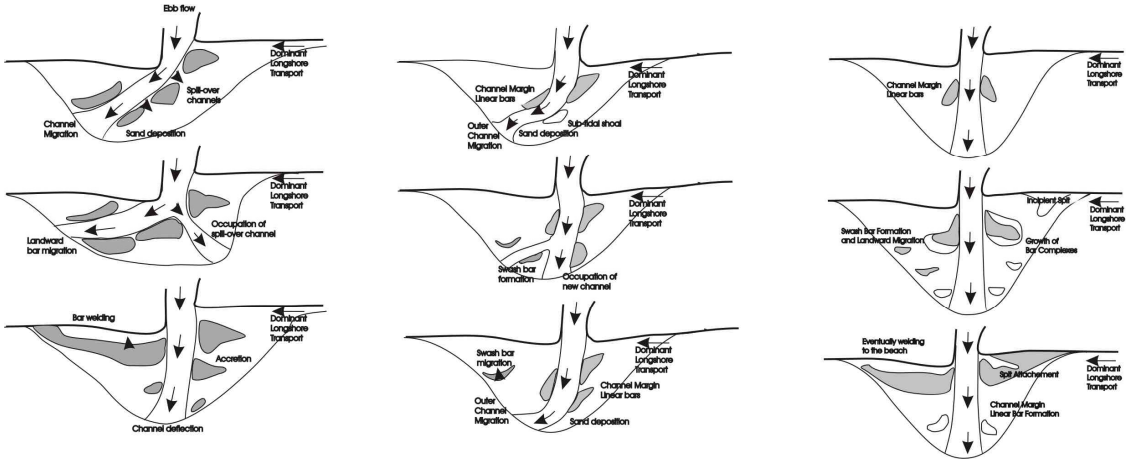

Figure 3.9: Models of sediment bypassing (a) Cyclic ebb-tidal delta breaching, (b) Outer channel shifting, (c) Stable inlet processes. (Redrawn after FitzGerald et al., 1988).

In the second model, stable inlet processes are considered. These are inlets with a stable throat position and a non-migrating ebb channel. The sediment bypassing occurs through the formation of bars, formed by the stacking and coalescing of wave built accumulations of sand on the ebb-tidal delta. By means of breaking and shoaling of waves the bars migrate and attach to the down drift coast. New bars will constantly develop due to a more or less continuous sand delivery by the ebb tidal channel. Therefore, the sediment bypassing in this model depends on sand deliveries through the channel system

The third model, ebb-tidal delta breaching, discusses similar to the second model inlets with a stable throat position. However, the ebb channel is not longer stable and the dominant littoral drift will push the ebb channel towards the down drift coast. As described in the first model, the flow efficiency of the elongated channel will decrease and hydraulic gradients over the bar will steadily increase. The inlet will divert its flow to a more seaward direction via the so-called spill over lobe channels. Consequently, the discharge through the old ebb channel decreases. The result is that large portions of the ebb-tidal delta sand bodies are bypassed.

3.5.2 Tidal basin

The tidal basin is located between the barrier islands and the mainland. The characteristic morphology of the Wadden Sea tidal basin is a meandering, branched channel system, with inter-tidal sand and mud flats and marshes. In the Dutch Wadden Sea, basins are often rectangular or near square, and the channel structure is often more branched than braided.

Flats

The tidal flat is defined as the area between mean high water (MHW) and mean low water (MLW). In the Wadden Sea, with a diurnal tide, the flats inundate twice a day.

Eysink (1993) noticed that from a morphological point of view, the tidal flats reduce the tidal prism of the basin and, consequently, affect the size of the channels. Hence, the larger and the higher the intertidal zone, the smaller the tidal prism is. This size of the flats, on their turn depend on the tidal range, the size and the shape of the basin, the orientation of the basin regarding the dominating wind, the width over depth ratio of the mean tidal channel and the local wind climate.

The crest of a flat is generally located at the tidal divide between two channels. When at flood the water spreads over the flats, the velocity decreases and sediment will be deposited. The level of the crest seems more or less to be related to the width of the flat (Eysink, 1993). Generally, the crest levels, in the Wadden Sea mostly range between MSL and MHW -0.3 m, while the level of the tidal divides roughly varies around MHW -1 m. The stability of the tidal divide appears to be another factor regulating the crest level. If the tidal divide is rather stable and the same for ebb and flood, the crest level will be relatively high. If not, the tidal flat may remain relatively low.

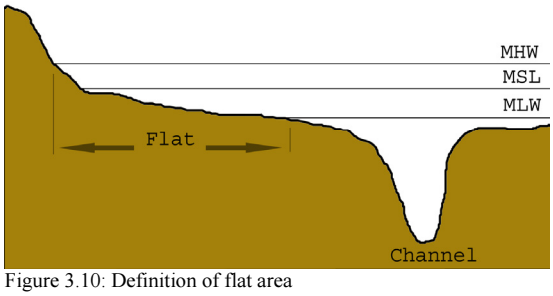

Figure 3.10: Definition of flat area

Channel

The area below mean low water is usually the definition of the channel area. From the inlet to the mainland and the tidal divides, the tidal volume decreases. As a result of decreasing cross-sectional channel areas the flow velocities in the channels decrease towards mainland and tidal divides (Oost, 1995).

According to Eysink and Oost (Eysink, 1979; Oost, 1995), most channels are dominated by the ebb flow. This ebb domination of the channels can be explained by the asymmetry of the vertical tide. Steijn (1991) explains that rather flat basins, with increasing surface area with rising tide, support the dominance of ebb currents. During falling tide, water from the (large) intertidal areas flows into the surrounding tidal channels, causing relatively higher ebb velocities. During rising tide, the flow velocities in the channels will be smaller due to the flooding of the intertidal areas and the higher flow resistance. When most of the intertidal areas are flooded, these flood currents may grow stronger in velocity. This results in an asymmetric flow velocity distribution over a tidal cycle, giving rise to ebb-dominance in large parts of the basin. If the basin is open, wide and has a mean depth larger than that of the inlet throat, the situation is reverse and the increased flow resistance for ebb may support flood dominance.

3.6 Equilibrium relations

A tidal inlet, and its several components, tends to equilibrium if the morphological factors are not changing. For the equilibrium situation several relationships exist between the equilibrium state and the hydrodynamic parameters. If one of the morphological factors will change, the new equilibrium can be predicted. In this section, several relationships will be described.

Most of the relations include a parameter related on the tide. Most of the time, this parameter is the tidal prism. However, often another tidal parameter is used like ebb volume (EV), flood volume (FV) and tidal volume. The tidal volume is the volume of water entering the basin during flood (FV) plus the volume of water leaving the basin during ebb (EV). The tidal volume is based on discharge measurements in the tidal basin. Eysink (1990) uses for his relations the characteristic tidal volume, which is equal to the prism

The tidal prism however, is equal to the water volume between MHW and MLW in the basin. In relatively short basins, like the Wadden Sea, the tidal motion is that of a standing wave. This results in a tidal volume of nearly twice the tidal prism. The tidal prism is based on systematic bathymetric surveys of the tidal basin.

3.6.1 Relation between cross-section and tidal prism

The morphology of tidal inlets can be very dynamic. Steijn (1991) did research on an inlet in South Carolina, which is subjected to an extreme situation, showing the possible dynamic character of an inlet. The width and the cross-sectional area of this inlet changes per tide as a consequence of the large differences in flow velocities. The morphology of the Wadden Sea inlets is less dynamic. Several relationships for cross-sectional areas and tidal prisms have been found, with the general form:

$$A_c = c \cdot P^n + a \tag{3.1}$$

in which:
A_c: cross-sectional area and mean sea level [m^2]
P: tidal prism [m^3]
a, c, n: empirical coefficients [-]

The empirical coefficients a, c and n depend on several aspects like tide, wave climate, dimension of the inlet and sediment characteristics.

For the Wadden Sea Gerristen and De Jong (1985) found the following relation:

$$TV_{inlet} = 3{,}3 \cdot 10^4 \cdot A_{inlet} - 79{,}2 \cdot 10^6 \tag{3.2}$$

in which:
TV_{inlet}: tidal volume of the inlet [m^3]
A_{inlet}: cross-sectional area of the inlet [m^2]

Misdorp et al. (1990) found another relationship for the Wadden Sea, comparable with relation (3.2).

$$TV_{inlet} = 3{,}6 \cdot 10^4 \cdot A_{inlet} - 152 \cdot 10^6 \tag{3.3}$$

Eysink (1990) stated that a fairly good relation between the inlet area and the tidal prism is presented by:

$$A_{MSL} = c_A \cdot P \tag{3.4}$$

in which:

A_{MSL}: flow area below MSL [m^2]
P: tidal prism [m^3]
c_A: empirical coefficient [m]

3.6.2 Relation between volume of ebb-tidal delta and tidal prism

As can be read in section 3.4.1, an ebb-delta will form in front of each tidal inlet as a result of a balance between the sediment leaving the tidal basin by the ebb currents and the pushing of waves and flood currents in the direction of the mainland.

Walton and Adams (1976) derived empirical relations for the amount of sand that is stored in a delta. They found that relations exist between the sand storage in the ebb-tidal delta and the tidal prism of the inlets and the local wave climate.

$$V_{delta} = c_{WA} \cdot P^{1,23} \tag{3.5}$$

in which:
V_{delta}: volume of the ebb-tidal delta [m^3]
c_{WA}: empirical coefficient [$m^{-1,23}$]

The value of c_{WA} depends on the wave climate. Walton and Adams (1976) distinguished three types of wave climate with each their own value of c_{WA}.

Table 3.1: Values of c_{WA}

Wave action	Value of c_{WA}[$m^{-1,23}$]
Low wave energy	$8,46 \times 10^{-3}$
Medium wave energy	$6,44 \times 10^{-3}$
High wave energy	$5,33 \times 10^{-3}$

In a recent study, Eysink (1990) determined the sand storage of the ebb-tidal delta of the inlets Marsdiep, Eierlandse Gat, Vlie and Borndiep and plotted them in the diagram of Walton and Adams. These data fitted quite well the relation fit the highly exposed coasts in which class they belong. However, Eysink (1990) found that the c_{WA} parameter had to be slightly adjusted, resulting in the following relation for the Wadden Sea:

$$V_{delta} = 6,57 \cdot 10^{-3} \cdot P^{1,23} \tag{3.6}$$

3.6.3 Relation between volume of tidal flats and size of basin

The relative flat area (A_{flat}/A_{basin}) depends on the total area of the basin and the tidal range.

Renger and Partensky (1974) found for the German Bight:

$$\frac{A_{flat}}{A_{basin}} = 1 - 2,5 \cdot A_{basin}^{0,5} \tag{3.7}$$

in which:
A_{flat}: surface area of flats [m^2]
A_{basin}: surface area of basin [m^2]

Eysink (1991) stated that the relative flat area is affects the tidal prism and found the following relation:

$$P = A_{basin} \cdot H - \alpha_f \cdot \left(\frac{A_{flat}}{A_{basin}} \right) \cdot A_{basin} \cdot H \tag{3.8}$$

A logical consequence of the relationship between the tidal flats and the basin is that the volume of the flats depends on the tidal range and on the basin area.

$$V_{flat} = \alpha_f \cdot \left(\frac{A_{flat}}{A_{basin}} \right) \cdot A_{basin} \cdot H \tag{3.9}$$

In the above relation, α_f is an empirical defined relation for the Wadden Sea.

$$\alpha_f = 0,41 - 0,24 \cdot 10^{-9} \cdot A_{basin} \tag{3.10}$$

Because the height of tidal flats is related to the tidal range, the average height of the flats ($h_{flat,av}$) compared to MLW is:

$$h_{flat,av} = \alpha_f \cdot H \tag{3.11}$$

3.6.4 Relation between channel volume and tidal prism

From the fact that a rather firm relation is present between the size of a tidal channel and the tidal prism, Eysink (1990) deduced that the volume of a channel system behind a certain channel cross-section should be related to the tidal prism at that cross-section.

For basins were the channels get narrower while approaching the mainland or a tidal divide, the follow relation is valid:

$$V_c = \alpha_c \cdot P^{1,5} \tag{3.11}$$

Eysink and Biegel (1992) also found a relation between the tidal prism and the channel volume below MLW:

$$V_c = 16 \cdot 10^{-6} \cdot P^{1,55} \tag{3.12}$$

In section 3.6 equilibrium relations for several elements in the tidal system have been described. Due to the construction of retention in either the Marsdiep or Vlie basin, several element of the tidal inlet system, like the tidal prism, the volume of channels and flats change. The new equilibrium value of these elements is subject of this study.

4 ASMITA

For this chapter articles of Stive et al. (1996), Kragtwijk (2001) and Van Goor et al. (2003) have been used.

4.1 Introduction

For the long-term morphological changes due to the construction of the reservoir in the western Wadden Sea, the ASMITA model is used. In the ASMITA model the elements of the tidal inlet system play a central role. For each element the morphological changes are modelled using empirical relations based on hydrodynamic and morphodynamic conditions.

The ASMITA model can be considered as an aggregation on the one hand and an extension on the other hand of the ESTMORF model (Wang et al., 1996; and Fokkink et al., 1996). The aggregation concerns the fact that the system elements are characterised by only one state variable (viz. a total wet or dry volume). The extension concerns the incorporation of formulations for the ebb tidal delta and directly adjacent coast.

4.2 ASMITA schematisation

In ASMITA, the degree of schematisation is determined by the element of the system, which delivers the lower boundary to the relevant spatial scale. This concerns typically the ebb-tidal delta, for which there is presently no other option than to consider its volume as an integral state variable, implying that the ebb tidal delta is modelled as a single element.

Starting with the same level of schematisation, i.e. using the same spatial scales, for all the elements in the system, the following basic elements are distinguished in the model (see also 3.5):

- the ebb-tidal delta as a whole;
- the total inner tidal flat area in the basin;
- the total channel volume in the basin;
- the adjacent coast at one side;
- the adjacent coast at the other side.

The morphological development of these elements cannot be considered independent (De Vriend, 1996). For the morphological development of the whole system as well of the individual elements, the interaction between different elements by sediment transport plays an important role. However, it is assumed that the sediment exchanges only occur between the tidal flat and the channel, between the channel and the ebb tidal delta, between the ebb tidal delta and the coasts and between the coasts and the adjacent boundaries (see figure 4.1).

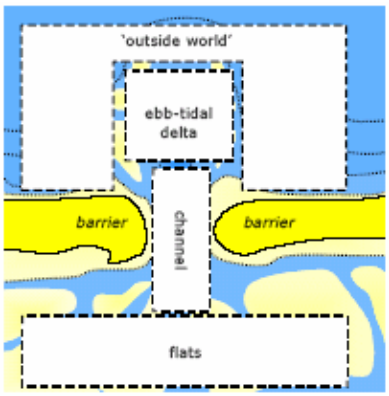

Figure 4.1: Schematisation of elements in ASMITA

Besides these elements, an outside world can be defined, for which an overall equilibrium state can be defined. This outside world compromises the coastal zone surrounding the ebb-tidal delta, which acts as a boundary for the system. An important hypothesis is the unconditionally ability of the outside world to provide sand, which is demanded by the ebb-tidal delta and basin.

The most important hypothesis used in the model concept is that a morphological equilibrium state can be defined for each element depending on the hydrodynamic conditions. The empirical relations between the equilibrium volume (V_e) and the tidal prism (P) are derived on basis of field data. In section 3.6 the empirical relations for the several elements can be found. The equilibrium volume of the elements channel and outer delta is related to the tidal prism:

$$V_{e\_d,c} = f(P) \tag{4.1}$$

while the equilibrium volume of the flats depend on the tidal range (H) and the basin's area (A_b).

$$V_{e\_f} = f(H, A_b) \tag{4.2}$$

If the length of the basin is small compared to the length of the tidal wave, spatial variations in water level may be neglected. The tidal prism may thus be defined by:

$$P = H \cdot A_b - V_f \tag{4.3}$$

In which V_f is the volume of flats between MLW and MHW [m^3].

In ASMITA the evolution of the elements towards a state of equilibrium is described on an aggregated scale, based on certain principles:

- All elements tend to progress towards an equilibrium state, which is defined for all elements.
- If an element is out of equilibrium, the element has a need or surplus of sediment. The amount of need or surplus depends on the extent of the disturbance.
- Whether this need results in sedimentation depends on the availability of sediment, which in turn depends on the sedimentation need of the adjacent elements.

Depending on the need and availability of sediment in the elements, the elements of the tidal inlet system exchange sediment with each other to achieve equilibrium. The exchange of sediment can be within an element or between two adjacent elements. The first process depends on the sediment concentration of the element and the equilibrium sediment concentration of the element. If the sediment concentration of the element is less than its equilibrium concentration, sedimentation occurs. Erosion occurs in the opposite situation. The exchange of sediment between two elements depends on the difference in sediment concentration of these elements. The sediment transport takes place from a high concentration towards a relatively lower concentration.

4.2.1 Equilibrium concentration

A key element in the modelling concept is the equilibrium concentration. When all the elements in the morphological system are in equilibrium a constant sediment concentration is present in the whole system. This constant concentration is called the equilibrium concentration c_E. For each element in the system a local equilibrium sediment concentration c_e is defined such that it is equal to c_E if the element is in morphological equilibrium. When the local equilibrium concentration c_e is larger than the equilibrium concentration c_E tendency of erosion exists. When the local equilibrium concentration c_e is smaller than the equilibrium concentration c_E tendency of accretion exists.

The local equilibrium concentration depends on the actual volume and the equilibrium volume. To represent this behaviour a simple power relation is used for the equilibrium concentrations. For the channel element the relation is:

$$c_{ce} = c_E \cdot \left(\frac{V_{ce}}{V_c} \right)^n \tag{4.4}$$

where:
c_E: overall equilibrium concentration [-]
c_{ce}: equilibrium concentration channel element [-]
V_{ce}: equilibrium volume channel element [-]
V_c: actual volume channel element [-]

The power n in relation 4.4 is larger than one and must commonly taken as 2 in compliance with a third power for the sediment transport as a non-linear function of the mean flow velocity. For the flat element and the ebb tidal delta element, the relation is inverted because for these elements the dry volume of the flat or channel is considered instead of the wet volume of the channel. Thus, for the flat element, the relation is:

$$c_{fe} = c_E \cdot \left(\frac{V_f}{V_{fe}} \right)^n \tag{4.5}$$

For the relation of the ebb-tidal delta, the volumes and concentrations of the flat have to be replaced by those of the ebb tidal delta.

4.2.2 Morphological change

In the case the local sediment concentration deviates from the local equilibrium sediment concentration morphological changes occur. The change in volume of a particular element depends on the availability of sediment in the surrounding elements and the transport capacity between these elements. The availability is assumed proportional to the difference in local equilibrium concentration c_e and the actual concentration c. If the sediment concentration is smaller than its equilibrium value, erosion occurs. When the opposite takes place ($c>c_e$) sedimentation occurs.

Relation 4.6 represents the volume change of the channel element:

$$\frac{dV_c}{dt} = w_s \cdot A_c \cdot (c_{ce} - c_c) \tag{4.6}$$

where:
w_s: vertical exchange coefficient [m/s]
A_c: horizontal area of the channel element [m^2]

Like for the equilibrium concentration, the relation for the change of volume is different for the flat and the ebb tidal delta element. For the flat element the relation is as follow:

$$\frac{dV_f}{dt} = w_s \cdot A_f \cdot (c_f - c_{fe}) \tag{4.7}$$

where A_f is the horizontal area of the flat element.

As mentioned, the sediment exchange between the elements depends on the availability of sediment per element. The amount of sediment in an element, available for transport between the elements depends on the sediment mass balance of the element. The second aspect determining the sediment exchange, the transport capacity depends is related to the hydrodynamic conditions in the inlet system. The transport capacity is determined by the tide and by wind-waves. The tide plays a dominant role in the sediment exchange. Combining the tide induced sediment exchange with an assumed unlimited availability of sediment at the seaward boundary of the system, the long-term tide-induced net exchange between elements takes the character of diffusion, represented by $\delta_{nm.}$

Relations 4.6 till 4.8 reflect the mass-balance for each element. In the formulated mass-balance an increase in volume of all the elements is considered. This implies an increase in water volume and in sand volume for respectively the channel, the flats and the ebb-tidal delta.

For the channel this reads

$$w_s \cdot A_c \cdot (c_{ce} - c_c) = \delta_{fc} \cdot (c_c - c_f) + \delta_{dc} \cdot (c_c - c_d) \tag{4.6}$$

For the flats:

$$w_s \cdot A_f \cdot (c_f - c_{fe}) = \delta_{fc} \cdot (c_c - c_f) \tag{4.7}$$

For the ebb tidal delta:

$$w_s \cdot A_d \cdot (c_d - c_{de}) = \delta_{do} \cdot (c_E - c_d) + \delta_{dc} \cdot (c_c - c_d) \tag{4.8}$$

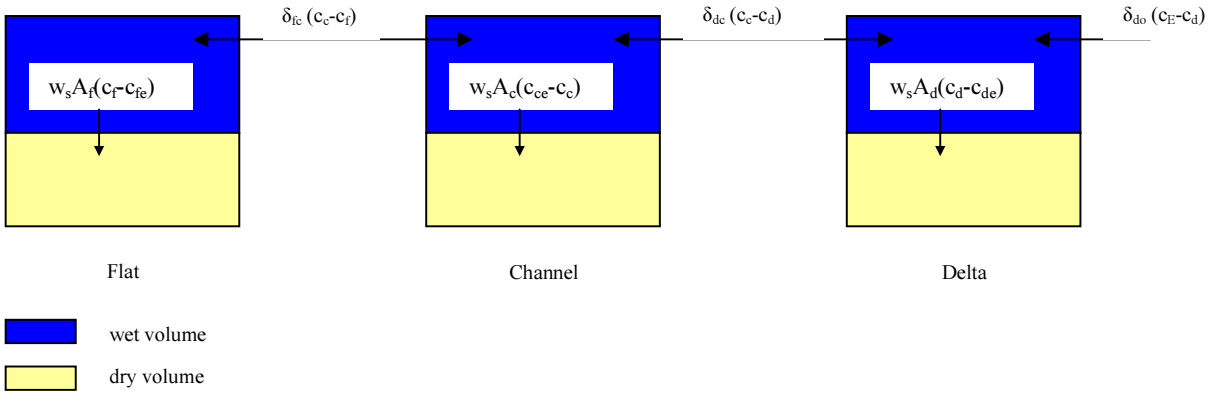

Figure 4.2: Sediment balance of elements in tidal inlet system

5 Delft3D

For this chapter reference is made to the Delft3D-FLOW manual.

5.1 Introduction

In this chapter the Delft3D model is described, based on the Delft3D-FLOW manual. As in this study we are interested in the hydrodynamic consequences caused by a reservoir, only the flow module is used. To prepare the files needed in the Delft3D-FLOW model, additional programs are used. Delft-quickin is used to change the bathymetry at the locations of the reservoir. The post-processing is done with Matlab routines and with Quickplot.

5.2 Theoretical background Delft3D-FLOW

The flow module of the Delft3D model system (Roelvink and Van Banning, 1994) is a multi-dimensional hydrodynamic simulation program which calculates non-steady flow and transport phenomena that result from tidal and meteorological forcing on a rectilinear or curvilinear, boundary fitted grid. Standard features in Delft3D-FLOW are:

- Tidal forcing.
- The effect of the earth's rotation (Coriolis force).
- Advanced turbulence models to account for the vertical turbulent viscosity and diffusivity based on the eddy viscosity concept.
- Time varying sources and sinks (e.g. discharge sluices).
- Robust simulation of drying and flooding of inter-tidal flats.
- Shear stress exerted by the turbulent flow on the bottom.

To make the calculations, the vertical accelerations are assumed to be small compared to the gravitational acceleration and are not taken into account. The momentum equations in x- and y-direction are:

$$\frac{\partial u}{\partial t}+u\frac{\partial u}{\partial x}+v\frac{\partial u}{\partial y}+g\frac{\partial \eta}{\partial x}-fv+\frac{g\cdot u\cdot|U|}{C^2(d+\eta)}-\frac{F_x}{\rho_w(d+\eta)}-K_x\left(\frac{\partial^2 u}{\partial x^2}+\frac{\partial^2 u}{\partial y^2}\right)=0 \qquad (5.1)$$

$$\frac{\partial v}{\partial t}+u\frac{\partial v}{\partial x}+v\frac{\partial v}{\partial y}+g\frac{\partial \eta}{\partial x}+fu+\frac{g\cdot u\cdot|U|}{C^2(d+\eta)}-\frac{F_y}{\rho_w(d+\eta)}-K_y\left(\frac{\partial^2 v}{\partial x^2}+\frac{\partial^2 v}{\partial y^2}\right)=0 \qquad (5.2)$$

(1) (2) (3) (4) (5) (6) (7) (8)

The formulas consist of the following terms:

(1)	Velocity gradient	(6)	Bottom stress
(2)&(3)	Advective terms	(7)	External forces (wind, waves, etc)
(4)	Barotropic pressure gradients	(8)	Viscosity
(5)	Coriolis force		

and the depth-averaged continuity equation is given by:

$$\frac{\partial \eta}{\partial t} + \frac{\partial (d+\eta)u}{\partial x} + \frac{\partial (d+\eta)v}{\partial y} = 0 \tag{5.3}$$

in which:
d: water depth below plane of reference [m]
f: Coriolis paramter [l/s]
$F_{x,y}$: x- and y-component of external forces [N/m^2]
u,v: depth averaged velocity [m/s]
U: absolute magnitude of total velocity, $U=(u^2+v^2)^{1/2}$ [m/s]
C: Chezy coefficient [$m^{1/2}/s$]
ρ_w: mass density of water [kg/m^3]
$K_{x,y}$: diffusion coefficient (eddy viscosity) [m^2/s]
η: water level variation above plane of reference [m]

The 2D-Chézy coefficient C, in the bottom stress term, can be determined with the Chézy, Manning or White Colebrook formulations.

The set of partial differential equations in combination with an appropriate set of initial and boundary conditions for water levels and horizontal velocities is solved on a staggered grid. The equations for the water levels are solved with an Alternating Direction Implicit (ADI) technique (Stelling, 1984). This means that the water levels and velocities in the x-direction are implicitly solved in the first half time step, while in the second time step y becomes the implicit direction for both water level and velocity.

Grid and bathymetry

In a staggered grid as applied in Delft3D-FLOW, not all quantities, such as water level, water depth or velocity components, are defined at the same location in the numerical grid. The water level points are defined in the middle of each cell and the current components are defined on the cell boundaries.

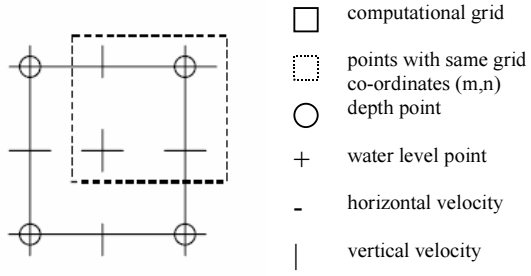

Figure 5.1: Staggered grid of Delft3D-FLOW

The orthogonal curvilinear grid is created using the additional program of Delft3D: Delft-RGFGRID. The advantage of an orthogonal grid is the possibility to create local situated high-resolution areas. Hereby the total number of cells and the computational time are reduced.

To obtain a bathymetry input file another program is needed: Quickin. By using interpolation, the data of sample points is assigned to the grid cells. The bathymetry observations are generally obtained by:

- Digitising bathymetric charts (Admiralty Charts, Fair Sheets).
- Extracting the bottom schematisation of the area to be modelled from the bottom schematisation of an overall coarser hydrodynamic model.
- Using available measurements (echo-soundings).

Initial and boundary conditions

To get a well-posed mathematical problem with a unique solution, a set of initial and boundary conditions for water levels and horizontal velocities must be specified. The contour of the model domain consists of parts along "land-water" lines (river banks, coast lines), which are called closed boundaries. Closed boundaries are natural boundaries. The velocities normal to a closed boundary are set to zero. Open boundaries are always artificial "water-water" boundaries. In a numerical model open boundaries are introduces to restrict the computational area and so the computational effort. They are situated as far as possible from the area of interest. Long waves propagating out of the model area should not be hampered by the open boundaries. The reflection should be minimal.

A large discrepancy between the initial condition and the boundary conditions at the simulation start time can result in short wave disturbances that propagate in the model area. The effects of a discrepancy between the initial condition and the boundary conditions at the start time of the simulation can be substantially reduced by applying a transition period from the initial condition to the actual boundary conditions and determine the intermediate values by a smooth interpolation.

Numerical stability

In Delft3D-FLOW the Courant number is an indication for numerical stability and accuracy. The directives for the Courant number are based on experience. The Courant number for two-dimensional problems is defined as (Stelling, 1984):

$$C = 2 \cdot \Delta t \sqrt{gh\left(\frac{1}{\Delta x^2} + \frac{1}{\Delta y^2}\right)} \tag{5.4}$$

in which:
C: Courant number
Δt: time step [s]
g: acceleration due to gravity [m/s^2]
h: local water depth [m]
Δx: grid mesh size in x-direction [m]
Δy: grid mesh size in y-direction [m]

The Courant number gives the relation between propagation speed and time step. The time step determined the total time needed for the computation. To reduce the total computational time, the

time step has to increase. However, a larger time step could decrease the accuracy and the stability. To define the best time step, the following parameters are important:

- Stability
- Required accuracy
- Size of the smallest grid cell
- Depth
- Available calculation time

5.3 Model description

After Elias E.P.L. et al. (2004).

The Texel Outer Delta (TOD) model application contains the Texel inlet and adjacent coastlines. The Eierlandse Gat and Vlie are included in the model domain to enable the simulation of the important internal residual volume transport between Vlie and Texel inlet (see e.g. Ridderinkhof, 1988). The well-structured orthogonal curvilinear grid has 38311 points, with a maximum resolution (80 * 120 m) at the location of Texel inlet (see figure 5.2). The North-Holland coastline, the landward coastline in the basin, and the island coastlines form closed boundaries. The northern basin periphery is chosen on the Terschelling tidal divide and prescribed as a zero velocity boundary. The open sea boundaries are located "far away" from the area of interest, outside the sphere of influence of Texel inlet and are prescribed as water level elevations.

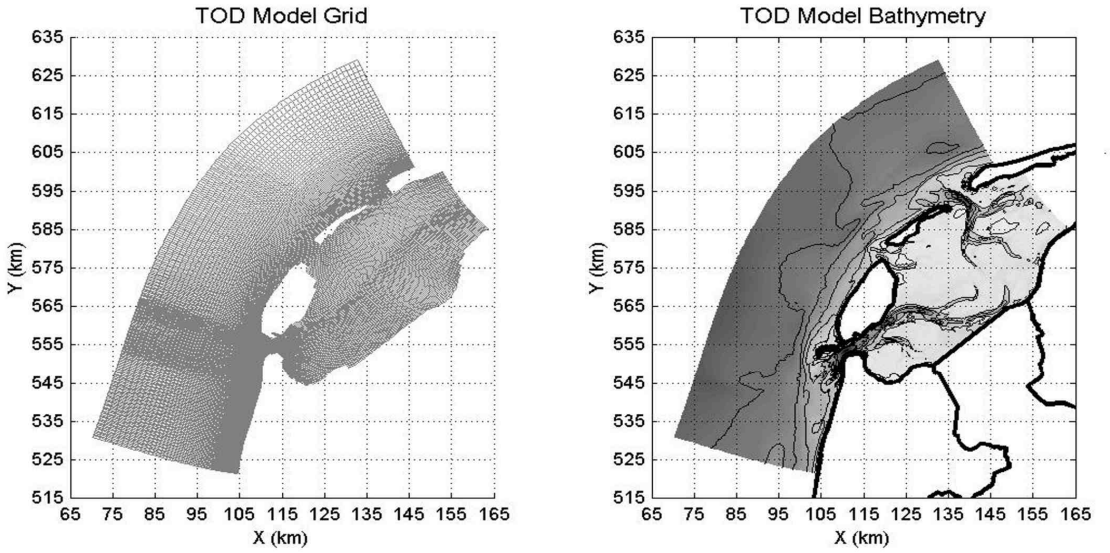

Figure 5.2: Delft3D model grid and bathymetry

The bed topography of the near shore, the inlets and the basin is based on the 1997 bed topography measurements. Depths in deeper region are generated using Dutch Continental Shelf data supplied by TNO-NITG (reference: FIY-LAND). Depth measurements were translated to the curvilinear grid using the Delft3D-Quickin discretiser. For the bottom roughness, a global Chézy coefficient of 61.5 $m^{1/2}/s$ was used. The time step for the flow computations is 60 seconds to fulfil the maximum courant number criterion of 15. Default settings for the uniform horizontal eddy viscosity and eddy diffusivity coefficients have been used of 1.0 m^2/s and 10.0 m^2/s respectively.

Computations start from a uniform water level. A two day spin-up and 60 minutes smoothing time prior to the actual computations is sufficient to dissipate the induces errors due to the discrepancy between boundary conditions and initial state.

To simulate the consequences resulting from the construction of the reservoir, the bathymetry is adapted at the location of the reservoir. The bathymetry at this location is changed to 5 m above the reference level.

Cross sections in the tidal inlets and several main channels provide for each alternative a new value for the ebb and flood volume.

5.4 Validation of model

After Elias E.P.L. et al. (2004).

To prove the validity of the Texel Outer Delta (*TOD*) model for the Texel case, long-term tidal flow through the inlet gorge is modelled and validated against the ADCP measurements.

Averaged over longer periods, e.g. with the exception of extreme storm events, water level variations are the governing forcing for flow in the inlet gorge, as the tidal water level variations are dominant over the non-tidal contributions. The tidally driven *TOD*-model set-up is used to simulate tidal flow through the inlet gorge.

These tidal flow model results provide a good indication of the longer-term flow. Salinity (density driven flow) is not included in the model. Roelvink et al. (2001) show the depth-averaged horizontal flow field not significantly being influenced by horizontal salinity gradients.

Using the tidally driven *TOD*-model set-up, flow through the inlet gorge is simulated over a 6-month period (01-12-1998 / 01-06-1999). The open sea water level boundaries are prescribed by representative harmonic constituents (frequencies, amplitudes and phases) of the water level elevations. The tidal boundary conditions are derived from nesting the TOD model in the larger-scale PROMISE model that describes the tidal movement of the southern North Sea with a realistic tidal height forcing at the northern boundary and in the English Channel (Gerritsen et al. 2001). Time series of simulated water levels are parsed on as a forcing at the nested boundaries. As a first calibration the simulated model output for the Den Helder tidal station was harmonically analysed for water level amplitudes and phases of the main tidal constituents in the same manner as the observed water levels. Main constituents have been selected based on the importance for flow through the inlet (see, Ridderinkhof 1999).

Table 5.1: Amplitudes and phases of water levels of the Texel Tidal station, both observations and model results

Tidal component	Amplitude (m)		Phase (deg)		Tidal component	Amplitude (m)		Phase (deg)	
	Obs	Model	*Obs*	Model		*Obs*	Model	*Obs*	Model
O1	*0.09*	0.09	*98*	97	S2	*0.19*	0.18	*259*	259
K1	*0.05*	0.05	*29*	29	K2	*0.04*	0.05	*130*	134
2N2	*0.02*	0.04	*323*	321	M4	*0.12*	0.12	*79*	78
mu2	*0.08*	0.08	*135*	135	MS4	*0.07*	0.07	*215*	214
N2	*0.10*	0.10	*94*	98	2MN6	*0.03*	0.03	*105*	102
nu2	*0.04*	0.06	*6*	-46	M6	*0.06*	0.06	*134*	137
M2	*0.68*	0.67	*119*	119	2MS6	*0.06*	0.06	*263*	262
L2	*0.06*	0.07	*310*	306					

Small corrections on the amplitudes and phases of the tidal components at the open sea boundaries are made until a good correspondence was observed in measured and modelled amplitudes and phases (Table 5.1).

The second calibration and validation step concerned the representation of the tidal flow through the inlet gorge focusing on the *TESO*-measurements. Time-series of simulated and observed depth-averaged flow and discharges were calculated at seventeen equidistantly distributed aggregation points. For each aggregation point the amplitude of depth-averaged residual velocity (A0), the contribution of the dominant M_2 and its first overtide (M_4) over the period are plotted (Figure 5.3). Results show that the *TOD*-model is able to simulate the tidally driven flow through the inlet accurately.

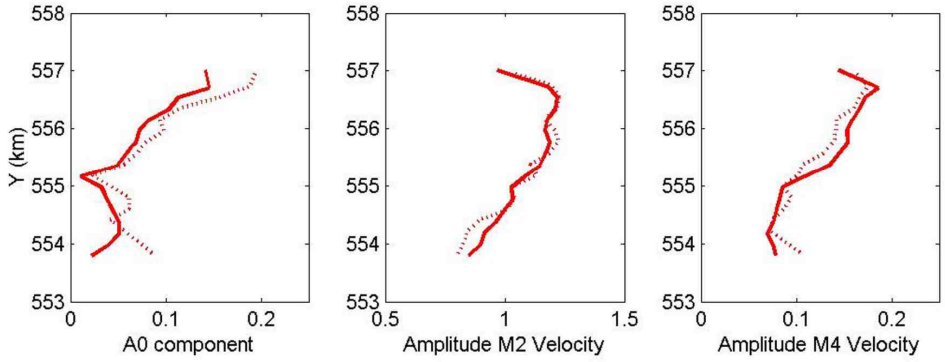

Figure 5.3: Tidally averaged flow constituents based on the TESO measurements (dashed) and model results (solid). Right to left: A0, M_2 and M_4 amplitude of velocity in (m/s)

6 Influence of reservoir on tidal prism basins

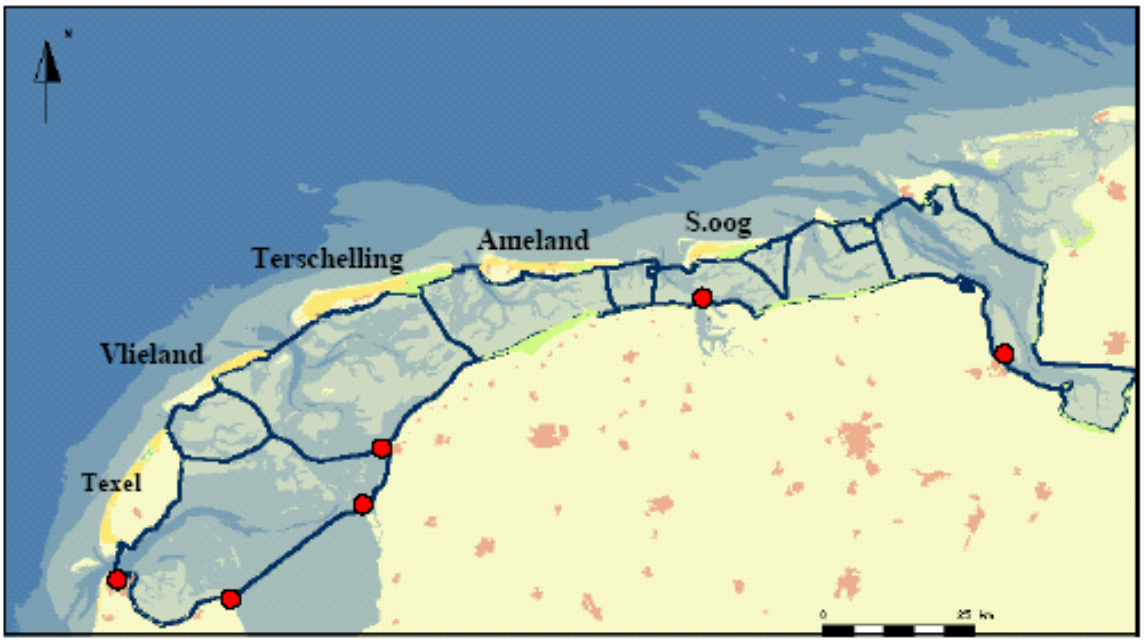

Figure 6.1: Different tidal basins and their tidal divides

6.1 Introduction

In the present study, the morphological effect of constructing a large-scale retention facility in the Wadden Sea is investigated. This structure causes a reduction of the tidal basin area and therefore influences the tidal prism. The morphological consequences of such an intervention depend on the size and location of the intervention. As the dimensions of the reservoir are significant compared to the dimensions of the Wadden Sea tidal basins, a noticeable effect on the morphological evolution in this area is expected. The empirical equations in chapter 3 (section 3.5) illustrate that tidal basin area and tidal prism are related.

The numerical model Delft3D-FLOW (chapter 5) is used to stimulate the effects of the reservoir on the basin hydrodynamics. On basis of the simulated tidal prism through the inlet, an increase or decrease of the tidal basin area can be estimated, assuming equal amplitude of the tidal wave (Eysink, 1992). In chapter 7 changes in location of the tidal divides are discussed. The shift of the tidal divides and the change in tidal prism are important parameters for the definition of the volumetric values of the characteristic elements of the basin (flat, channel and delta). With the new values for the tidal prism, the morphological consequences for the basins, inlets and adjacent coast are calculated with the semi-empirical model ASMITA (chapter 8).

6.2 Tidal prism of western Wadden Sea basins

With the closure of the Zuider Sea, the tidal area was reduced and although a decrease of the tidal prism was expected (see relation 3.8) an increase occurred. The tidal prism increase was due to the changed tidal wave characteristics in the Wadden Sea. After the closure, the length of the

Marsdiep and Vlie basin are short compared to the tidal wave length resulting in a standing wave (chapter 2). To investigate the influence of the reservoirs, it is assumed that the geometric values of the reservoir are too small to influence the tidal wave length. With this assumption a change in tidal prism can only imply a change in tidal basin area. The correctness of this assumption is discussed in section 6.5.

In this section the simulated tidal volumes of the Marsdiep, Eierlandse Gat and Vlie are discussed and compared with measured tidal volumes, in order to get an indication of the validity of the model results.

6.2.1 Marsdiep

After the construction of the Afsluitdijk multiple discharge measurements have been made at the Marsdiep inlet. In table 6.1 some of these data and the results of Delft3D-FLOW are presented.

Based on the values in table 6.1 it can be concluded that the Marsdiep is an ebb dominant basin, meaning a larger volume of water flowing out of the basin at ebb than entering at flood. This ebb surplus is due to the residual flow from the Vlie to Marsdiep (Ridderinkhof, 1988) and due to the discharges of the discharge sluices at Den Oever and Kornwerderzand.

A large variety in ebb and flood volumes is observed, see table 6.1. These variations can partly be explained by different accuracy of measurements, meteorological forcings and possibly different measurement locations. Due to the variations in ebb and flood volumes, the residual volumes through the inlet fluctuates between 0 and -200 Mm^3 per tide except for two field data sets in 1966 and one field data set in 1971 (see figure 6.2). For these three field data sets the residual volume is positive meaning flood dominance; most likely due to a period with strong western wind preceding the measurement. The dotted line in figure 6.2 represents the residual volume modelled by Delft3D-FLOW.

Model results are in the range of the measured volumes (10% deviation) and for the purpose of this research the model results are satisfying enough for the simulation of hydrodynamic consequences caused by an intervention like the reservoir.

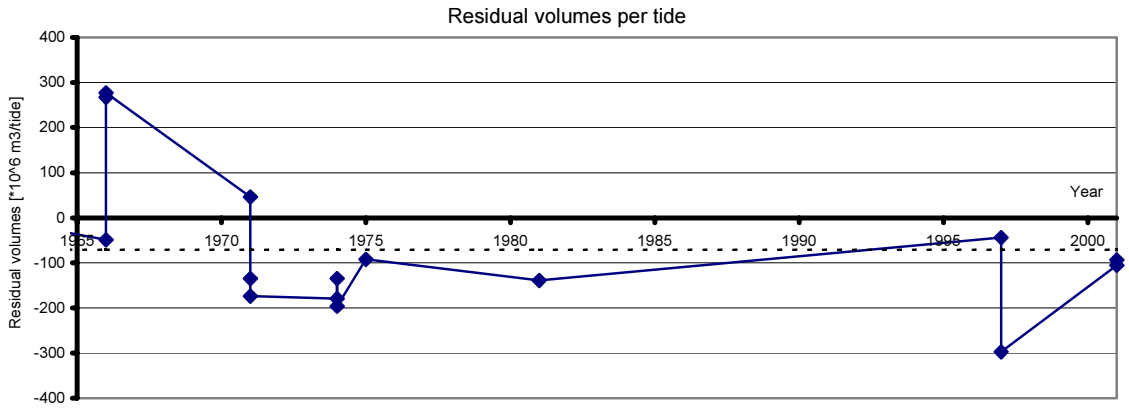

Figure 6.2: Residual volumes [m^3/tide] through the Marsdiep inlet

Table 6.1: Ebb and Flood volumes Marsdiep

	Flood volume (10^6 m^3/tide)	Ebb volume (10^6 m^3/tide)
Endema, 1979 (measurements between 1951 and 1971)	925	1005
Rakhorst, 2004 (corrected measurement 1959)	945.6	912
De Reus, 1980 (measurement 1966)	1052	1101
Rakhorst, 2004 (corrected measurement 1966)	1110	843
Rakhorst, 2004 (corrected measurement 1966)	1137	860
Rakhorst, 2004 (corrected measurement 1971)	1159	1113
Rakhorst, 2004 (corrected measurement 1971)	948	1083
Rakhorst, 2004 (corrected measurement 1971)	942	1116
Rakhorst, 2004 (corrected measurement 1974)	811	1060
Rakhorst, 2004 (corrected measurement 1974)	590	725
De Reus, 1980 (measurement 1974)	896	1092
De Reus, 1980 (measurement 1975)	953	1045
De Blok et al., 2001 (measurement 1981)	910	1049
De Blok et al., 2001 (measurement 1997)	904	948
Rakhorst, 2004 (corrected measurement 1997)	787.1	1084.4
De Blok et al., 2001 (measurement 2001)	1010	1115
Rakhorst, 2004 (corrected measurement 2001)	899.4	992.9
Simulation Delft3D-FLOW	1025	1096

6.2.2 Eierlandse Gat basin

In table 6.2 the ebb and flood volumes through the Eierlandse Gat inlet are shown. There is also a large variation in the data. Figure 6.3 and 6.4 show the ebb and flood volumes of obtained by measurements and the result of Delft3D-FLOW (dotted line). The dotted line is situated between the measured values. The difference between the measured data and the model results is the direction of the residual flow. For most of the measured date the basin is flood dominant, while the model shows ebb dominance.

Table 6.2: Ebb and Flood volumes Eierlandse Gat

	Flood volume (10^6 m^3/tide)	Ebb volume (10^6 m^3/tide)
Endema, 1979 (measurements between 1951 en 1971)	165	130
Studiedienst Hoorn, date is unknown	138	142
Rakhorst, 2004 (corrected measurement 1948)	150	141
Rakhorst, 2004 (corrected measurement 1971)	202.4	174.3
Rakhorst, 2004 (corrected measurement 1971)	180.2	172.1
Rakhorst, 2004 (corrected measurement 1971)	185	178.5
Rakhorst, 2004 (corrected measurement 1979)	239.5	260.9
Rakhorst, 2004 (corrected measurement 1979)	184	180
Rakhorst, 2004 (corrected measurement 1980)	256.5	235.7
Rakhorst, 2004 (corrected measurement 1980)	230.5	213.8
Rakhorst, 2004 (corrected measurement 1996)	244.4	221.5
Simulation Delft3D-FLOW	192	210

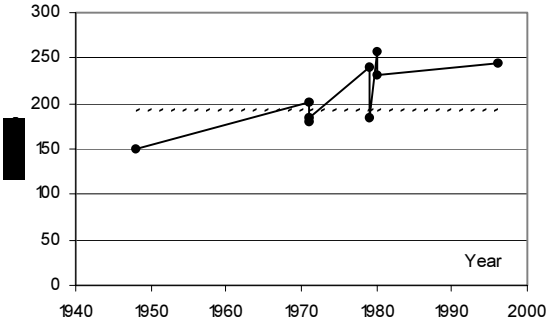

Figure 6.3: Flood volumes through Eierlandse Gat

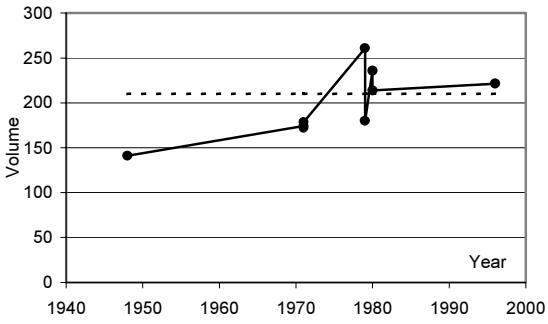

Figure 6.4: Ebb volumes through Eierlandse Gat

6.2.3 Vlie basin

Compared to the Marsdiep and Eierlandse Gat less data is available, but with the data obtained from publications can be seen that the model results correspond quite well to the measured volumes.

From table 6.3 can be seen that the Vlie basin is a flood dominant basin. This flood dominance corresponds with the through flow from the Vlie towards the Marsdiep basin, as is mentioned in section 6.2.1.

Table 6.3: Ebb and Flood volumes Vlie

	Flood volume (10^6 m^3/tide)	Ebb volume (10^6 m^3/tide)
Endema, 1979 (measurements between 1951 en 1971)	885	810
Studiedienst Hoorn, date is unknown	832	791
Rakhorst, 2004 (mean values)	1088.8	1076
Simulation Delft3D-FLOW	892	848

6.2.4 Conclusion

In table 6.1 till 6.3 can be seen that the values for ebb and flood volumes through the inlets show large variations. The variety in ebb and flood volumes of the several inlets can partly be explained by different accuracy of measurements and meteorological forcings.

As the used Delft3D-FLOW model has been calibrated on the Marsdiep inlet and basin, the model results of the Marsdiep inlet should be comparable with the measured ebb and flood values. Indeed, comparing the model results and the measured ebb and flood values, we see comparable values for the measured and modelled ebb and flood volumes.

The model results of the Vlie inlet are comparable with the measured volume (less than 10% deviation), while the model has not been calibrated on the Vlie inlet. The good correspondence is most likely due to the through flow from the Vlie towards Marsdiep basin.

For the Eierlandse Gat such a connection with the Marsdiep is not present and the match between the model results and the measured data is less. Therefore the results obtained for the Eierlandse Gat basin should be interpreted with caution.

As for this study we are interested in the hydrodynamic change due to an intervention, we are interested in the relative change in ebb and flood volumes compared to the current situation. In spite of the fact that differences are present between the model results and the measured values, a further calibration is thus not necessary.

6.3 Reservoir alternatives

To investigate the hydrodynamic and morphodynamic influence of an intervention like the construction of a retention facility, several locations have been investigated. The AD alternative cut off one or two channels (the Doove Balg and the Scheurrak), while the other two alternatives, KZ and LW, are located between channels.

6.3.1 Alternative AD (AD1, AD2 and AD3)

The reservoirs of alternative AD are attached to the Afsluitdijk between the sluices in Den Oever and Kornwerderzand. The largest reservoir does not only cut off the Doove Balg, but also the Scheurrak. The surface area of the reservoir is 180 km^2, which corresponds to 1/4th of the total Marsdiep basin area. The surface of the second reservoir AD2 is about 120 km^2 and corresponds to 1/6th of the total Marsdiep basin area. The smallest reservoir AD3 has a surface of 90 km^2, which corresponds to 1/8th of the Marsdiep basin area.

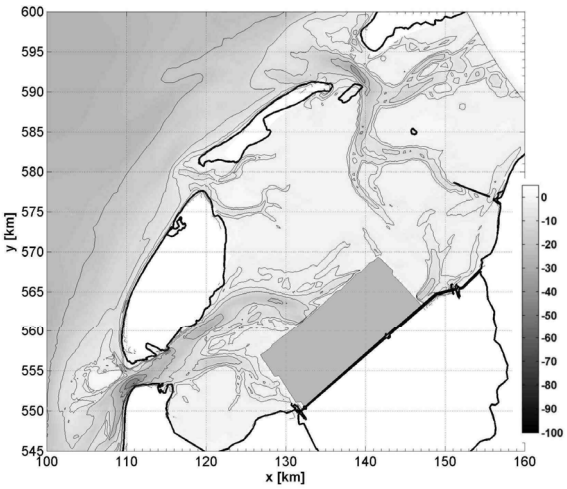

Figure 6.5: Reservoir AD1

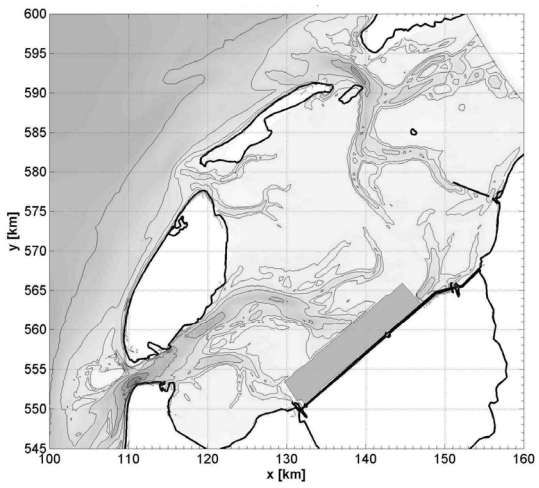

Figure 6.6: Reservoir AD3

6.3.2 Alternative KZ (KZ1 and KZ2)

Alternative KZ is situated between two channels, the Inschot and the Blauwe Slenk. The KZ reservoir is mostly situated in the Vlie basin, however a part is situated in the Marsdiep basin. The largest reservoir (120 km^2) is as large as the reservoir could be, without cutting off one of the surrounding channels.

The other reservoir has a surface area of 90 km2. Due to the same surfaces as the AD alternative, the influence of cutting off can be inquired. The surface areas of the reservoirs are respectively 1/6th and 1/8th of the Vlie basin's surface.

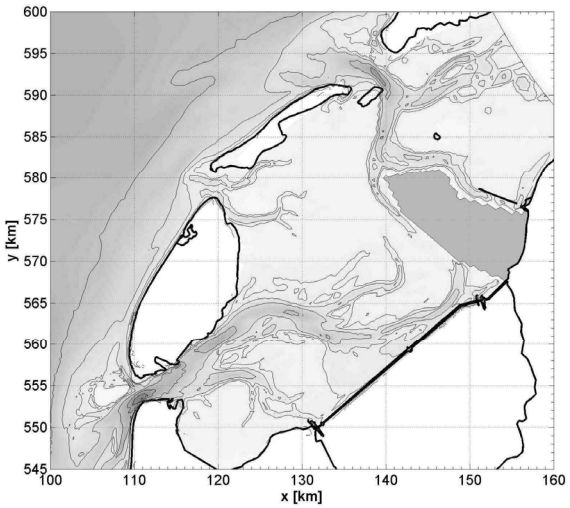

Figure 6.7: Reservoir KZ1

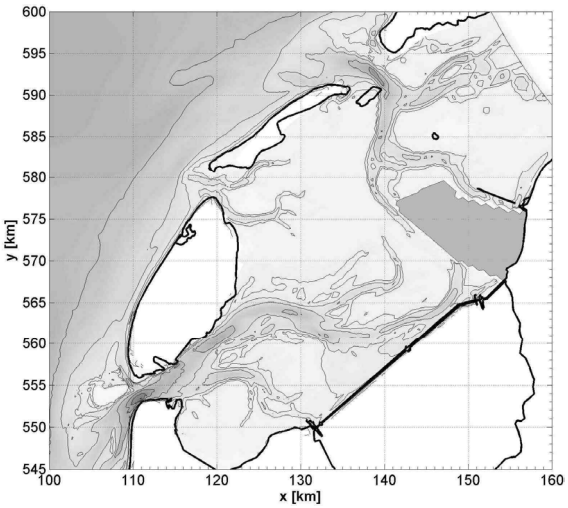

Figure 6.8: Reservoir KZ2

6.3.3 Alternative LW (LW1 and LW2)

Approximately the same as for alternative KZ holds for the LW alternatives. The surrounding channels are the Texelstroom and the Malzwin. The largest reservoir LW1 is 120 km^2, while the other one is 90 km^2.

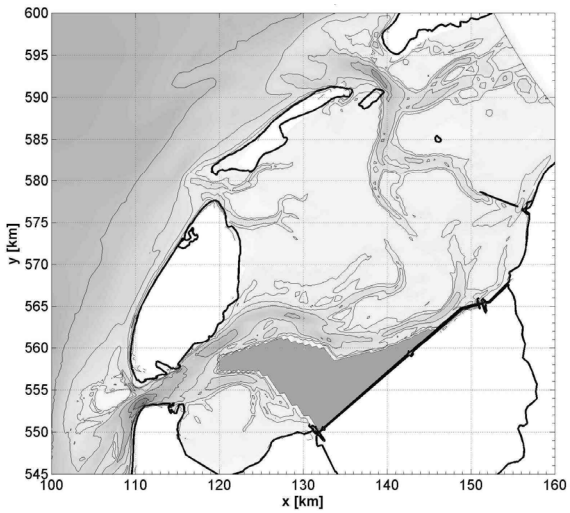

Figure 6.9: Reservoir LW1

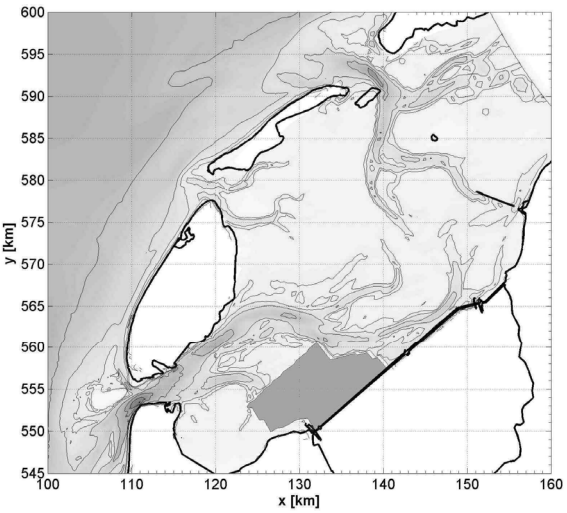

Figure 6.10: Reservoir LW2

6.4 Results

In this section an interpretation is given of the hydrodynamic changes due to constructing the reservoir. For each alternative, the change in tidal volume through the inlets and the change in the through flow from the Vlie to Marsdiep basin, the Vlie current, is explained. Based on equation 3.8, we assume that the basin area is related to the tidal volume, if the tidal range remains unchanged. The correctness of the assumed unchanged tidal range is subject of section 6.5.

As described in section 6.3, the alternatives differ from each other by the location of the reservoirs. Not only a difference in basin (Marsdiep or Vlie) is made, but also a difference between flat and channel areas is made. The last distinction is made to investigate the consequences induced by cutting off channels, as is the case for alternative AD. In appendix A the residual discharges in the current situation and after the construction of a reservoir are presented.

6.4.1 Alternative AD

Due to the construction of the reservoir a decrease of the Marsdiep tidal volume is expected. The model results in table 6.4, figure 6.11 and figure 6.12 confirm this expectation. The reduction in ebb volume is larger than the reduction in flood volume. The stronger reduction in ebb volume is due to the decreased through flow from Vlie to Marsdiep inlet. The affected Vlie current also results in a decreased flood volume flowing through the Vlie inlet.

The tidal volume of the Eierlandse Gat remains practically unchanged (a small decrease).

Table 6.4: Ebb- and flood volumes of alternative AD

	Flood volume (10^6 m^3/tide)				Ebb volume (10^6 m^3/tide)			
Tidal basin	Present	AD1	AD2	AD3	Present	AD1	AD2	AD3
Marsdiep	1025	756	845	899	1096	758	869	925
Eierlandse Gat	192	166	175	178	210	196	201	203
Vlie	892	832	849	853	848	845	843	847

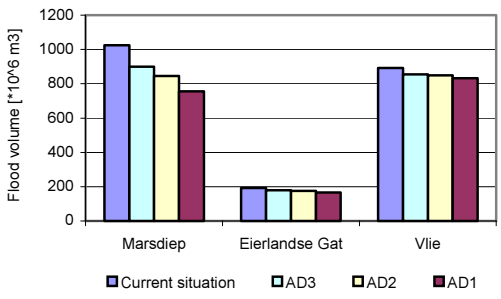

Figure 6.11: Flood volumes per tide through tidal inlet [$*10^6$ m^3], alternative AD

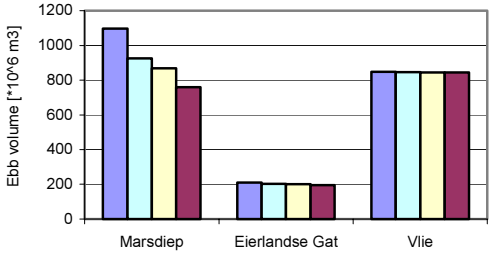

Figure 6.12: Ebb volumes per tide through tidal inlet [$*10^6$ m^3], alternative AD

6.4.3 Alternative KZ

Separating the tidal volume of the Marsdiep in ebb and flood volumes, an increase in flood volume is seen, while the ebb volume stays unchanged. An increase in flood volume does not correspond with the relation between tidal volume and tidal basin area (relation 3.8). Two possibilities are conceivable and the first concerns the tidal divide between the Marsdiep and the Vlie. Because this tidal divide is not as clearly defined as other tidal divides, it is possible that the KZ reservoir is completely situated in the Vlie basin and will therefore not diminish the tidal volume of the Marsdiep. Still, a different location of the tidal divide does not explain the increase in flood volumes through the Marsdiep inlet, after the human intervention. Due to the diminished through flow from the Vlie to the Marsdiep, the tidal current from the Vlie towards the Marsdiep becomes less. The tidal current in the Marsdiep basin experiences less resistance and the flood volume therefore increases. It is possible that the increase in tidal current is such that the reduction of the tidal volume due to the intervention is negligible. However, if the reservoir would be partly in the Marsdiep basin, the ebb volume would have shown a reduction.

If we consider the Vlie basin, the decrease in ebb volume corresponds with the reduction of the basin area caused by the reservoir.

Like for alternative AD, the tidal volume of the Eierlandse Gat basin remains practically unchanged.

Table 6.5: Ebb- and flood volumes of alternative KZ

	Flood volume (10^6 m^3/tide)			Ebb volume (10^6 m^3/tide)		
Tidal basin	Present	KZ1	KZ2	Present	KZ1	KZ2
Marsdiep	1025	1054	1053	1096	1097	1095
Eierlandse Gat	192	183	184	210	215	216
Vlie	892	835	854	848	802	823

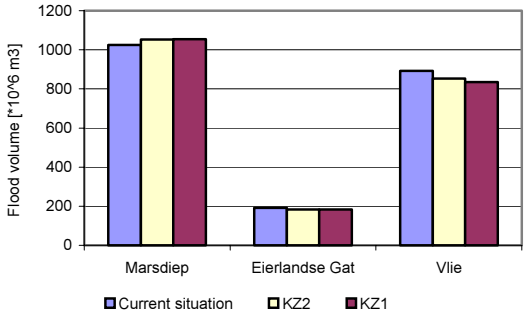

Figure 6.13: Flood volume per tide through tidal inlet [*10^6 m^3], alternative KZ

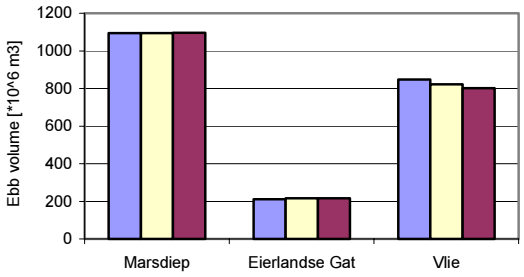

Figure 6.14: Ebb volumes per tide through tidal inlet [*10^6 m^3], alternative KZ

6.4.4 Alternative LW

The tidal volume of the Marsdiep inlet decreases due to the construction of the reservoir, as relation 3.8 implies. The decrease in ebb volumes is of the same order as the decrease in flood volumes, which implies an undisturbed through flow from the Vlie to the Marsdiep inlet.

The tidal volume of the Vlie mainly retains its ebb- and flood discharges and confirms that the Vlie current is not affected by reservoir LW.

Similar to the Vlie basin, the Eierlandse Gat mainly retains its tidal volume.

Table 6.6: Ebb- and flood volumes of alternative LW

	Flood volume (10^6 m^3/tide)			Ebb volume (10^6 m^3/tide)		
Tidal basin	Present	LW1	LW2	Present	LW1	LW2
Marsdiep	1025	848	892	1096	913	957
Eierlandse Gat	192	189	188	210	209	209
Vlie	892	887	884	848	847	843

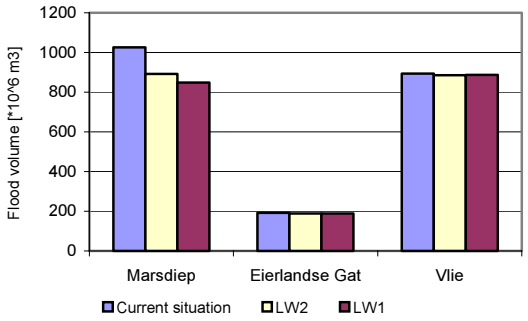

Figure 6.15: Flood volume per tide through tidal inlet [$*10^6$ m^3], alternative LW

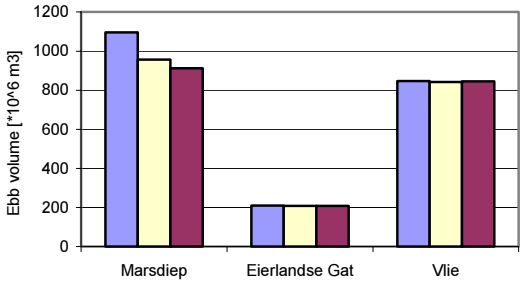

Figure 6.16: Ebb volume per tide through tidal inlet [$*10^6$ m^3], alternative LW

6.5 Tidal wave envelope

To verify the assumed constant tidal range (section 6.2) in this section study is done to the alteration of the tidal wave to the construction of the reservoir. For the modification of the tidal wave, the variation in M_2, M_4 and a0 component and in the form of the tidal wave envelope is studied. Change in the form of a tidal wave envelope causes alteration in the wave propagation, while change in the M_2 and M_4 components result in an increase or decrease in amplitude of the tidal wave. In appendix C, plots of the variation in the M_2 component and of the tidal range in several points are presented. The M_4 plots show the same results as the M_2 component, but have smaller values. The a0 component mainly shows an increase where the M_2 shows a decrease.

6.5.1 Influence of reservoir on tidal wave envelope, inlets

Marsdiep basin

Due to the construction of the AD reservoir the tidal wave envelope in the Marsdiep inlet shows both a change in form and in amplitude. The magnitude of the increased amplitude corresponds with the magnitude of the increased M_2 component. As a result of the changed tidal wave propagation high water is reached earlier, as can be seen in Figure C.8

In Figure C.9 can be seen that the KZ reservoir does not affect the propagation of the tidal wave. However, the amplitude of the tidal wave increases

The alteration in tidal wave envelope due to the LW reservoir is comparable with the alterations due to the AD reservoir. Both reservoirs cause increased amplitude and changed wave propagation, though the magnitude of the alteration due to the LW reservoir is less.

Eierlandse Gat

The magnitude of change in the tidal wave envelope in the Eierlandse Gat basin is less than in the Marsdiep basin. The construction of the AD reservoir affects both the propagation of the tidal wave in the basin as well as the amplitude of the tidal wave through the Eierlandse Gat basin (see figure C.11).

After the construction of the KZ and LW reservoir the propagation of the tidal wave remains unchanged. The amplitudes show a slight increase.

Vlie basin

Due to the construction of the reservoirs only the amplitude of the tidal wave envelope is affected. The M_2 component decreases for the AD reservoirs, while it increases for the KZ alternative. The LW alternative does not influence the M_2 component of the tidal wave.

6.5.2 Influence of reservoir on tidal wave envelope, discharge sluices

Due to the construction of the AD alternative the tidal range at the discharge sluices in Den Oever is considerably affected (see figure C.17). In Kornwerderzand on the other hand the mainly the ebb amplitude of the tidal wave diminishes, but the form of the wave remains the same. Alternative LW shows the same development of the tidal divide after the construction of the reservoir. The KZ reservoir does barely affect the tidal wave in both locations. The main reason for the larger influence of the reservoirs in Den Oever than in Kornwerderzand is due to the location of the reservoir. Because the reservoir is constructed near to the Den Oever sluices, the tidal wave enters a region where the wave will be reflected and distorted. The distance between the sluices in Kornwerderzand and the reservoir is larger, resulting in less influence of the reservoir on the tidal wave.

6.5.3 Conclusion

Considering the figures presenting the change in M_2 and the tidal range before and after the construction of the reservoir, the deviations in amplitude of reservoir KZ and LW are less than 10 percent of the original value. The AD alternative shows areas where the deviation is close to or slightly more than 10 percent.

6.6 Conclusion

In this chapter the influence of a reservoir on the tidal prism of a basin is investigated. Model results are according Eysink's relation between the tidal prism and the tidal basins area: constructing a reservoir in a basin results in a smaller tidal basin and thus a smaller tidal prism.

By constructing the AD reservoir in the Marsdiep basin, not only the Marsdiep's tidal volume is affected but, as a result of the affected through flow from the Vlie towards the Marsdiep basin (the Vlie current), the tidal volume of the Vlie basin is affected too.

The KZ reservoir, in the Vlie basin and near the tidal divide between the Vlie and Marsdiep basin, also influences the tidal volume of both the Vlie and Marsdiep basin. The tidal volume of the Marsdiep basin enlarges due to the reduced Vlie current.

The only alternative that mainly influences its own basin is the LW alternative. Like the AD reservoir the LW reservoir is constructed in the Marsdiep basin, however, the LW basin does not cut off the Doove Balg or other important channels. Because of this the Vlie current is not disturbed and the Vlie basin is not affected. The expectation that cutting off channels will influence the hydrodynamics of the concerning basin and possibly adjacent basins is therefore confirmed by the results of the model.

With the model results the flow direction of the Vlie current (the through flow from the Vlie basin to the Marsdiep basin) is deduced. Because cutting off the Doove Balg largely influences the Vlie current, and because constructing the KZ reservoir slightly influences the Vlie current, it is expected that the Vlie current enters the Vlie basin by the inlet and flows through the Vlie and Inschot towards the Marsdiep basin. To reach the Marsdiep inlet, the Vlie current flows through the Doove Balg and the Texelstroom.

The assumption made about the tidal range staying unchanged after the human intervention, seems to be applicable for the alternatives KZ and LW. For the AD alternative, this assumption is possibly not completely correct. However, for the further research of this study the assumption will be kept.

Note:
Due to the closure of the Zuider Sea, the Marsdiep basin became small compared to the tidal wave and a more or less standing wave was formed, resulting in an increased tidal prism of the Marsdiep basin (chapter 2). Till now, the Marsdiep basin is still not in equilibrium. By constructing a reservoir in this basin, the surface area reduces and the Marsdiep basin will be closer to its equilibrium. However, it is shown that a large human intervention can have hydrodynamic consequences for the adjacent basins and that a good research has to be done to find a good location for such an intervention. Based on the hydrodynamic consequences for the several basins in the Western Wadden Sea, the LW alternative seems to be the best.

7 Influence of reservoir on tidal divides

7.1 Introduction

In the previous chapter the reservoir induced tidal volume change in the inlets is studied. In the basin where the reservoir is constructed, the tidal volume decreases, as was predicted using Eysink's (1991) relation. The reservoir also influences the flow patterns in the basin. Changes in the flow induce displacements of the tidal divides. As a result the surface area and the related tidal prism in the adjacent basins are also influenced.

The displacement of the tidal divides is characterised by (1) the amount of displacement and (2) the location of displacement. We assume that the tidal prism change only induces a basin area alteration (section 7.2), while the tidal range remains constant. Based on this assumption, in this chapter, an estimation of the tidal divide displacement is given (section 7.3, 7.4 and 7.5).

To estimate the location of the displacements, the behaviour of the basins channels before and the expected behaviour after the intervention are compared. The expected behaviour is predicted by an expert judgement based analysis of e.g. channel flow. When the tidal prism entering a tidal basin decreases, the tidal prism through the channel decreases as well and the area reached by the concerned channel reduces. (In appendix A the values of the channel's tidal volume for the different alternatives are given.) We have to rely on interpretation as we have only computed hydrodynamics. In reality due to the dynamic character of the Wadden Sea, morphological alteration of the channels occurs and the tidal volumes of the channels will deviate from the modelled volumes.

In the following sections we focus on four tidal divide locations (see figures 7.1, 7.2 and 7.3). The first tidal divide, at location A, is situated between the Eierlandse Gat and the Vlie basin. The channels Keteldiep, Robbengat, Vlie and Inschot influence this tidal divide. The tidal divide at location B is situated between the Marsdiep and Vlie basin, near the Scheurrak and the downstream part of the Inschot. The third location, C, is located between Marsdiep and Eierlandse Gat and is influenced by the Keteldiep, Texelstroom and Scheurrak channels. Location D is situated between the Marsdiep and Vlie basin, in the vicinity of the Doove Balg, the downstream part of the Inschot and the downstream part of the Blauwe Slenk.

With these tidal divide displacements, new values for the geometric parameters of the basin are calculated. These new values are used as input parameters for ASMITA to predict the long-term morphological effect caused by the AD, KZ and LW reservoirs. The long-term morphological effect of the reservoir is described in chapter 8.

7.2 Change in tidal basin surface area

As explained in the introduction, the amount of displacement of the tidal divides is based on the change in tidal volume flowing through the inlet of the concerning basin. Because an exact displacement at each tidal divide location is not necessary for the prediction of the long-term development (chapter 8) and because it is complicated to estimate the exact amount of displacement per tidal divide, only a total change in tidal basin area is determined. The change in tidal volumes and in basin areas is given in table 7.1, 7.2 and 7.3.

Table 7.1: Change in basin area for alternative AD

Alternative	Tidal basin	Change in tidal volume [%]	Change in basin area [%]
AD1	Marsdiep	- 28.6%	- 28.6%
	Eierlandse Gat	- 10%	- 10%
	Vlie	- 3.6%	- 3.6%
AD2	Marsdiep	- 19.2%	- 19.2%
	Eierlandse Gat	- 6.6%	- 6.6%
	Vlie	- 2.75%	- 2.75%
AD3	Marsdiep	- 14%	- 14%
	Eierlandse Gat	- 5.3%	- 5.3%
	Vlie	- 2.3%	- 2.3%

Table 7.2: Change in basin area for alternative KZ

Alternative	Tidal basin	Change in tidal volume [%]	Change in basin area [%]
KZ1	Marsdiep	+ 1.4%	+ 1.4%
	Eierlandse Gat	- 0.9%	- 0.9%
	Vlie	- 6%	- 6%
KZ2	Marsdiep	+ 1.3%	+ 1.3%
	Eierlandse Gat	- 0.6%	- 0.6%
	Vlie	- 3.7%	- 3.7%

Table 7.3: Change in basin area for alternative LW

Alternative	Tidal basin	Change in tidal volume [%]	Change in basin area [%]
LW1	Marsdiep	- 17%	- 17%
	Eierlandse Gat	- 1.1%	- 1.1%
	Vlie	- 0.4%	- 0.4%
LW2	Marsdiep	- 12.9%	- 12.9%
	Eierlandse Gat	- 1.3%	- 1.3%
	Vlie	- 0.7%	- 0.7%

7.3 Alternative AD

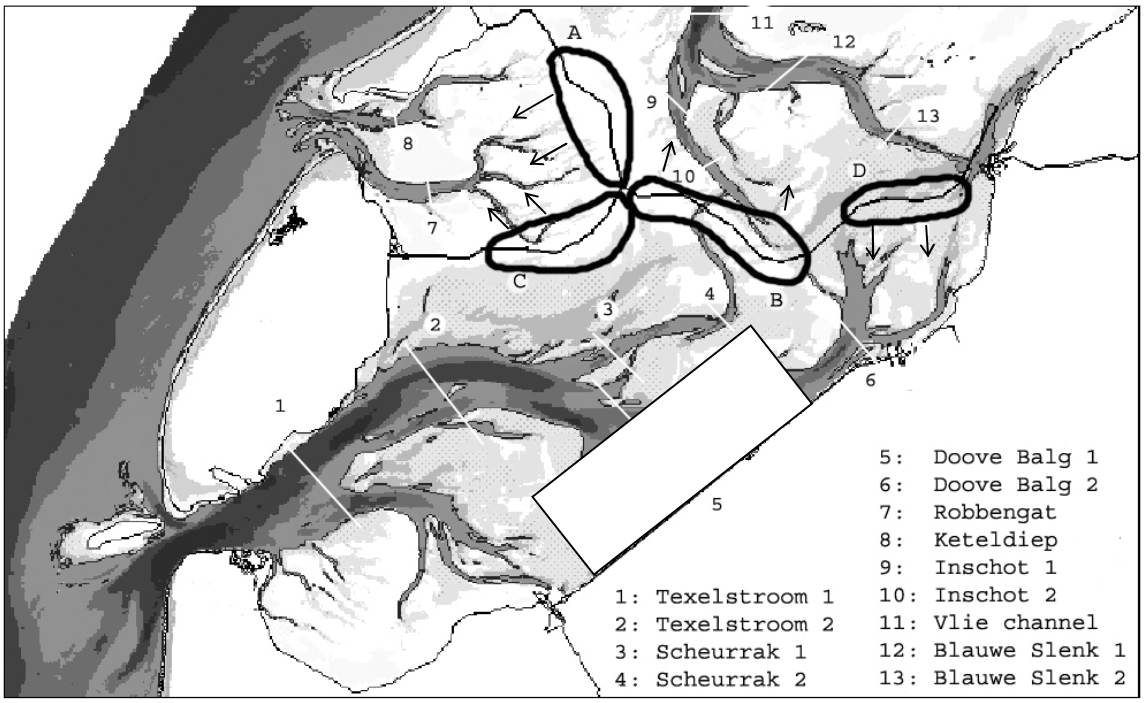

Figure 7.1: Location of possible change in tidal divides for alternative AD

Before the construction of the AD reservoir, the main flow path of the Vlie current is through the Inschot into the Doove Balg. Due to the construction of the reservoir, the Doove Balg is cut off and the through flow is affected. Immediately after construction the downstream part of the Inschot reduces as a result of the reduced flood volume (due to affected Vlie current), while the tidal prism of the Scheurrak increases. This increase is a result of the changed flow pattern in the Marsdiep basin, caused by the cut off Doove Balg. Plausibly, a connection will be formed from Vlie to Marsdiep basin through Inschot and Scheurrak.

Based on the discharges through several channels (see figure 7.1) directly after construction of the reservoir and based on the probable development of the channels, the estimated displacement of the tidal divides is:

Location A

The reduction of the tidal prism through the Eierlandse Gat implies a reduction of both the Robbengat as Keteldiep tidal volumes. This reduction in tidal volume induces a displacement of the tidal divide in the direction of the Eierlandse Gat inlet.

Location B

Considering the development of the Scheurrak directly after the construction of the reservoir and the expected development, the displacement of the tidal divide is in the direction of the Vlie inlet.

Location C

Due to the northwards displacement of the main flow in the Marsdiep basin, the tidal divide probably shifts in the direction of the Eierlandse Gat inlet. The reduction of the Robbengat's tidal volume confirms this displacement.

Location D

As a result of the constructed reservoir the tidal flow entering the Marsdiep is not able to reach the downstream part of the Doove Balg. The Blauwe Slenk and the Inschot push the tidal divide at location D southwards, into the Marsdiep basin.

7.4 Alternative KZ

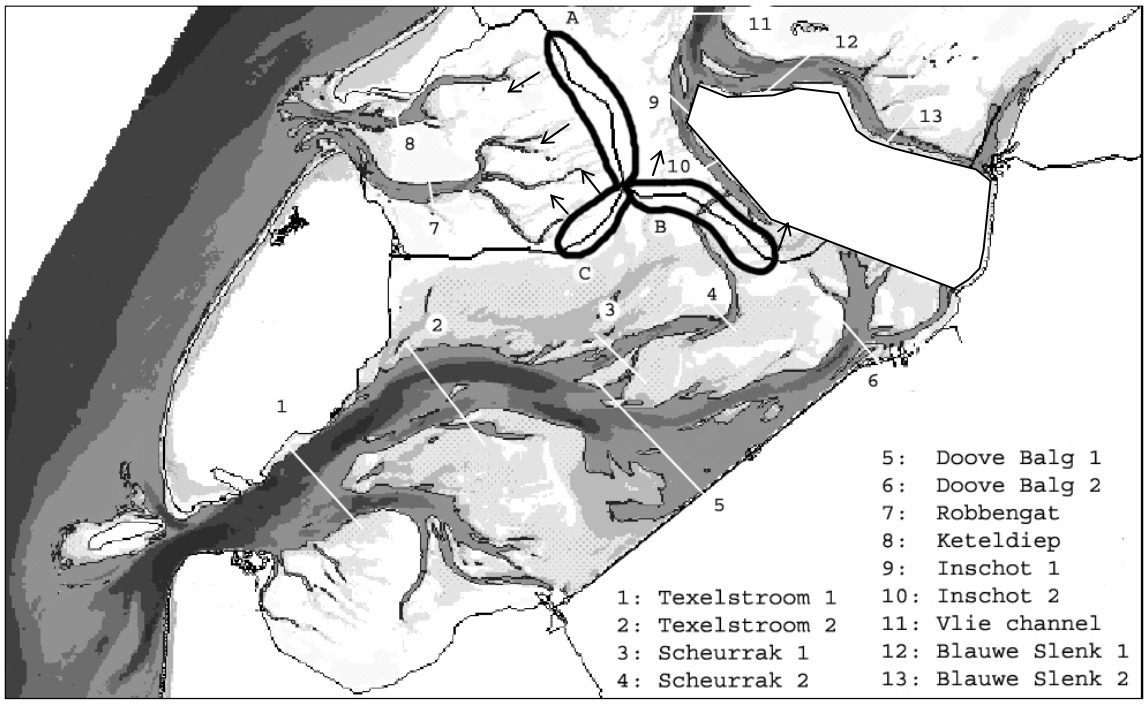

Figure 7.2: Location of possible change in tidal divides for alternative KZ

The KZ reservoir is located on the tidal divide between the Vlie and Marsdiep basin, on the Kornwerderzand flat. Because the reservoir doesn't close off the Inschot or Doove Balg, it is expected that the Vlie current is not affected by the reservoir. However, model results for the Vlie inlet show a larger reduction in ebb volume than in flood volume, indicating that the through flow is disturbed (chapter 6).

Since channels are likely to adapt themselves to the altered situation the Vlie current probably recovers. It is difficult to estimate whether the flow path of the Vlie current develops from the Inschot towards the Doove Balg or towards the Scheurrak. Another possible scenario is the development of the Blauwe Slenk at the cost of the Inschot, resulting in a disappearance of the through flow between the Vlie and Marsdiep basin. As a consequence, the interaction between the Marsdiep and Vlie basin ends and two separate systems develop.

Location A

After the construction of the reservoir the tidal prism of the Eierlandse Gat decreases, resulting in decreased tidal volumes of the Robbengat and Keteldiep. As a result the Vlie channel pushes the tidal divide at location A inwards the Eierlandse Gat basin.

Location B

Both the Inschot and the Scheurrak channels near location B decrease in ebb and flood volume. However, the increased tidal volume of the Marsdiep basin indicates an enlargement of the Marsdiep basin area resulting in a displacement of this tidal divide inwards the Vlie basin. This displacement is larger when the Vlie current disappears.

Location C

It is expected that the tidal divide at location C shifts inwards the Eierlandse Gat as a result of a decreased tidal volume of the Robbengat as well as an increased tidal volume of the Marsdiep basin. When the reduction of the Eierlandse Gat surface area (due to the displacement of the tidal divide at location A) is larger than the reduction in tidal prism, the tidal divide at location C probably shift in the opposite direction: inwards the Marsdiep basin.

7.5 Alternative LW

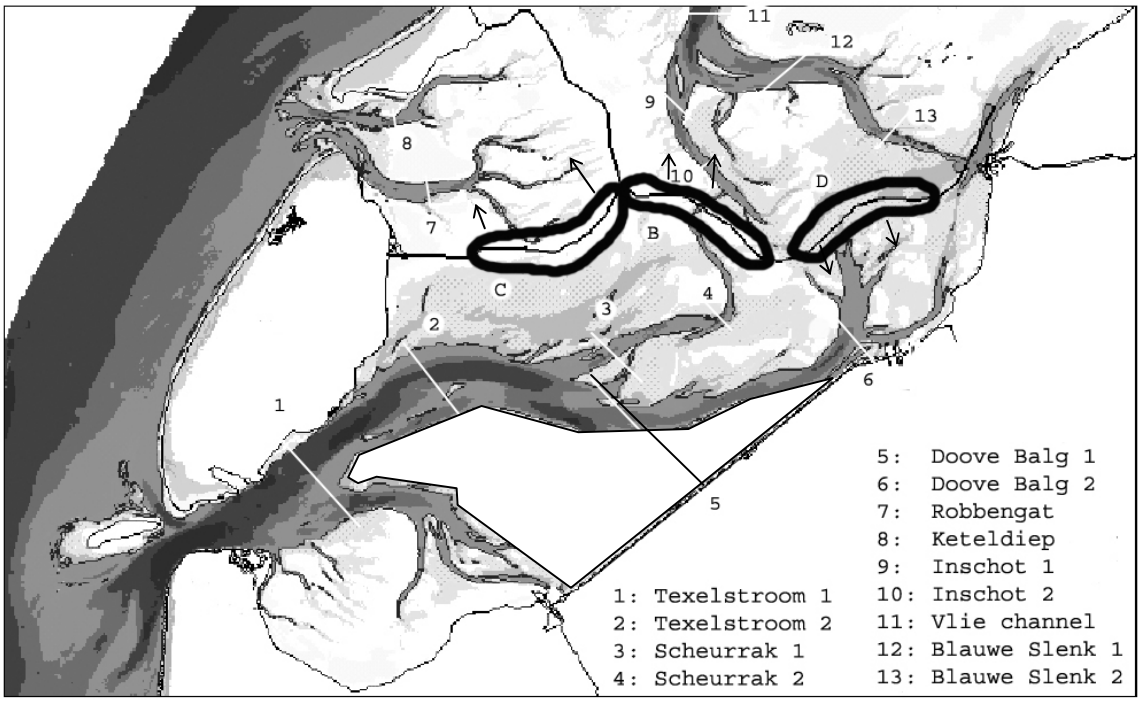

Figure 7.3: Location of possible change in tidal divides for alternative LW

The LW reservoir is located on the Lutjeswaard flat, enclosed by the Malzwin, the Texelstroom and the Afsluitdijk. In contrast to LW1 reservoir, LW2 reservoir partly closes off the Malzwin. Interpreting the simulations, the smallest reservoir LW2 has a stronger influence on the channels and on the tidal prism of both the Eierlandse Gat as the Vlie basin, than the larger LW1 reservoir. The slightly different form of the LW2 reservoir resulting in a partly closed off Malzwin, is probably the main reasons for the bigger influence of the LW2 reservoir (chapter 6).

The probable displacement of the tidal divides is determined with the discharges through channels (see figure 7.3) directly after construction of the reservoir and with the probable (long-term) development of the channels:

Location B

Directly after the construction of the reservoir the tidal volume of the Scheurrak increases. The increase of the Scheurrak's tidal volume is due to the occupation of the Lutjeswaard by reservoir LW, resulting in a different flow pattern. The increased pressure from the Scheurrak causes a displacement of the tidal divide in the direction of the Vlie basin.

Location C

At this location, the tidal divide will probably move in westward direction, inwards the Eierlandse Gat basin. The displacement in this direction is caused by the decreased tidal volume of the Eierlandse Gat basin and the northwards displacement of the Marsdiep main flow.

Location D

Due to the construction of reservoir LW, the tidal flow is not able to pass the Lutjeswaard flat resulting in a decrease of the Doove Balg's tidal volume. However, the tidal volumes of the Inschot and Blauwe Slenk decrease too, due to the reduction of the Vlie basin's tidal prism. Based on these two developments and based on the southwards displacement of the tidal divide at location B, it is expected that the tidal divide at location D displaces inwards the Marsdiep basin.

7.6 Conclusion

Due to construction of the reservoir the tidal prism of the basin in which this reservoir is constructed decreases. Changed flow patterns in the basin with reservoir induce displacements of tidal divides, resulting in area reduction of the adjacent basins and thus a diminution of their tidal prisms. An exception is made for the Marsdiep basin after construction of the KZ reservoir (see chapter 6).

To predict the location of the displacement, the behaviour of the channels before and after the construction is investigated. Due to the dynamic character of the Wadden Sea, morphological alteration of the channels occurs and the tidal volumes of the channels will deviate from the modelled volumes. To estimate the behaviour of the channels both tidal volumes as well as expected long-term development of the channels is used. We focussed on four different tidal divide locations: location A between the Eierlandse Gat and the Vlie basin, location B between the Marsdiep and Vlie basin, location C between the Marsdiep and Eierlandse Gat basin and location D between the Marsdiep and the Vlie basin.

The tidal prism of the Eierlandse Gat decreases for all the alternatives. The latter results in a displacement of the tidal divide at location A and location C inwards the Eierlandse Gat basin for all alternatives, except for alternative KZ. Due to the KZ reservoir the direction of the tidal divide displacement at location C depends on the amount of the tidal divide displacement at location B. At location B, the tidal divide moves inwards the Vlie basin for all alternatives. The tidal divide at location D is displacing towards the Marsdiep basin for alternative AD and alternative LW.

8 Influence of reservoir on development tidal basins

8.1 Introduction

To predict the long-term morphological development of the western Wadden Sea after the construction of a reservoir, the ASMITA model and data of Biegel (1993), Eysink (1993) and Kragtwijk (2001), are used. The ASMITA model needs several input parameters such as volumetric values (volume and area) for the characteristic elements of the tidal inlet (flat, channel and delta) and parameters expressing the sediment transport capability. Because these sediment transport parameters are empirical determined and difficult to estimate, for this study we assumed that the sediment exchange capability between elements remains unchanged. The values for these sediment transport capability parameters are derived from previous studies such as Buijsman (1997) and Van Goor (2001).

In chapter 7, a decrease in the surface area for the basin with reservoir as well as for the adjacent basins is observed. The decrease in the adjacent basins is caused by the displacement of tidal divides. For both the basin with reservoir as well as for the adjacent basins, the intervention results in new volumetric values for the elements. To predict the long-term morphological development after the intervention, these new volumetric parameters must be determined. The determination of these new parameters is done in Appendix D.

In this chapter, the development of the tidal basins after the intervention is modelled and discussed. To understand the influence of the reservoir on the morphological development of the western Wadden Sea the development after the intervention is compared with the development in the present situation (CS), without sea level rise. In order to scale the consequences of the reservoir to the consequences induced by natural forcing like sea level rise, the development of the western Wadden Sea is modelled including the most probable sea level rise of 17 cm/century (Van Goor, 2001) as well (CS + SLR).

8.2 Development of elements tidal inlet system

The ASMITA model distinguishes several elements of the tidal inlet system: channels, flats and the delta. Each element strives for equilibrium. Only when all elements are in equilibrium, the system is in equilibrium too. The equilibrium volume for the elements mainly depends on the tidal prism (see equilibrium relations in chapter 3). In appendix E, the development of the several elements (for all the alternatives) towards equilibrium is presented, expressed in the deviation of the element from equilibrium state (in volume) and expressed in the cumulative sediment import for each element needed to achieve the equilibrium state. The development of the basins in the current situation is explained in section 8.2.1, 8.2.2 and 8.2.3.

The equilibrium degree of the tidal system can also be expressed in terms of system time scales (Kragtwijk, 2001). The magnitude of these system time-scales is determined by inlet geometry and sediment exchange processes. The smallest time scale dominates the initial development. When the initial development damps out, only the response of the largest time-scale remains.

The development of the elements modelled with ASMITA is in accordance with the results of Kragtwijk (2001). However, the values of the equilibrium volumes differ. The tidal prism used in this study is modelled with Delft3D-FLOW. These modelled tidal prisms differ from the tidal

prism used by Kragtwijk (2001) explaining the different values for the equilibrium volumes of the elements.

8.2.1 Development of Marsdiep basin

Based on the sediment demand in the current situation (CS), without sea level rise, of the elements in the Marsdiep basin, we conclude that this basin is currently not in equilibrium. Apparently, the basin is not fully adapted to the altered situation after the construction of the Afsluitdijk. Due to the construction of the Afsluitdijk the tidal prism through the Marsdiep inlet increased and the remaining shoal area of the Marsdiep basin became too small relative to the area of channels (see chapter 2). Based on the increased tidal prism it is expected that the volumes for the channel and delta elements increase. On the other hand, as the relative depth of the Marsdiep increased after the closure, not only an increase in flat volume is expected but also a decrease in (wet) channel volume. In figure 8.1 we observe a sediment demand for all elements. Apparently, the increase of the channel volume caused by the construction of the Afsluitdijk has been larger than the tidal prism increase.

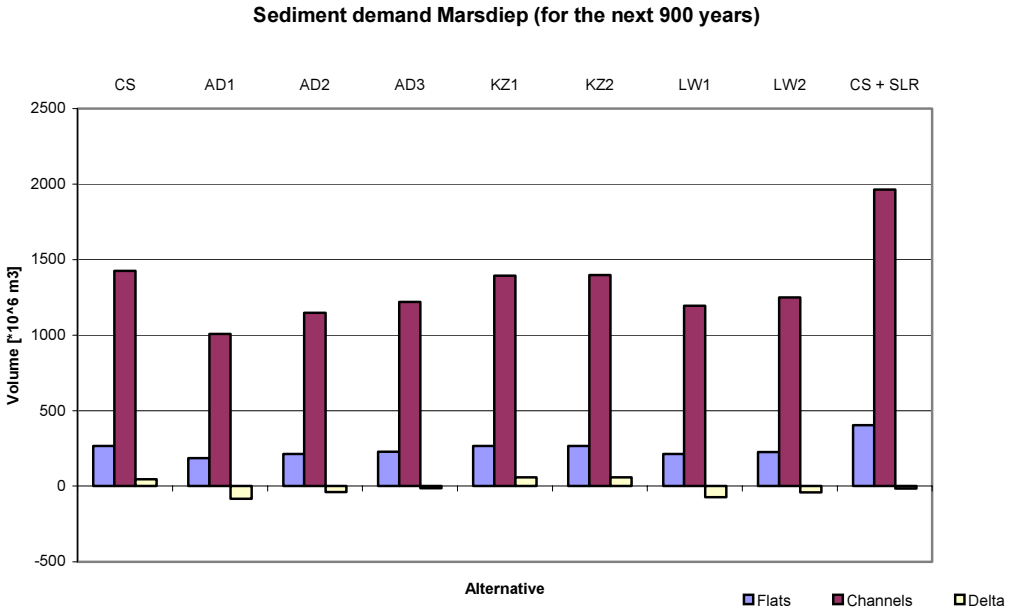

Figure 8.1: Sediment demand elements Marsdiep basin

The elements in the Marsdiep basin have different system time scales: two in the order of decades and one in the order of centuries. Moreover, the flat and delta elements show a bump in their development to equilibrium (figure E.2 and E.4). This indicates that these elements initially develop away from their equilibrium to the benefit of the channels.

Due to the construction of a reservoir in the Marsdiep basin, (alternatives AD and LW) the channel and flat area, and the tidal prism are reduced. As a result, the tidal inlet system is closer to its equilibrium as can be seen in table 8.1, where the adaptation time towards equilibrium is presented for the several alternatives. The development of the elements towards the equilibrium remains the same as it is in the current situation (compare figures in appendix E). The only

alternative that slightly elongates the adaptation time of the basin is the KZ reservoir. This is a consequence of the enlarged basin area (by the increased tidal prism, see chapter 6) causing a larger gap between the situation after human intervention and the corresponding equilibrium situation.

In figure 8.1, the sediment demand of each element of the Marsdiep basin is reflected. Due to the construction of reservoir AD and LW, the increase in flat volume and the decrease in channel volume are diminished in the Marsdiep basin. This is explained by the reduction of the basin area due to the reservoir. Because the channel area in reservoir AD and LW are comparable and because a mean channel depth (appendix D) has been used, comparable channel volumes for these reservoirs are obtained. As a result, the sediment demand for the channel element in the AD and LW alterative are similar. The increase in delta volume changes to a decrease in delta volume for the AD and LW alternative. Considering the net sediment balance, the sediment demand from the outside world and the adjacent coasts decreases for alternatives AD en LW. The sediment demand for alternative KZ shows a slight decrease, caused by the smaller reduction of the channel volume.

Due to the most probable scenario of sea level rise (17cm/century), the system needs more sediment from the outside world than in the situation without sea level rise. Interpretation of figure 8.1 for the current situation with sea level rise suggests a decrease in sediment demand for the delta element. However, figure 8.1 represents the sediment demand for the coming 900 years and since the system (with SLR) is not in equilibrium after 900 years (figure E.121), the figure is not the sediment demand needed for equilibrium (contrary to the other alternatives).

Table 8.1: System time scales of Marsdiep for the various alternatives [in years]

CS	AD1	AD2	AD3	KZ1	KZ2	LW1	LW2	CS + SLR
180	137	152	160	184	184	142	151	380
30	23	26	27	30	30	26	27	27
46	36	39	41	47	47	37	40	40

8.2.2 Development of Eierlandse Gat basin

Like the Marsdiep basin, the Eierlandse Gat basin is not in equilibrium in the current situation (CS). However, due to both a smaller basin area and a smaller influence of the Zuider Sea closure, compared to the Marsdiep and Vlie basin, the Eierlandse Gat has a smaller adaptation time than the other two basins. In the development towards equilibrium, all elements show an asymptotic development as can be seen in figure E.6, E.7 and E.8. To reach the equilibrium state the flat element shows an increase in volume, while both the delta and the channel elements show a decrease in volume. The sediment demand for the increase in flat volume and for the decrease in channel volume is less than the sediment obtained by the decrease of the delta volume, resulting in sediment transport to the outside world.

Considering the adaptation time of the Eierlandse Gat basin after the construction of a reservoir in one of the adjacent basins (Vlie or Marsdiep), the results obtained with ASMITA show a shorter adaptation time for all the reservoirs. In addition, for all alternatives the net sediment surplus of the basin decreases, while the reduction of the delta volume increases. The decrease in sediment surplus is caused by an increase in sediment demand of the channel element (due to decreased tidal prism) and of the flat element (due to displacement of tidal divides, on the shallow areas). The AD alternatives have the largest consequences, probably due to the northwards displacement of the Texelstroom and Scheurrak caused by the blocked Doove Balg and Scheurrak (see chapter 6).

The evolution of the Eierlandse Gat basin towards equilibrium with a sea level rise of 17 cm per century (but without reservoir) has a longer adaptation time than without sea level rise. As expected, the sediment demand of the channel and flat element increases. The increased sediment demand of the channel and flat element results in a reduction of the basins sediment surplus.

Table 8.2: System time scales of Eierlandse Gat for the various alternatives [in years]

CS	AD1	AD2	AD3	KZ1	KZ2	LW1	LW2	CS + SLR
36	31	32	33	35	35	35	35	40
12	11	11	11	12	12	12	11	11
21	18	19	19	21	21	21	20	21

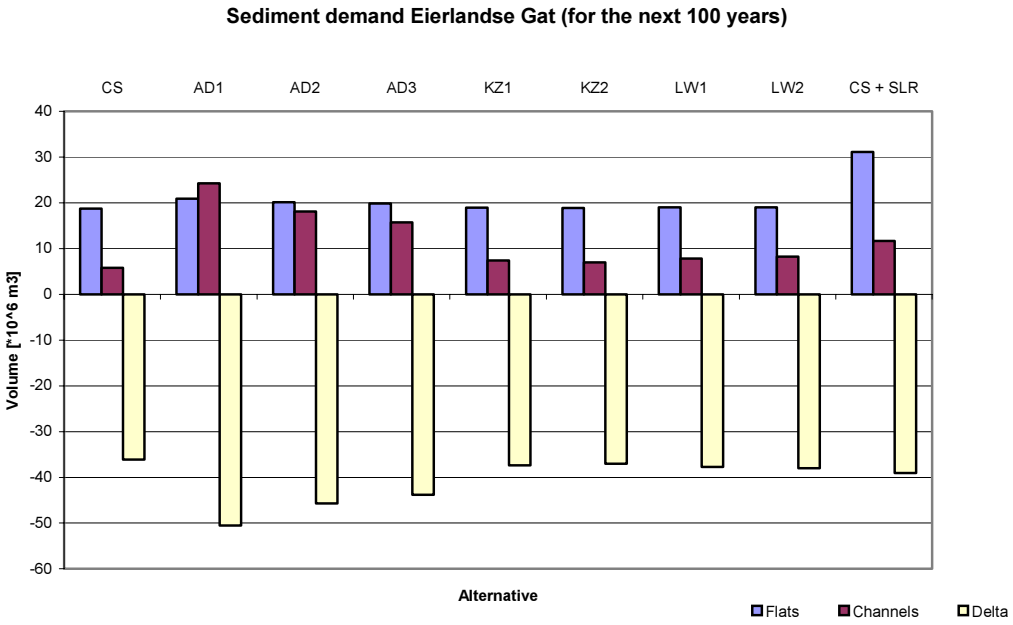

Figure 8.2: Sediment demand elements Eierlandse Gat basin

8.2.3 Development of Vlie basin

Just like the other concerned basins, the Vlie basin is not in equilibrium yet. With ASMITA the development of the elements in the basin for the current situation (without SLR) are modelled. Results show that the elements are currently close to their equilibrium state. However, as can be seen in figure E.13, the development of the channel element towards equilibrium first moves away from its equilibrium to provide sediment to the adjacent elements (flats and delta). Due to the development of the channel, the adaptation time for the total inlet system is in the order of centuries.

Constructing a reservoir, either in the Marsdiep as in the Vlie basin, diminishes the adaptation time of all elements in the tidal inlet system. Due to the construction of the KZ reservoir the tidal prism of the basin diminishes resulting in a decreased sediment demand of the delta element and

an increased sediment demand of the channel element. The reduction in surface area results in a decreased sediment demand for the flat element.

Less increase in volume for the delta element and a larger decrease in volume of the channel element is the consequence of reduction of the tidal prisms (chapter 6). For the KZ alternative, the decrease in channel volume is also due to the disturbed through flow from the Vlie to the Marsdiep basin. The latter is supported by the larger decrease in channel volume for the AD alternative, where the through flow is nearly completely blocked.

Due to the construction of the KZ reservoir, the initial volumes of the channel and flat elements and the tidal prism are reduced. A consequence of these volumetric and hydrodynamic changes is that the basin is closer to equilibrium. This can be seen in table 8.3, were the adaptation times of the basin are presented.

For the other alternatives, (AD and LW) it holds that the system time scales of the basin are slightly smaller than those in the current situation. However, this does not mean that the total amount of sediment needed to reach the equilibrium state is less than in the current situation.

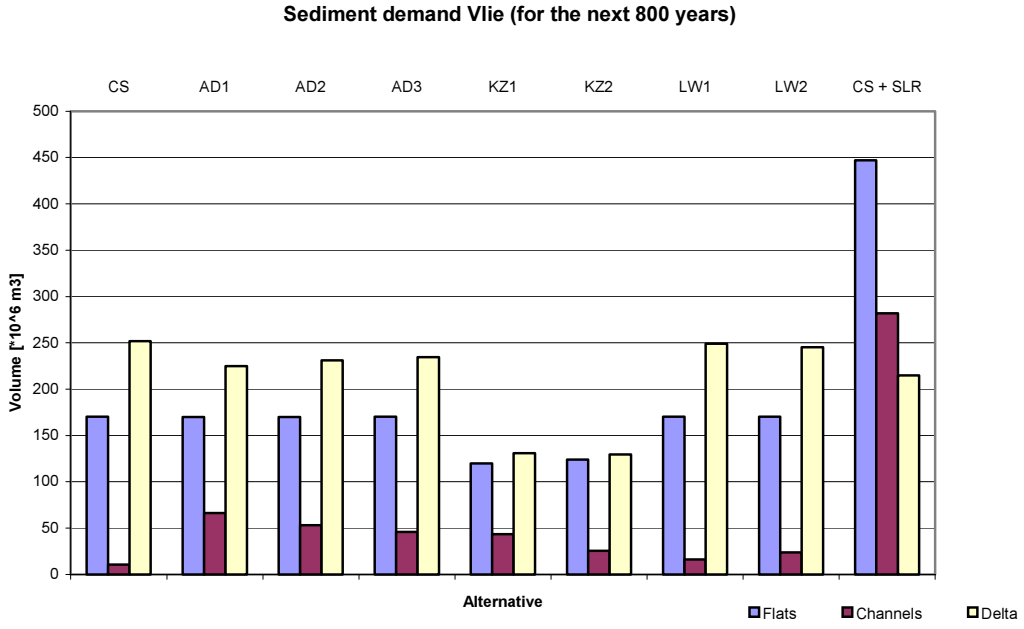

Figure 8.3: Sediment demand elements Vlie basin

For the development of the basin with sea level rise, a larger amount of sediment is needed than in the current situation (see figure 8.3). The increase in sediment demand seems to be larger than for the Marsdiep basin. However, the scale of the figure is different and the Vlie basin is closer to equilibrium than the Marsdiep basin in the current situation.

Table 8.3: System time scales of Vlie for the various alternatives [in years]

CS	AD1	AD2	AD3	KZ1	KZ2	LW1	LW2	CS + SLR
157	148	150	152	113	119	157	155	276
25	24	24	25	21	22	25	25	21
44	42	43	43	32	34	44	44	41

8.3 Sensitivity analysis

For the derivation of the volumetric values of the characteristic elements of the tidal inlet system, the main parameter is the tidal prism. With the new values of the elements, the development of the basins after construction of the reservoir is modelled. This means that the results of both the change in geometric parameters as well as the future development of the Wadden Sea basins are dependent of the results of Delft3D-FLOW. In fact, the tidal prism is the only link between the process-based Delft3D-FLOW and the semi-empirical ASMITA model. If the value of the tidal prism, given by the Delft3D-FLOW model is overestimated or underestimated, the volumetric values of the several tidal inlet elements are over - or underestimated too. Therefore, a sensitivity analysis has been carried out for the tidal prism. Two different cases are studied: a case where the tidal prism is 10% overestimated for the basin with reservoir (basin p, appendix D) and a case were the tidal prism is 10% overestimated for one of the basins without reservoir, adjacent to basin p (basin n/m, appendix D). This distinction has been made because the volumetric values of the characteristic elements in basin p depend on the new geometric values of basin n and m (due to tidal divide displacements). The calculation method is explained in appendix D.

The tidal prism, in the above cases, can be overestimated either in all the three basins either in one basin. Results obtained during the sensitivity analysis showed a minor difference (1%) between these two situations. For the sensitivity analysis in this chapter, the tidal prism is overestimated in one basin.

Overestimation of 10 percent in basin n/m

The volumetric values of the characteristic elements in basin n/m are directly related to the tidal prism and calculated by means of the (equilibrium) relations described in chapter 3 (see appendix D). The overestimation of the volumetric parameters is proportional to the power of the tidal prism in the applied (equilibrium) relations. In figure 8.4, the overestimation of the elements due to a 10 percent overestimation of the tidal prism is presented.

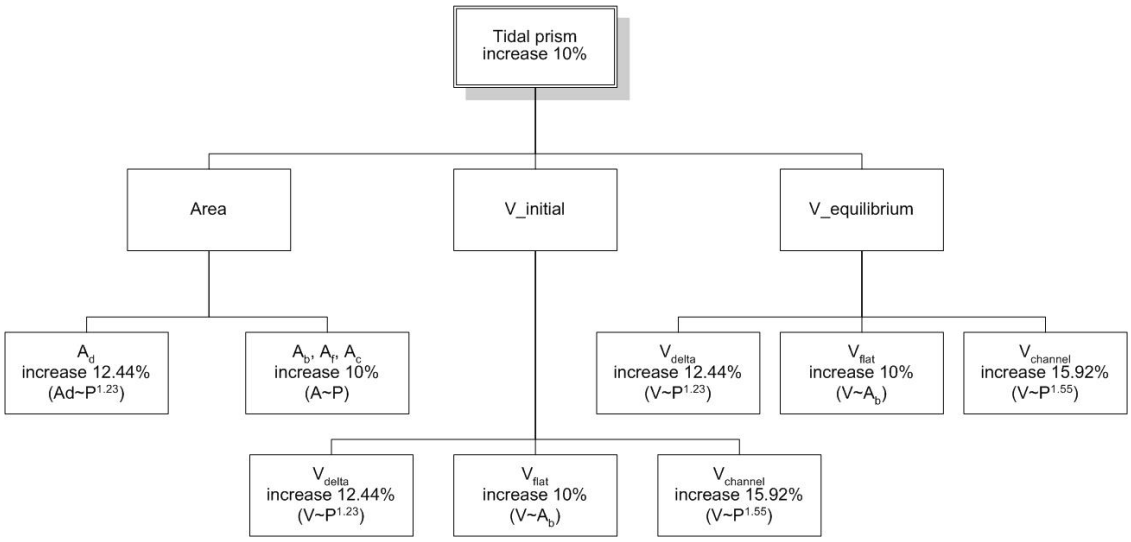

Figure 8.4: Overestimation of volumetric parameters in basin n/m due to overestimation of tidal prism basin n/m

Overestimation of 10 percent in basin p

If the tidal prism in basin p is overestimated, the consequences are different than in the first case. The volumetric parameters of the tidal inlet system are still dependent on the tidal prism. However, these parameters are also dependent on the volumetric values of the constructed reservoir. These values are fixed and independent of the tidal prism.

In figure 8.5 and in figure 8.6, the averaged overestimation of the volumetric parameters for the Marsdiep and Vlie are presented.

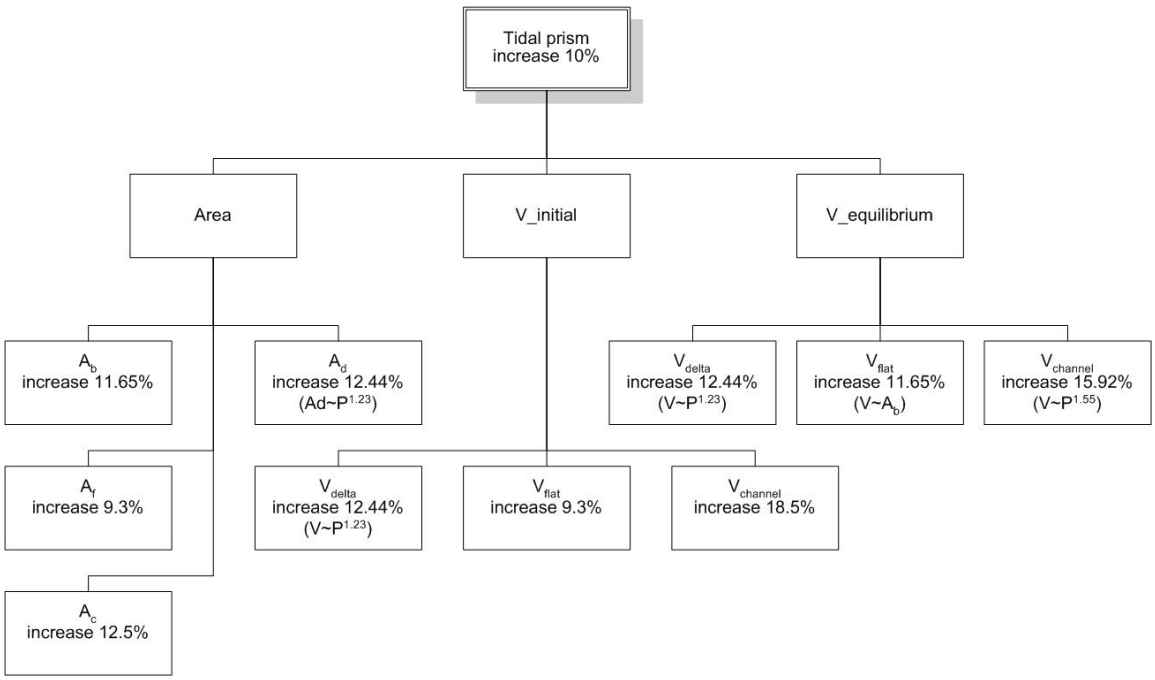

Figure 8.5: Overestimation of volumetric parameters in Marsdiep due to overestimation of tidal prism Marsdiep

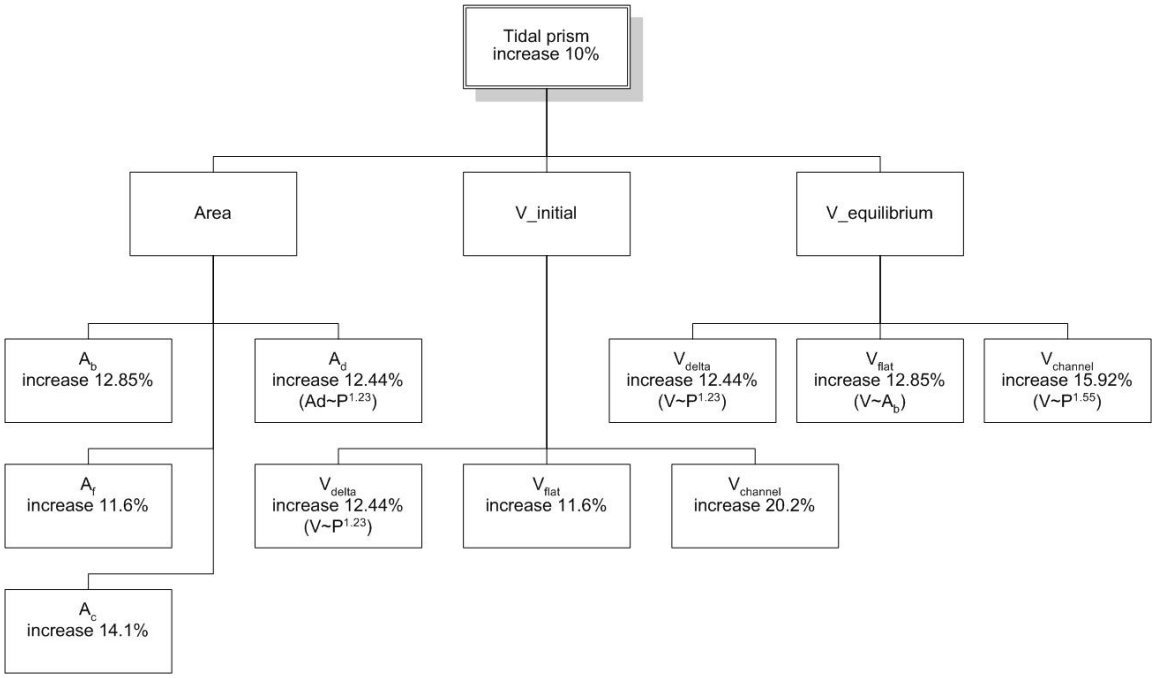

Figure 8.6: Overestimation of volumetric parameters in Vlie due to overestimation of tidal prism Vlie

From figure 8.4 until 8.6 can be concluded that the overestimation of the volumetric parameters of the tidal inlet mainly depends on which tidal prism is overestimated. If the tidal prism of basin n/m is overestimated, the volumetric parameters are completely depending on the power of the tidal prism in the used (equilibrium) relation. When the tidal prism of basin p is overestimated, the relative surface area of the reservoir and the location of the reservoir are important. The larger the area of the reservoir compared with the basin, the larger the increase in overestimation of the geometric parameters. The location of the reservoir is mainly important for the overestimation of the flat element. If the reservoir covers a small flat area, the overestimation is smaller then when a large flat area is covered by the reservoir.

8.4 Conclusions

In this chapter the morphological evolution of the several basins, after the construction of the reservoir has been studied. In the previous chapters is explained that the area of the basin after the construction of the reservoir depends on the surface area of the reservoir and the eventual displacement in tidal divide. Most basins, with or without reservoir are reduced due to the human intervention. Alternative KZ is the only alternative with an enlargement of a basin area (Marsdiep, see chapter 6).

To investigate the influences of the human intervention a distinction is made for the basin where the reservoir is constructed and the adjacent basins. Because of the reduced area of basin p, the basin is closer to its equilibrium state resulting in a smaller sediment exchange with the outside world. If the basin has a sediment need from the outside world in the current situation, this sediment need reduces. Reduced sediment demand can have positive effects regarding the erosion

of the adjacent coastal stretch. Both the Marsdiep and the Vlie basin currently have sediment need form the outside world (see table 8.4). For the Marsdiep basin the sediment need diminishes with 36 percent in the most advantageous case (AD1) and 18 percent in the less advantageous case (AD3 and LW2). The sediment need of the Vlie basin reduces with 35 percent in the most positive of the investigated cases.

Due to the shift in tidal divides, the basin adjacent to the basin with reservoir is reduced. Because of this reduction, this basin is closer to its equilibrium. For the Eierlandse Gat this implies a smaller sediment surplus than in the current situation, which could imply less sediment deposit on the adjacent coast. The reduction of the surplus is around 50 percent for alternative AD1. Alternative LW and KZ cause a reduction of less than 10 percent. The Vlie basin has a different result. Instead of a smaller sediment need from the outside world, a larger amount of sediment is needed due to the disturbed Vlie current (section 6.6).

Table 8.4: Sediment demand from the outside world [$*10^6$ m^2]

	CS	AD1	AD2	AD3	KZ1	KZ2	LW1	LW2
Marsdiep	1738	1111	1322	1433	1720	1722	1336	1434
EG	-12	-5	-8	-8	-11	-11	-11	-11
Vlie	433	461	454	451	294	279	436	439

If we compare the morphological consequences for all alternatives, the LW1 reservoir is probably the best option. The LW1 reservoir has not the largest reduction on the Marsdiep sediment demand, but the consequences for the Eierlandse Gat and the Vlie basin are negligible compared to the consequences due to the AD reservoirs.

9 Conclusions and Recommendations

This study focuses on the estimation of the hydrodynamic and morphodynamic effects of constructing a reservoir in either the Marsdiep or Vlie basin. The hydrodynamic impact of the reservoir is investigated using the Delft3D modelling system. Changes in tidal prism are determined for the Marsdiep, Eierlandse Gat and Vlie basin. The changes in tidal prism, and alterations in flow patters through the main channels are used for an expert-judgement based prediction of tidal divide displacements. These tidal prism changes and tidal divide displacements are important factors for the morphologic, reservoir related, basin changes. The long-term morphological evolution of the basins is determined by applying the semi-empirical model ASMITA.

For the research three alternatives have been used:

- AD alternative. This reservoir is situated at the original location of Boorsma (2003), against the Afsluitdijk and cuts off the Doove Balg (and AD1 also the Scheurrak)
- LW alternative. Constructed against the Afsluitdijk, but only on flat area.
- KZ alternative. Constructed on the Kornwerderzand flat between the Inschot and Blauwe Slenk, on the tidal divide separating the Marsdiep and Vlie basin.

For each of the alternatives hydrodynamic simulations (Ddelft3D-FLOW) and morphodynamic simulations (ASMITA) are made. Delft3D-FLOW results show a tidal prism decrease in Marsdiep and Vlie inlet for alternatives AD and LW, due the reduction of basin area. The above average ebb volume decrease in the Vlie inlet for the AD and KZ reservoir points to the disruption of the important through flow between the Vlie and Marsdiep basin. The LW alternative does not disrupt this through flow.

The tidal divide displacements, between Marsdiep and Vlie, are determined using the computed tidal prism changes, and the expected morphological development of the channels. The part of the tidal divide near the Inschot, displaces into the Vlie basin for all investigated alternatives, the part near the Kornwerderzand flat, displaces into the Marsdiep basin for alternative AD and LW.

The ASMITA based results show that construction of the reservoirs has positive effects on the morphological development of the basins and the adjacent coasts. Basin area reduction results in shorter adaptation time towards an equilibrium state. Especially, alternatives AD and LW reduce the adaptation time to equilibrium for the Marsdiep basin, while the adaptation time of the Vlie basin reduces with the construction of the KZ reservoir.

From this study follows, that the LW alternative is the best option. This alternative is completely constructed in the Marsdiep basin and has only limit influence on the through flow between Vlie and Marsdiep. Thus, effects on the Vlie basin are small. The reduction of the Marsdiep basin is beneficial. After closure of the Zuider Sea the tidal prism increased considerably, and the basin had not yet reached equilibrium. After construction of the reservoir, equilibrium is reached in a shorter period.

Note: One should be aware that this study was a first pilot in order to obtain indications of morphological effects of constructing reservoirs in the Wadden Sea. Therefore a number of simplifications and assumptions had to be made. For example, tidal range was assumed constant, empirical relations are used, and the flow computations were only made for the initial state, not taking into account morphological alterations of the Wadden Sea bathymetry resulting from the

reservoir. It is doubtful that such alterations can be modelled accurately, due to the complex and highly-dynamic nature of the Wadden Sea. Possibly, the modelled tidal prism change and interpretations of tidal divide displacement are not fully representative. As these are used as an input for the ASMITA model, the prediction of the long-term development of the channel, flat and delta elements can deviate.

Table 9.1: Overview hydrodynamic and morphodynamic consequences for the investigated reservoirs

		AD1	AD2	AD3	KZ1	KZ2	LW1	LW2
Hydrodynamic consequences [Tidal prism (P)]	MD	P decreased 28%	19%	14%	P increased 1%	1%	P decreased 17%	13%
	EG	P decreased 10%	7%	5%	P decreased 1%	1%	P decreased 1%	1%
	Vlie	P decreased 4%	3%	2%	P decreased 6%	4%	P decreased 0%	1%
Morphological consequences [Sediment (S)]	MD	S demand decreased 36%	24%	18%	S demand decreased 1%	1%	S demand decreased 23%	18%
	EG	S surplus decreased 54%	36%	29%	S surplus decreased 5%	3%	S surplus decreased 6%	7%
	Vlie	S demand increased 7%	5%	4%	S demand decreased 32%	36%	S demand increased 1%	2%

9.1 Conclusions

9.1.1 Hydrodynamic and Delft3D-FLOW related conclusions

- Analysis of the model results shows that due to the construction of a reservoir the tidal prism decreases. The reduction of the tidal prism results from the reduction in basins area caused by the reservoir.

- Model results show that the through flow from the Vlie towards the Marsdiep basin, the Vlie current, enters the Vlie basin at the inlet and flows through the Vlie channel and Inschot into the Marsdiep basin. In the Marsdiep basin the Vlie current flows through the Doove Balg and the Texelstroom before it leaves the Marsdiep basin. This is in accordance with Ridderinkhof (1990).

- Comparing the reduction in tidal prism for alternatives AD and LW we can conclude that the hydrodynamic consequences for the adjacent basins are larger when the Doove Balg is closed off (AD), than when this channel is not closed off. The latter is due to the altered through flow between the Vlie and Marsdiep basin.

- Due to the construction of the KZ reservoir, the tidal prism of the Marsdiep basin increases, while a decrease is expected. An increased flood volume simultaneously with a constant ebb volume implies that the KZ reservoir is not situated in the Marsdiep basin and implies another position of the concerning tidal divide.

- Comparing the modelled ebb and flood volumes of the Eierlandse Gat with the field data we observed opposite tide dominance. In the modelled case the Eierlandse Gat is ebb dominant, while field data imply a flood dominant basin. Therefore the results of the Eierlandse Gat should be interpreted with caution.

9.1.2 Morphodynamic and ASMITA related conclusions

- The Marsdiep and Vlie basin are too large in the present situation. These basins import sediment in order to reach their equilibrium. The Eierlandse Gat is too small and exports sediment. Due to the construction of the reservoir, the basins show for every alternative, except the Marsdiep basin for alternative KZ, a reduction of their surface area. Due to the reductions in the basins surface area, less sediment exchange is needed to reach the equilibrium volume of the delta, channel and flat elements in the tidal inlet system.

- The development of the flat, channel and delta elements towards equilibrium does not change after the construction of the investigated reservoirs. This means that if the element shows an asymptotic development curve towards its equilibrium in the present situation, the development of the element shows also an asymptotic behaviour towards equilibrium after the realisation of the construction. The behaviour of an element towards equilibrium is not always asymptotic. The element can also overshoot its equilibrium or first move away from the equilibrium.

- An overestimation / underestimation of the modelled tidal prism results in an overestimation / underestimation of the basin's geometric parameters (area and volume of flat, channel and delta elements).

  The degree of overestimation of the geometric parameters depends on the tidal prism. When the tidal prism of a basin with reservoir is overestimated, the relative surface area of the reservoir and the location of the reservoir are important for the degree of overestimation.

  When an overestimation of the tidal prism occurs in an adjacent basin, the overestimation of the geometric parameters only depends on the power of the tidal prism in the used (equilibrium) relation.

- The consequences of the construction of the studied reservoirs are limited compared to the influence of a Sea Level Rise of 17 cm/century. In some cases the construction of the reservoir does diminish the sediment need of all sediment demanding basins, implying that the basin is able to cope with a larger Sea Level Rise, than in the present situation. As a result of the reduced basin area, the construction of the reservoir could imply a more stable tidal basin system. After all a reduction in basin area results in smaller equilibrium system time scales: the system needs less time to respond on an imposed disturbance.

9.2 Recommendations

9.2.1 Hydrodynamic and Delft3D-FLOW related recommendations

- The field data of the ebb and flood volumes through the inlet fluctuates considerably, due to different measurement accuracies and due to meteorological forcings. The model approaches the field data, but a further calibration (for the Eierlandse Gat and Vlie basin) is recommended to reach more realistic results.

- The construction of the KZ reservoir, probably changes the flow through the Westmeep and the location of the tidal divide between the Vlie and Borndiep basin. For an accurate modelling of the KZ reservoir an extension of the model, up to the Borndiep, is recommended.

- Further research on the position of the tidal divide near the Doove Balg, Scheurrak and Inschot is recommended.

- For a better prediction of both the area and volume of the channel and flat elements (ASMITA input parameters) and to limit the need of expert-judgement based predictions, it is recommended to extend the model to a morphological updating model able to simulate morphological change of a basin and tidal divide displacement.

9.2.2 Morphodynamic and ASMITA related recommendations

- The tidal range is needed to define the volumetric parameters (area and volume) of the channel, flat and delta elements. In this study it is assumed that compared to the length of the tidal wave, the length of the reservoir is too small to influence the amplitude of the tidal wave. However, during this study the change in tidal range is investigated and for the worst case alternative the tidal range changed 10 percent. It is recommended to take the change in tidal range into account to obtain a better estimation of the volumetric parameters of the elements.

- The volumetric parameters for the flat, channel and delta elements are derived from the values of Eysink (1993). For a better prediction of the consequences of a reservoir, it is recommended to find more and recent data.

- Because constructing a reservoir implies a large artificial disturbance in the tidal basins, it is questionable if the used equilibrium relations are still valid.

- For this study general values have been used for the transport capacity parameters. It is recommended to calibrate the parameters for the several basins. Because the flow conditions change per alternative it is also recommended to calibrate these transport parameters for each alternative.

- The volumes of the channel and flat elements in the reservoir are used to calculate the volumes of these elements after the construction. The volumes of these elements are determined by the mean channel and flat heights of the tidal basin. For a better estimation of the new flat and channel volumes in the basin with reservoir, 'real' flat and channel heights in the reservoir, obtained from chart analysis, should be used.

References

Berendsen, H.J.A, 1997. De vorming van het land. Inleiding in de geologie en de geomorfologie. Van Gorcum, Assen.

Berger, G.W.; Eisma, D.; Bennekom, A.J. van, 1987. 210Pb derived sediment rate in the Vlieter, a recently filled-in channel in the Wadden Sea. Netherlands Journal of Sea Research, Volume 21, pp. 287-294

Biegel, E.J., 1993. Morphological changes due to sea level rise in the Dutch Wadden Sea versus concepts morphological response model MORRES. Report IMAU-93.14. Institute for Marine and Atmospheric Research Utrecht, Utrecht University.

Blok, M.; Mol, J.W., 2001. Debietmetingen van Texel. Report Rijkswaterstaat, Directie Noord-Holland, Informatiedienst Water, IJmuiden, the Netherlands.

Boorsma, K., 2003. Onderloopboezem in Waddenzee houdt Nederland droog. Land + Water, nr. 9, Septmber 2003, blz 36-37.

Bruun, P; and Gerristsen, F., 1959. Natural bypassing of sand at coastal inlets. Journal of the Waterways and Harbours Div. ASCE, 85, pp. 75-107.

Buijsman, M.C. 1997. The impact of gas extraction and sea level rise on the morphology of the Wadden Sea, Delft Hydraulics, Report H3099.30

Dean, R.G., 1988. Sediment interaction at modified coastal inlets: processes and policies. In: Aubrey D.G. & Weishar, L. (Eds.): Hydrodynamics ans Sediment Dynamics of Tidal Inlets. Lecture Notes on Coastal and Estuarine Studies, 29: 412-439; New York, Springer.

Dean, R.G.; and Walton, T.L., 1975. Sediment transport processes in the vicinity of inlets with special reference to sand trapping. In Estuarine Research, L.E. Cronin, Academic press, 2, pp. 129-150.

Donselaar, M.E., 1996. Barrier island coast and relative sea level rise: preservation potential, facies architecture and sequence analysis, Delft.

Elias, E.P.L.; Stive, M.J.F.; Bonekamp, J.G.; Cleveringa, J., 2003b. Tidal inlet dynamics in response to human intervention. Coastal Engineering Journal. Vol. 45, No. 4 (2003) 629-658.

Elias, E.P.L. Stive, M.J.F.; Cleveringa, J., 2004. Hydrodynamics and Morphodynamics of the Texel inlet, the Netherlands. Paper in progress.

Endema, D., 1979. Grootheden / gegevens Waddenzee, Waddeneilanden en Noordzeekust. Rijkswaterstaat nota WWKZ-97.H003

Eysink, W.D., 1979. Morfologie van de Waddenzee, gevolgen van zand- en schelpenwinning, Delft Hydraulics, Report of literature survey, Rep. R1336.

Eysink, W.D., 1990. Morphological response of tidal basins to change. Proc. 22nd Coast. Eng. Conf., ASCE, Delft, July 2-6, Vol. 2, The Dutch Coast, Paper no. 8, 1990, pp. 1948-1961.

Eysink, W.D., 1991. ISOS*2 Project, phase 1. Impact of sea level rise on the morphology of the Wadden Sea in the scope of its ecological function. Inventory of available data and literature and recommendations on the aspects to be studied. Delft Hydraulics. Report H1300.

Eysink, W.D.; Biegel E.J., 1992. ISOS*2 Project, phase 2. Impact of sea level rise on the morphology of the Wadden Sea in the scope of its ecological function. Investigations on morphological relations. Delft Hydraulics. Report H1300.

Eysink, W.D., 1993. ISOS*2 Project, phase 4. Impact of sea level rise on the morphology of the Wadden Sea in the scope of its ecological function. General considerations on hydraulic conditions, sediment transports, sand balance, bed composition and impact of sea-level rise on tidal flats. Delft Hydraulics. Report H1300.

Fokkink, R.J.; Karssen, B.; Wang, Z.B.; Kerckhoven, J. van; and Langerak, A., 1996. Morphological modelling of the Western Scheldt estuary. 8th International Biennial Conference on Physics of Estuaries and Coastal Seas, The Hague, September 1996

FitzGerald, D.M. (1988). Shoreline erosional-depositional processes associated with tidal inlets. In Aubrey, D.G. & Weishar, L. (eds.): Hydrodynamics and sediment dynamics of tidal inlets, Springer-Verlag, N.Y., pp 186-225

Gerritsen, F.; and Jong, H. de, 1985. Stability of flow profiles in the Wadden Sea. Rijkswaterstaat, Adviesdienst Vlissingen, Nota WWKZ-84, Vol. 6.

Gerritsen F., 1990. Morphological stability of inlets and channels of the western Wadden Sea. Ministerie van verkeer en waterstaat, dienst getijdewateren. Nota GWAO - 90.019.

Gerritsen, H.; Boon, J.G.; Kaaij, T. van der; and Vos, R.J., 2001. "Integrated modelling of Suspended Matter in the North Sea", Estuarine, Coastal and Shelf Sciences Vol. 53,4, pp. 581-594

Goor, M.A. van, 2001. Influence of Relative Sea Level Rise on Coastal Inlets and Tidal basins. Delft Hydraulics, Note Z2822.

Goor, M.A. van; Zitman, T.J.; Wang, Z.B.; Stive, M.J.F., 2003. Impact of sea-level rise on the morphological equilibrium state of tidal inlets. Elsevier, Marine Geologie 3391 (2003) 1-17.

Hayes, M.O., 1979. Barrier island morphology as a function of tidal and wave regime. In Barrier Islands, S.P. Leatherman (editor), Academic Press, New York, pp. 1-28.

Hayes, M.O.; Goldsmith, V.; and Hobb, C.H., 1970. Offset coastal inlets. Proc. 12th Coast. Eng. Conf. ASCE, pp. 1197-1200.

Kolk, B; and Schalkers, K.M., 1980. De veranderingen in de Waddenzee ten gevolge van de afsluiting van de Zuider Sea. Report Rijkswaterstaat, 78H238, 22 pp, The Hague

Kragtwijk, N.G., 2001. Aggregated Scale Modelling of Tidal Inlets of the Wadden Sea; Morphological Response to the Closure of the Zuiderzee. Delft Hydraulics, Note Z2822.

Louters, T.; Gerritsen, F., 1994. The Riddle of the Sands, a Tidal System's Answer to a Rising Sea Level. Report RIKZ-94.040, The Hague.

Misdorp, R.; Steyaert, F.; Hallie, F.; and Ronde, J. de, 1990. Climate change, sea level rise and morphological developments in the Dutch Wadden Sea, a marine wetland. RWS, The Hague.

Oost, A.P., 1995. Dynamics and Sedimentary Development of the Dutch Wadden Sea with emphasis on the Frisian Inlet. A Study of the barrier islands, ebb-tidal deltas, inlets and drainage basins. Geologica Ultrajectina 126, Proefschrift Rijksuniversiteit Utrecht.

Oost, A.P., 2004 Autonome ontwikkeling Westelijke Waddenzee, personal communications

Rakhorst, H.D., 2004. Personal communications

Reijngoud, T.T., 1998. De morfodynamica van de Waddenzee op verschillende ruimte- en tijdschalen, Waddenvereniging, Harlingen, 1998

Renger, E.; and Partenscky, H.W., 1974. Stability criteria for tidal basins, Proc. 14th Coast. Eng. Conf., ASCE, 2, pp. 1605-1618.

Reus, J.H. de; Lieshout, M.F.M., 1982. Debieten Zeegat van Texel. Rijkswaterstaat, WWKZ-82.H205

Ridderinkhof, H., 1988 a. Tidal and residual flows in the western Dutch Wadden Sea. I: Numerical model results. Netherlands Journal of Sea Research, volume 22 (1), pp 1-21.

Ridderinkhof, H.; Haren, H. Van; Eijgenraam, F.; Hillebrand, T., 1999. Ferry observations on temperature, salinity and currents in the Marsdiep tidal inlet between the North Sea and Wadden Sea. Proc. of Eurogoos Conf., Rome, Italy.

Roelvink, J.A.; Kaaij, T. Van der; Ruessink, M.G. (2001). Set-up, calibration and verification of large-scale hydrodynamic models. Report ONL, Coast and Sea studies. Project 2, Hydrodynamics and Morphology. Z3029.10. Delft Hydraulics, Delft

Roelvink, J.A. and Banning G.K.F.M. van, 1994, Design and Development of Delft3D and application to coastal morphodynamics, Proceedings of Hydroinformatics 1994, Verwey, Minns, Babovic and Maksimovic eds., A.A. Balkema Publishers, Rotterdam, 451-456.

Sha, L.P., 1990. Sedimentological studies of the ebb-tidal deltas along the West Frisian Islands, the Netherlands, Geologica Ultrajectina 64, Proefschrift Rijksuniversiteit Utrecht.

Sha, L.P.; Berg, J.B. van den, 1993. Variation in Ebb-tidal Geometry along the past of the Netherlands and the German Bright, Journal of Coastal Research, 9(3), pp 730-746.

Spek, A.J.F. van der; Noorbergen, H.H.S., 1992, Morfodynamica van intertijde gebieden. Beleidscommissie Remote Sensing (BCRS). Report NRSP-1 92-03

Staatscommissie Zuiderzee (Lorentz, H.A; Lely, C.W. et al.), 1926. Verslag Staatscommissie Zuiderzee 1918-1926. Algemeene Landsdrukkerij, 's Gravenhage.

Steijn, R.C., 1991. Some considerations on tidal inlets; a literature survey on hydraudynamic and morphodynamic characteristics of tidal inlets with special attention to "Het Friesche Zeegat". Delft Hydraulics, WL H 840.

Stelling, G.S., 1984. On the construction of computational methods of shallow water flow problems, Rijkswaterstaat communications, No. 35

Stive, M.J.F.; Capobianco, M.; Wang, Z.B.; Ruol, P.; Buijsman, M.C., 1996. Morphodynamics of a tidal lagoon and the adjacent coast. 8th International Biennial Conference on Physics of Estuaries and Coastal Seas, The Hague, September 1996.

Stive, M.J.F.; Roelvink, D.J.A.; Vriend, H.J. de, 1990. Large-scale coastal evolution concept. Proc. 22nd Coast. Eng. Conf., ASCE, Delft, July 2-6, Vol. 2, The Dutch Coast, Paper no. 9, 1990, pp. 1962-1974

Thijsse, J.Th., 1972. Een halve eeuw Zuiderzeewerken 1920-1970. H.D. Tjeenk Willink B.V. Groningen.

Wang, Z.B.; Karssen, B.; Fokkink, R.J.; and Langerak, A., 1996. A dynamic/empirical model for estuarine morphology. 8th International Biennial Conference on Physics of Estuaries and Coastal Seas, The Hague, September 1996.

Walton, T.L.; Adams, W.D., 1976. Capacity of Inlet outer bars to store sand, Proceedings of 15th Coastal Engineering Conference, ASCE, Honolulu, Hawaii, pp 1919-1937

WL | Delft Hydraulics, Delft3D-FLOW, User manual, release 3.06, August 2001.

Zagwijn, W.H., 1991. Nederland in het Holoceen, Rijks Geologische Dienst Haarlem, Staatsuitgeverij, 's Gravenhage.

Zitman, T.J.; Stive, M.J.F.; and Wiersma, H.J., 1990. Reconstruction of the Holocene evolution of the Dutch coast. Proc. 22nd Coast. Eng. Conf., ASCE, Delft, July 2-6, Vol. 2, The Dutch Coast, Paper no. 9, 1990, pp. 1962-1974

Internet adresses

www.getij.nl
www.waddenzee.nl

Appendix A

Tidal volume inlets and channels

Appendix B

Residual velocities

The figures in this appendix show the residual velocities in the Western Wadden Sea for one of the several situations. The colours in the figures represent the magnitude of the residual flow, while the vectors represent the direction of the residual flow.

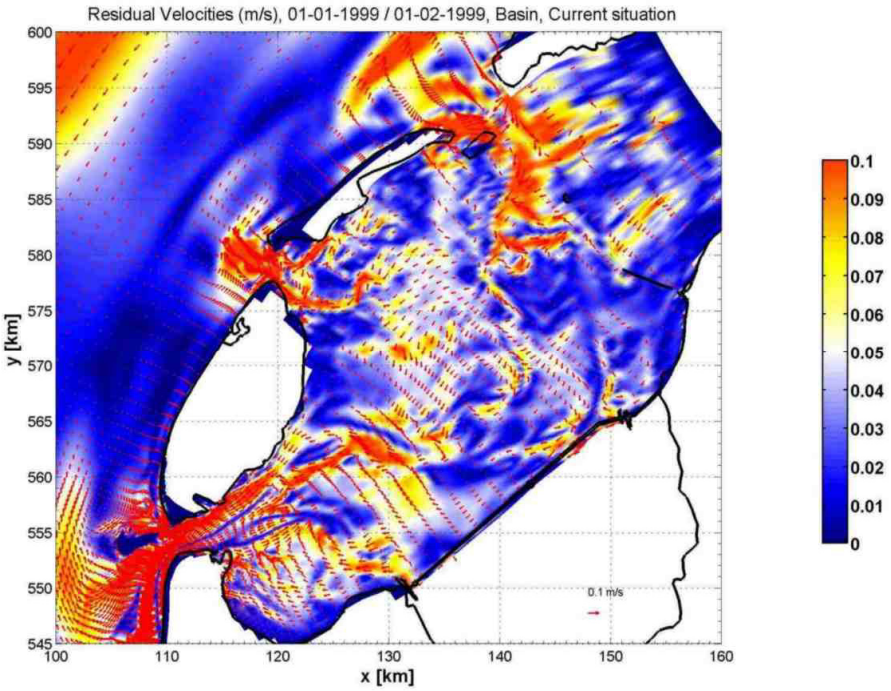

Figure B.1: Residual velocities in Current Situation.

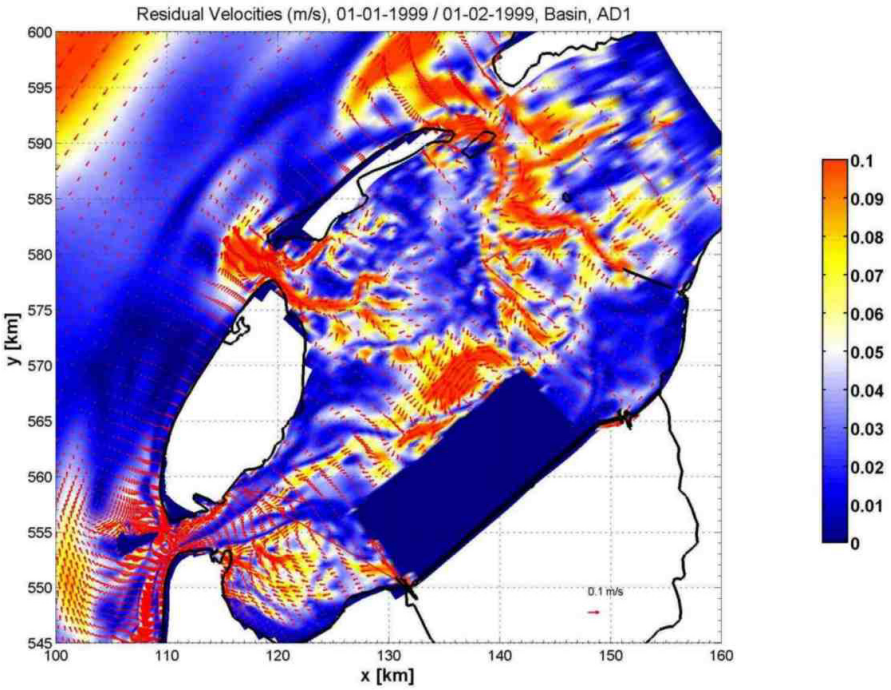

Figure B.2: Residual velocities in alternative AD1.

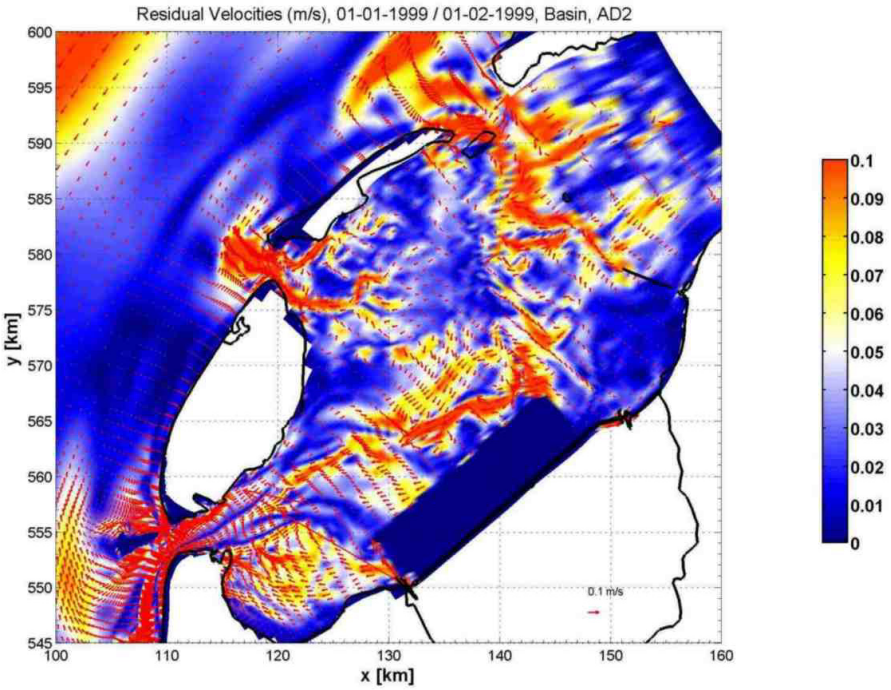

Figure B.3: Residual velocities in alternative AD2.

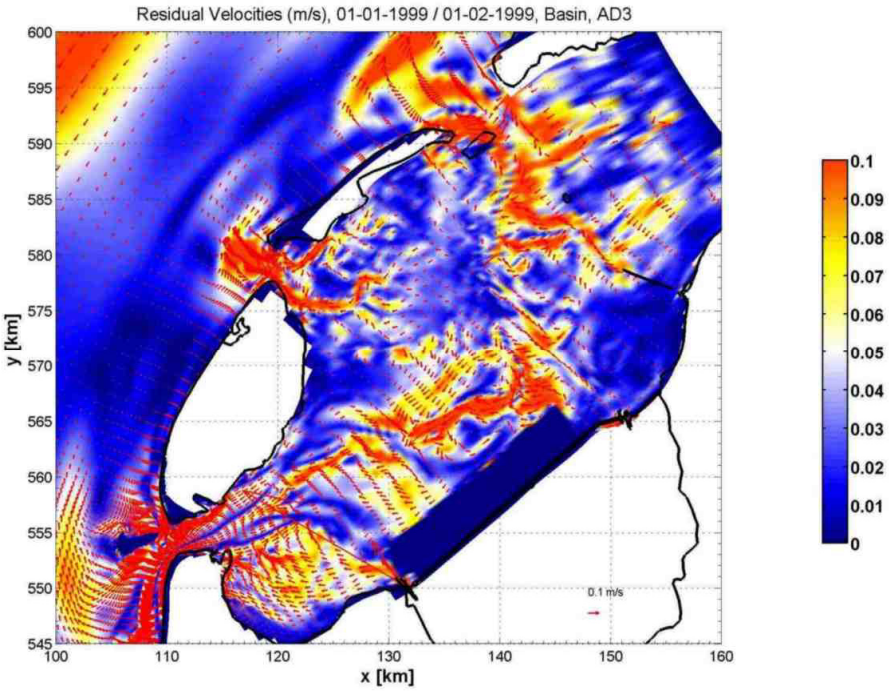

Figure B.4: Residual velocities in alternative AD3.

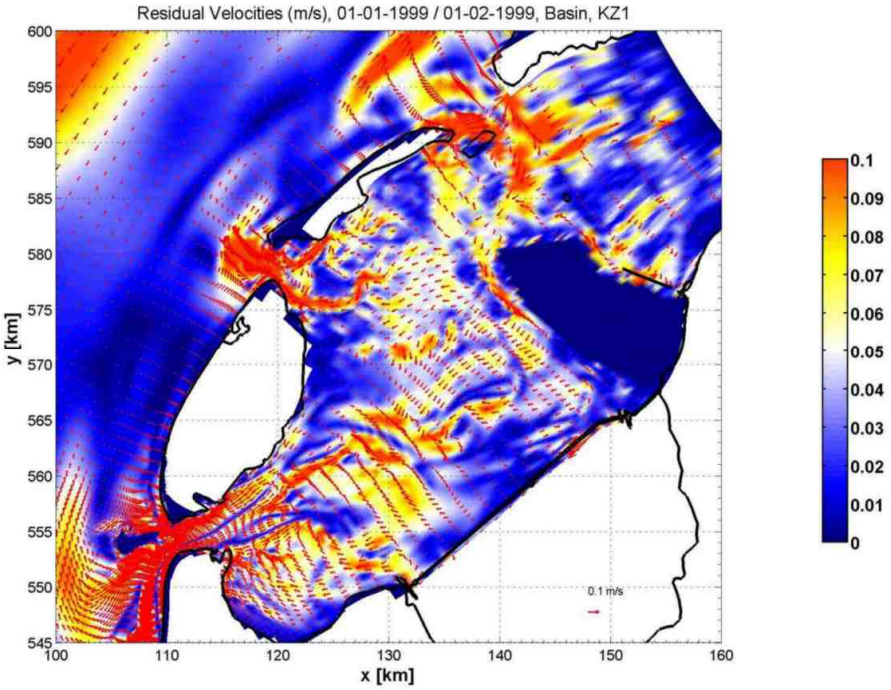

Figure B.5: Residual velocities in alternative KZ1.

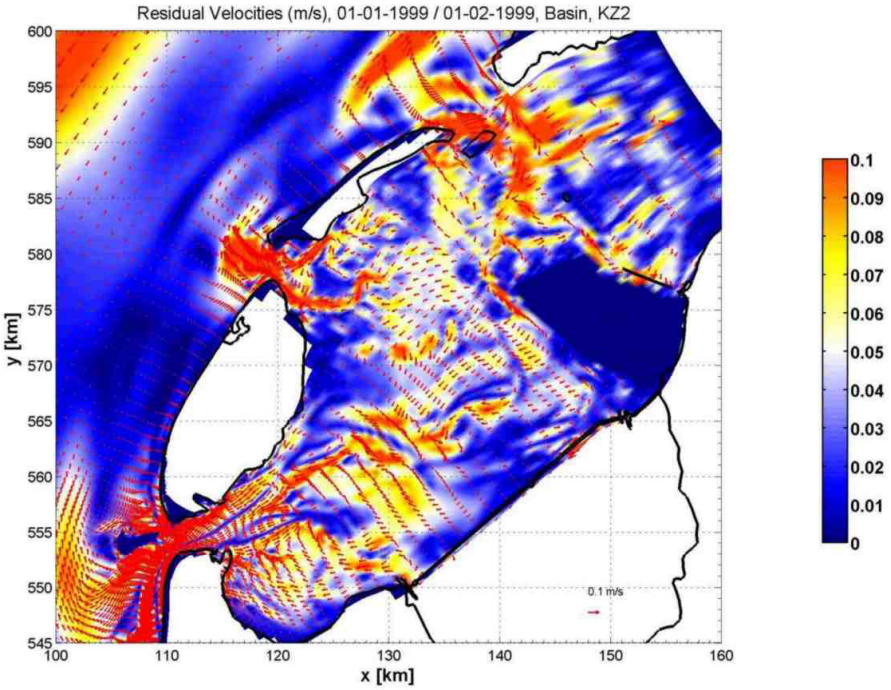

Figure B.6: Residual velocities in alternative KZ2.

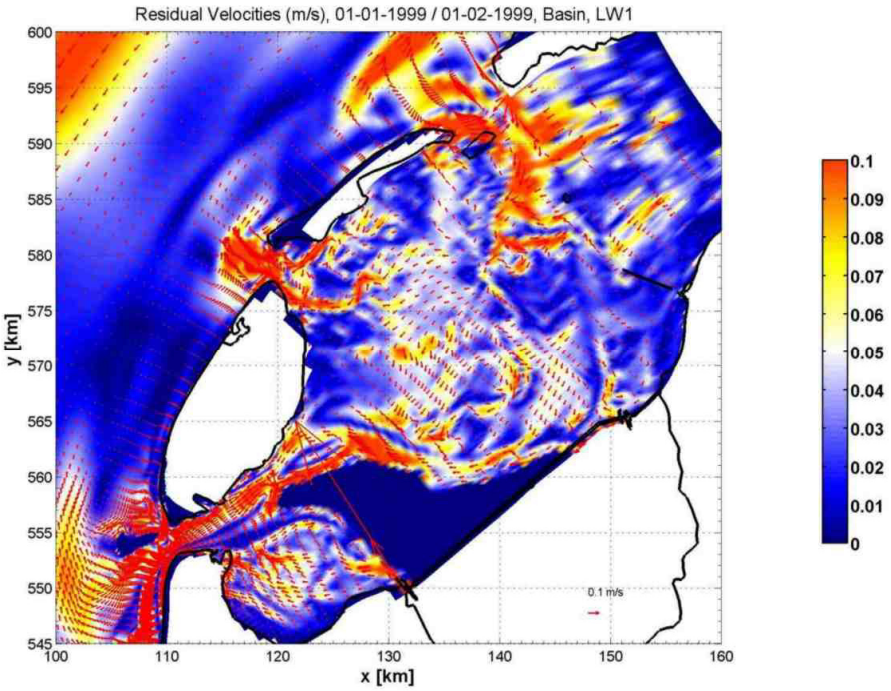

Figure B.7: Residual velocities in alternative LW1.

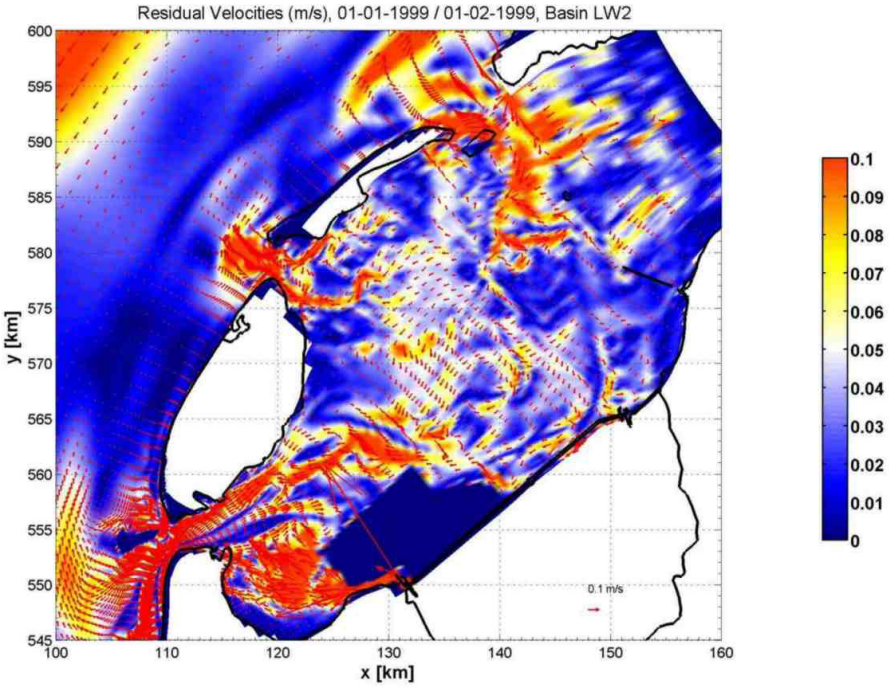

Figure B.8: Residual velocities in alternative LW2.

Appendix C

Tidal range

In this appendix the change in tidal range is presented by means of figures. Delft3D-FLOW, quick-plot and matlab, are used to obtain these figures. The first figures are an overview of the western Wadden Sea with the degree of change in the M_2 component due to the construction of the reservoir.

In the other figures the water level is represented for both the current situation (straight line) and the situation with the constructed reservoir (dashed line).

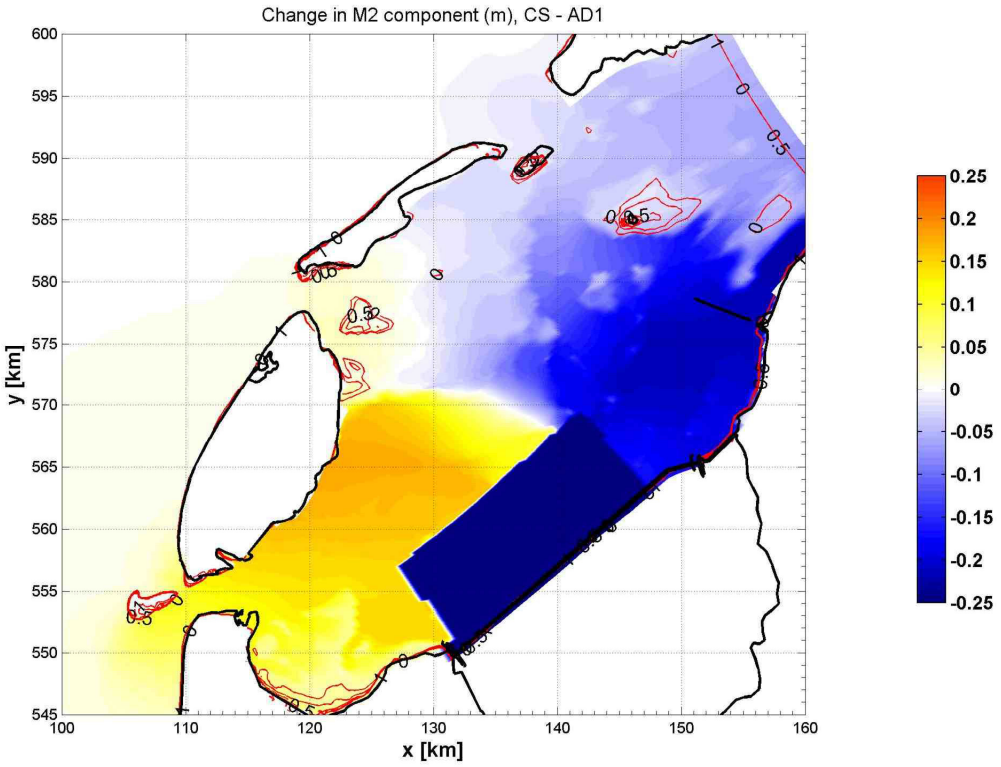

Figure C.1: Change in M_2 component due to reservoir AD1, compared to the Current Situation

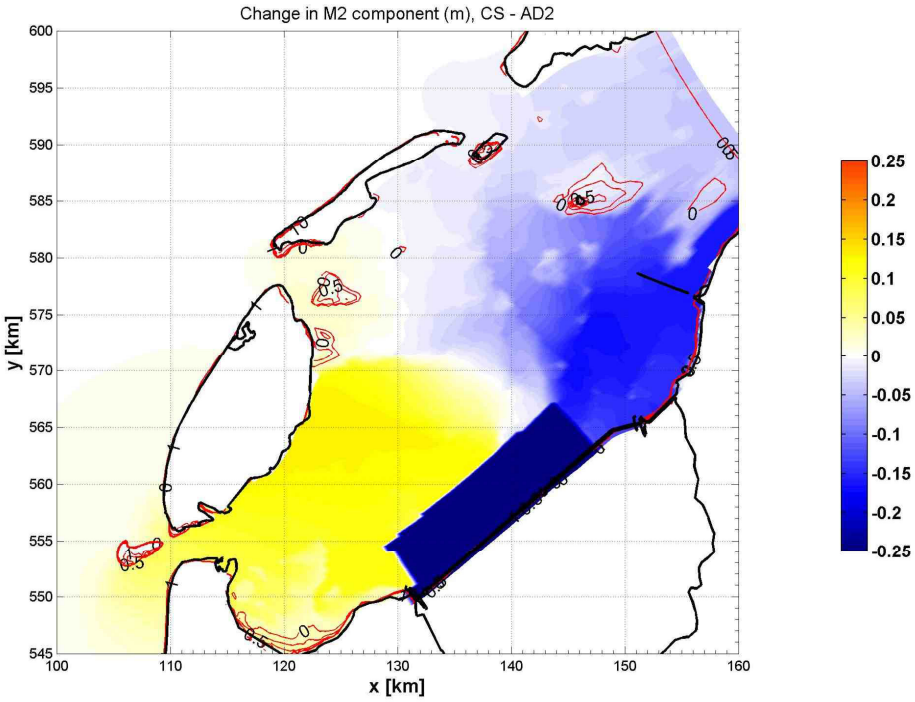

Figure C.2: Change in M_2 component due to reservoir AD2, compared to the Current Situation

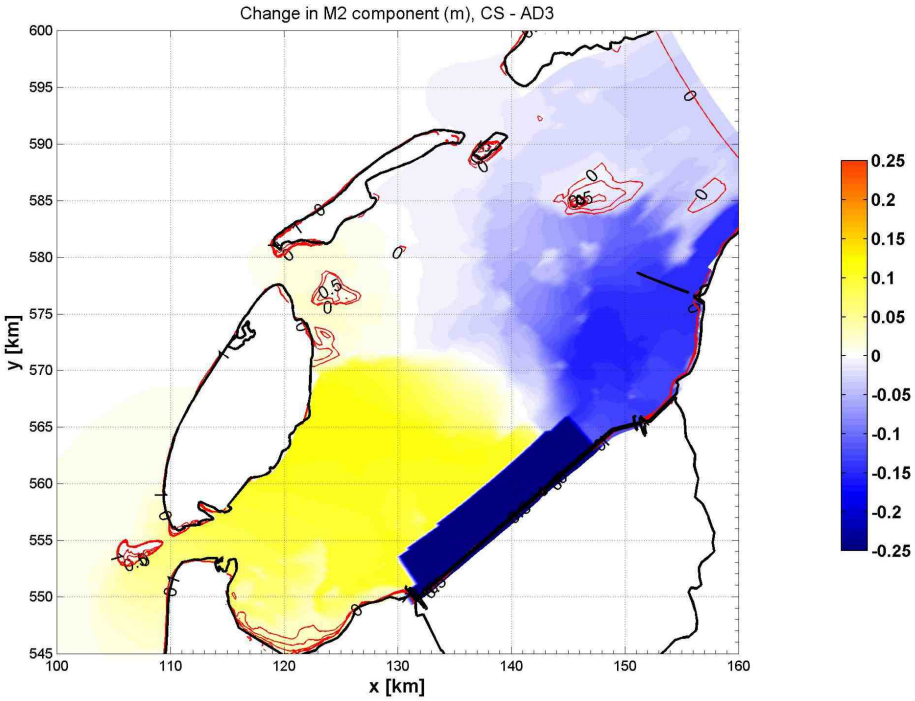

Figure C.3: Change in M_2 component due to reservoir AD3, compared to the Current Situation

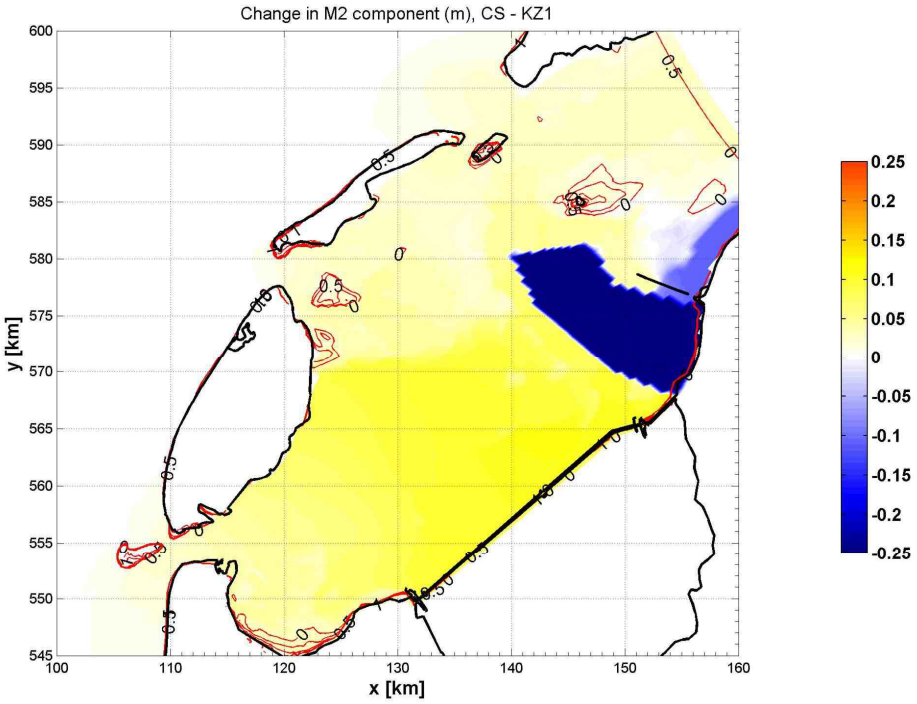

Figure C.4: Change in M_2 component due to reservoir KZ1, compared to the Current Situation

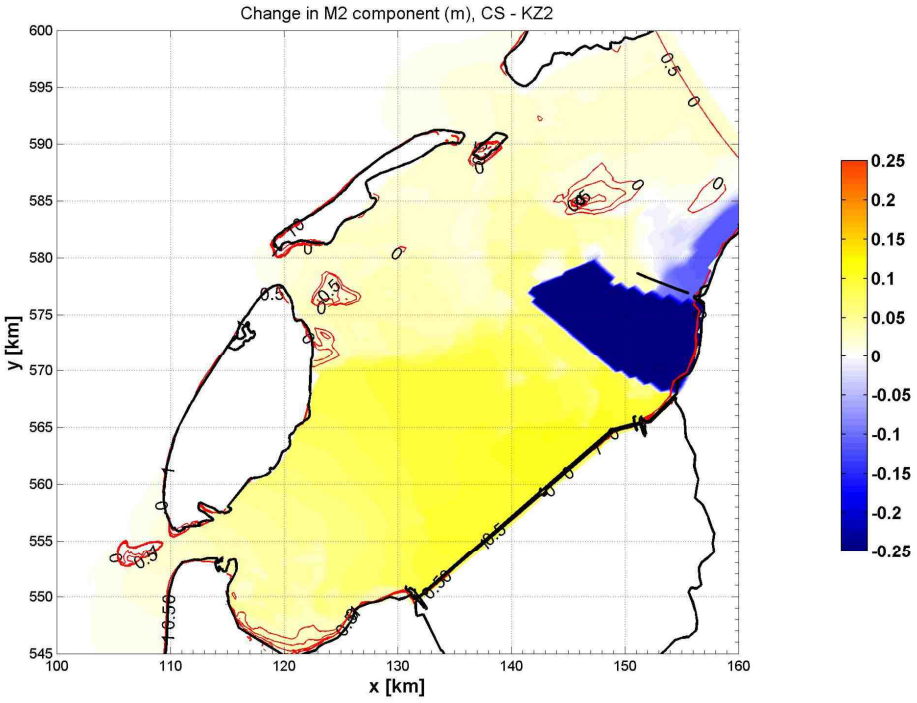

Figure C.5: Change in M_2 component due to reservoir KZ2, compared to the Current Situation

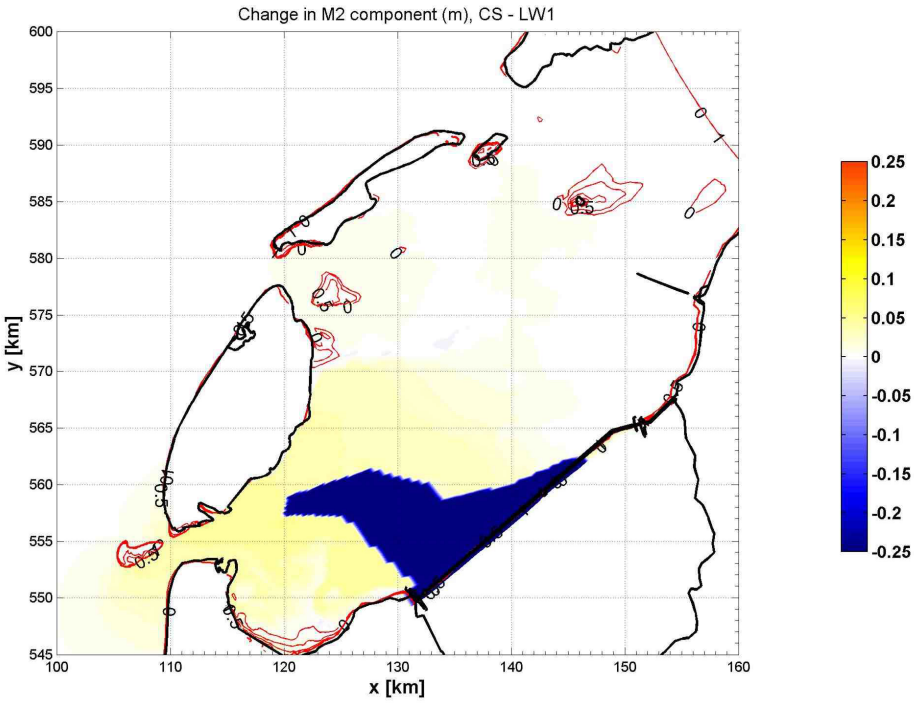

Figure C.6: Change in M_2 component due to reservoir LW1, compared to the Current Situation

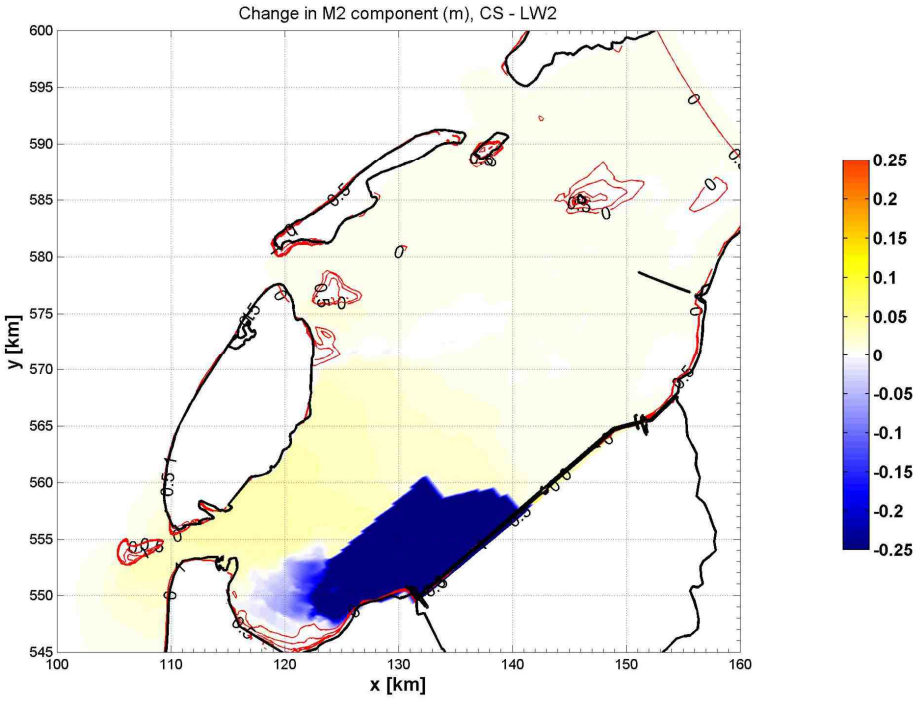

Figure C.7: Change in M_2 component due to reservoir LW2, compared to the Current Situation

Marsdiep basin

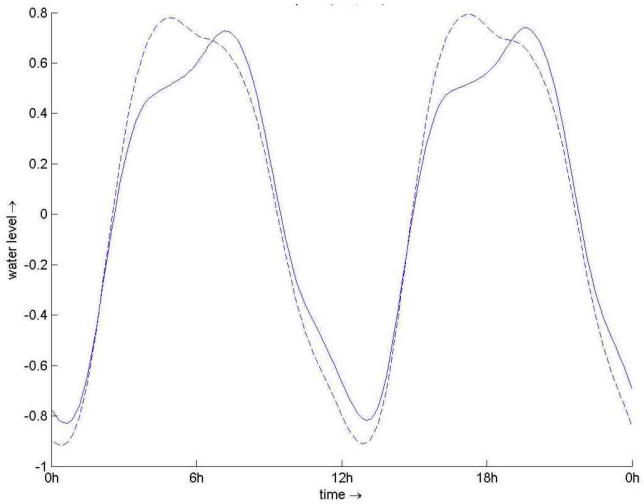

Figure C.8: Tidal range through Marsdiep inlet for Alternative AD1

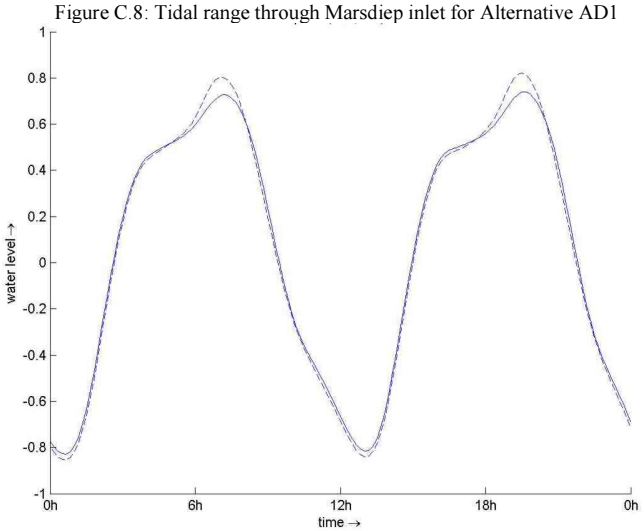

Figure C.9: Tidal range through Marsdiep inlet for Alternative KZ1

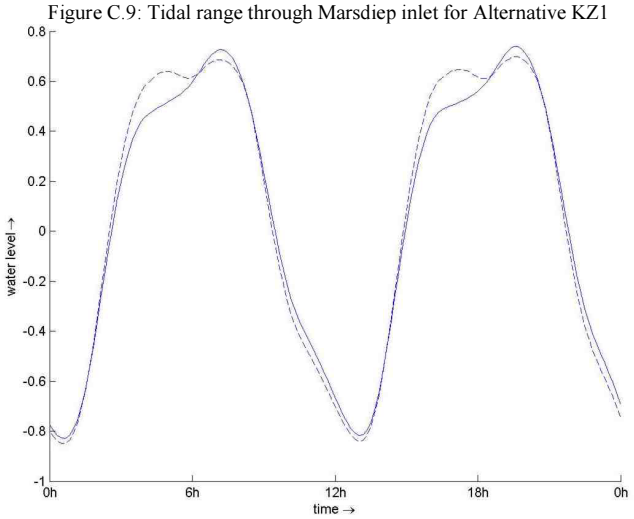

Figure C.10: Tidal range through Marsdiep inlet for Alternative LW1

Eierlandse Gat

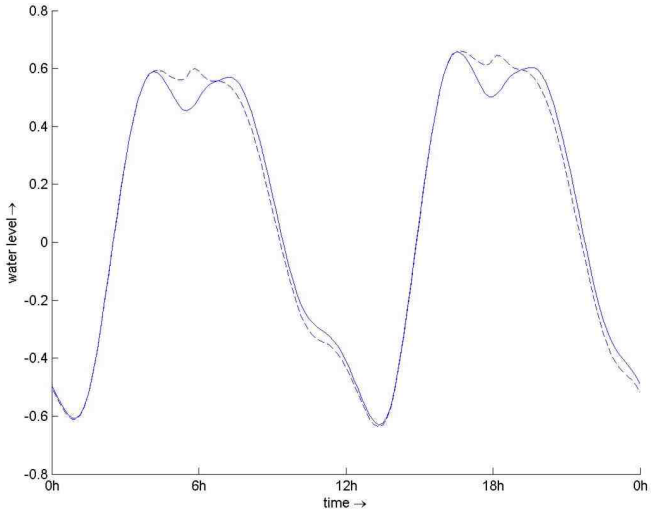

Figure C.11: Tidal range through Eierlandse Gat inlet for Alternative AD1

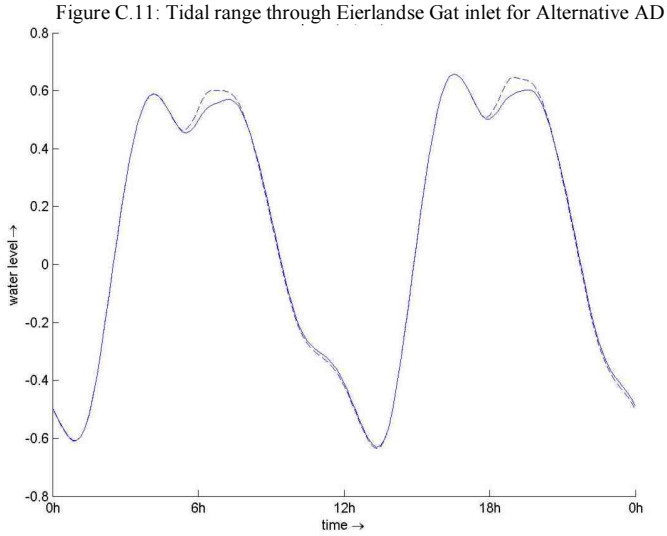

Figure C.12: Tidal range through Eierlandse Gat inlet for Alternative KZ1

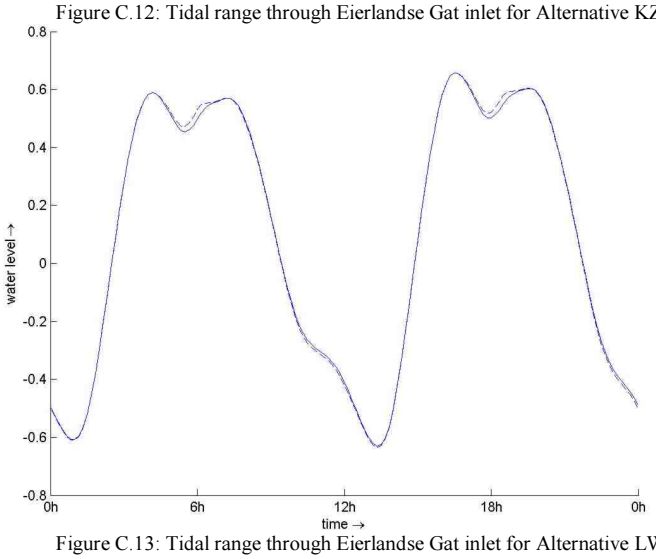

Figure C.13: Tidal range through Eierlandse Gat inlet for Alternative LW1

Vlie

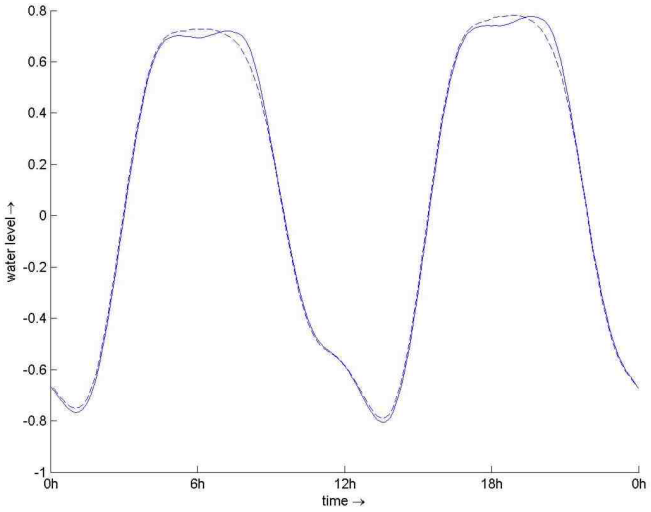

Figure C.14: Tidal range through Vlie inlet for Alternative AD1

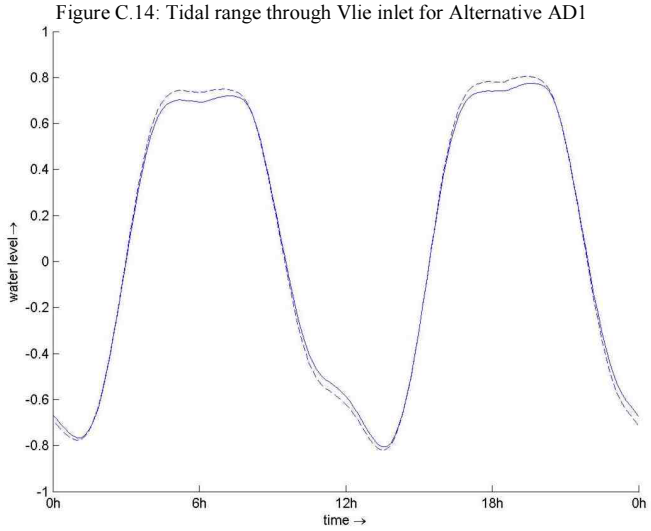

Figure C.15: Tidal range through Vlie inlet for Alternative KZ1

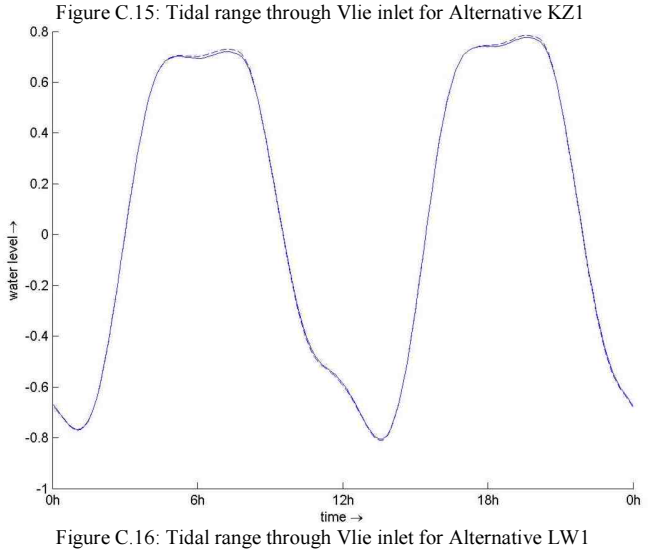

Figure C.16: Tidal range through Vlie inlet for Alternative LW1

Discharge sluices at Den Oever

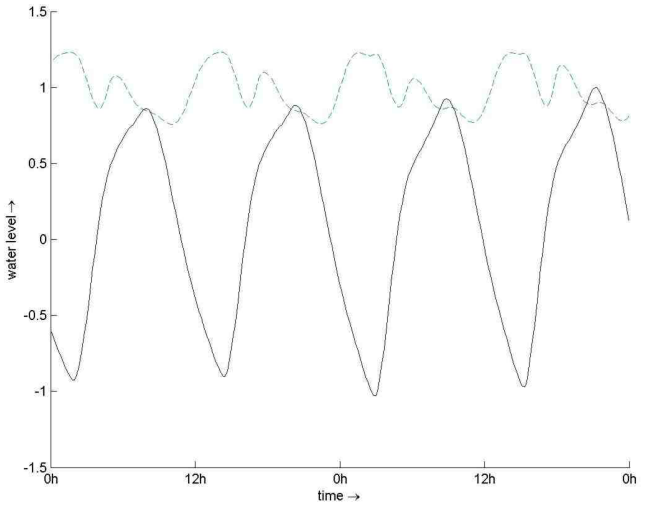

Figure C.17: Tidal range in Den Oever for alternative AD1

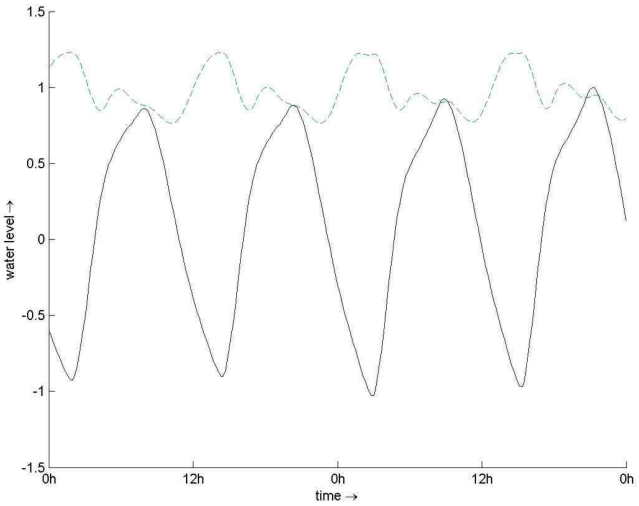

Figure C.18: Tidal range in Den Oever for alternative AD2

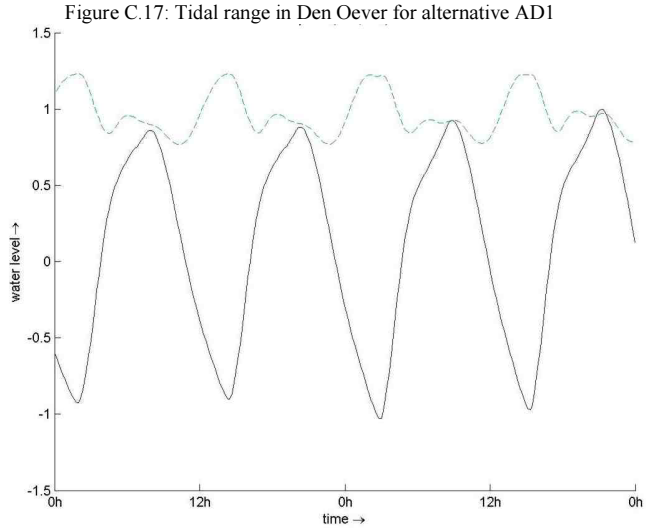

Figure C.19: Tidal range in Den Oever for alternative AD3

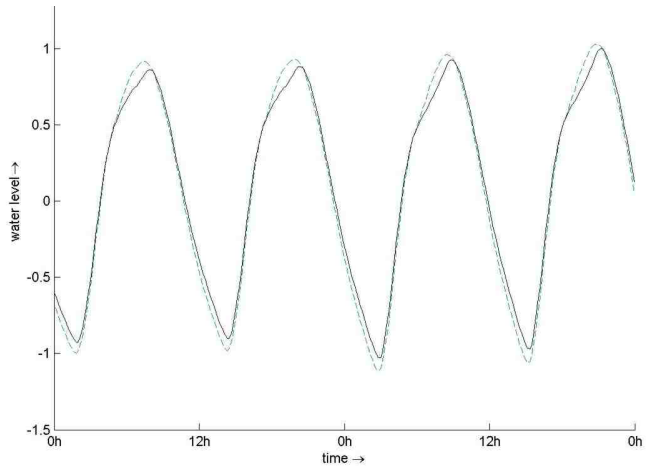

Figure C.20: Tidal range in Den Oever for alternative KZ1

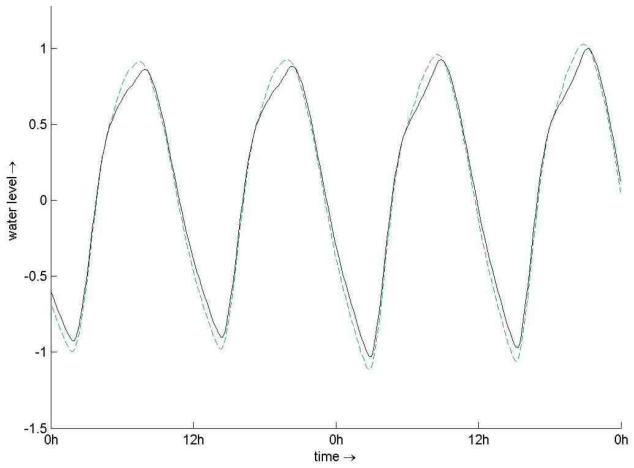

Figure C.21: Tidal range in Den Oever for alternative KZ2

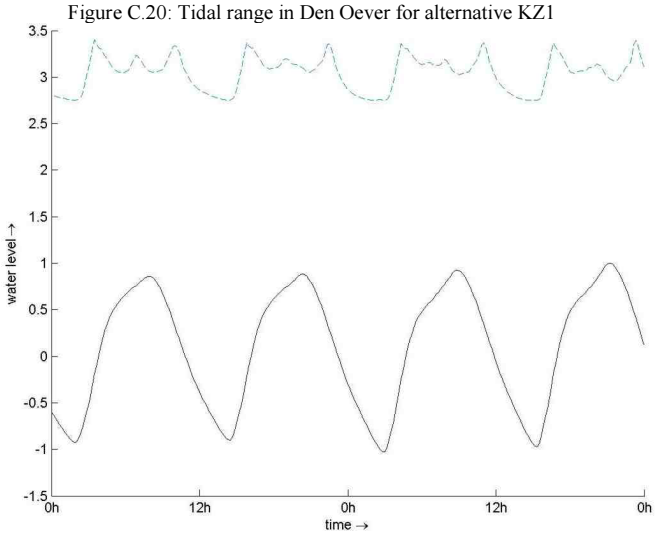

Figure C.22: Tidal range in Den Oever for alternative LW1

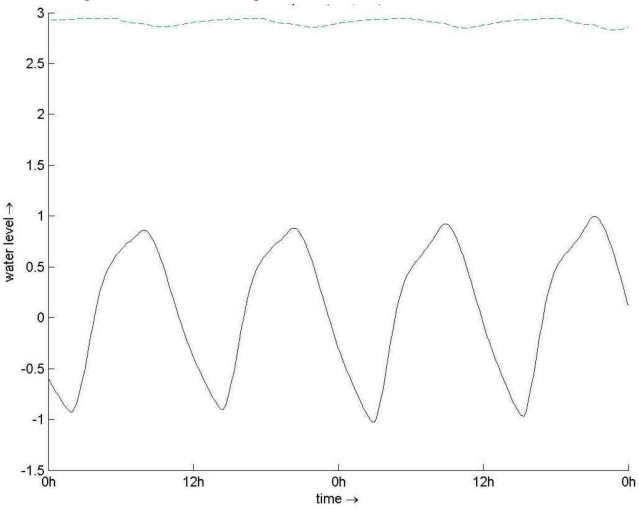

Figure C.23: Tidal range in Den Oever for alternative LW2

Discharge sluices at Kornwerderzand

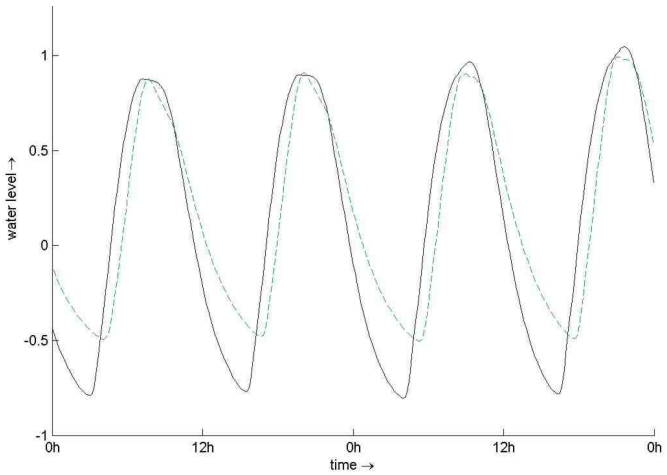

Figure C.24: Tidal range in Kornwerderzand for alternative AD1

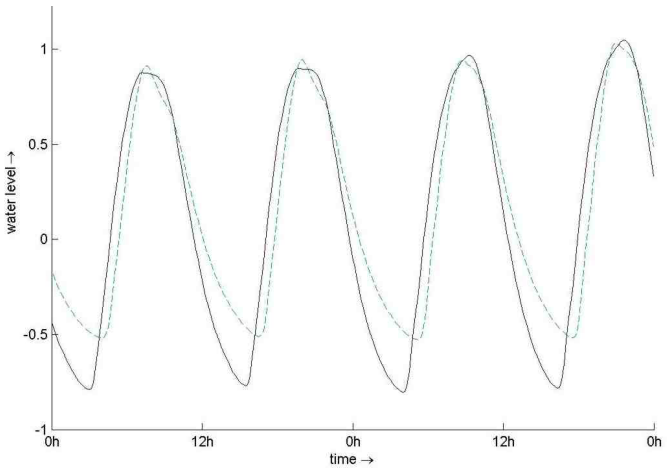

Figure C.25: Tidal range in Kornwerderzand for alternative AD2

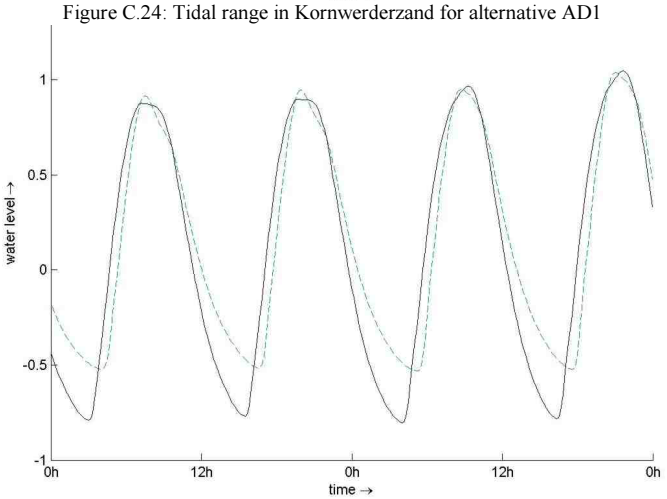

Figure C.26: Tidal range in Kornwerderzand for alternative AD3

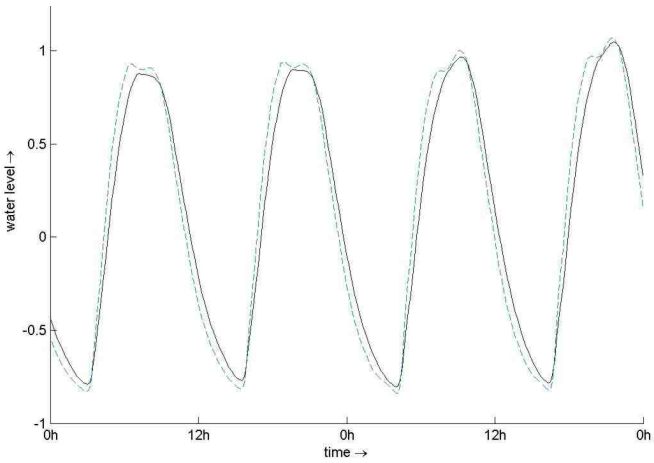

Figure C.27: Tidal range in Kornwerderzand for alternative KZ1

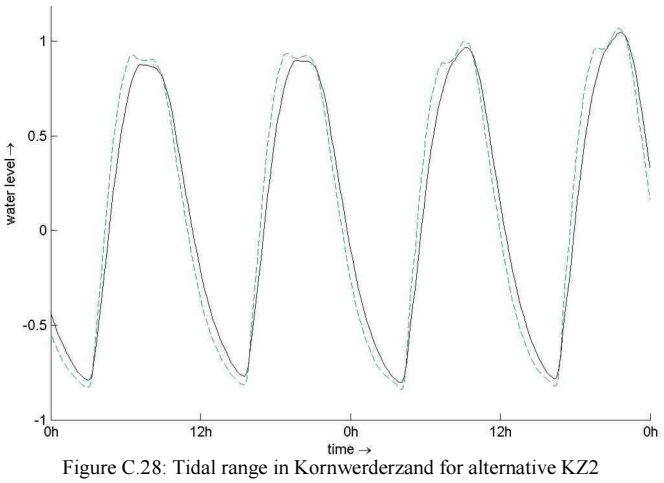

Figure C.28: Tidal range in Kornwerderzand for alternative KZ2

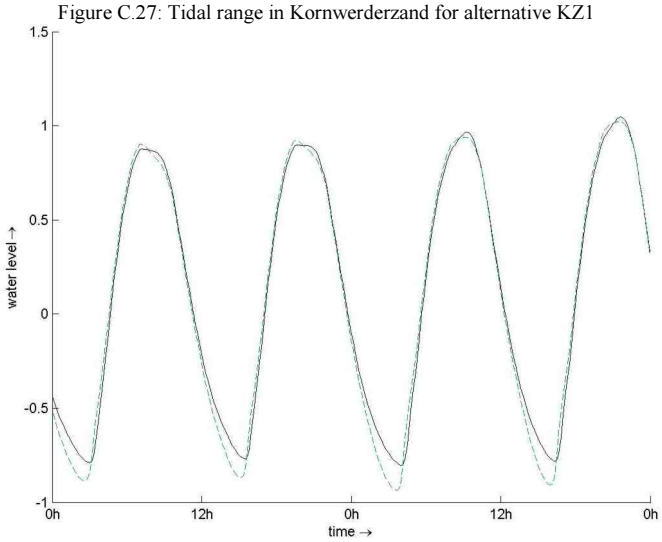

Figure C.29: Tidal range in Kornwerderzand for alternative LW1

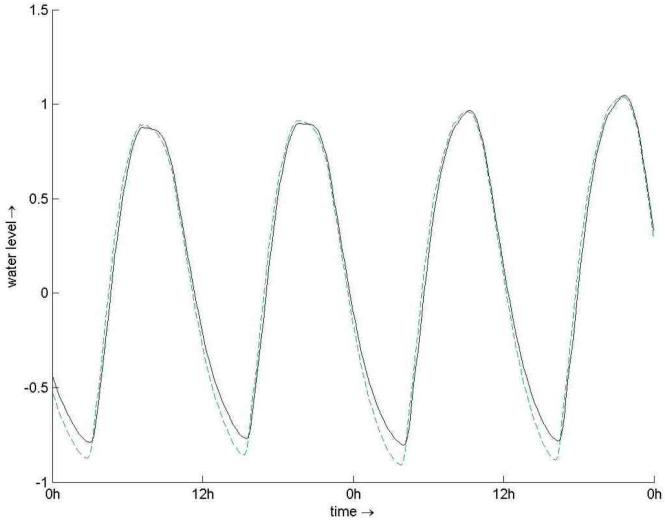

Figure C.30: Tidal range in Kornwerderzand for alternative LW2

Appendix D

Parameters ASMITA

The derivation of the volumetric parameters: area and volume of the channel, flat and delta elements is subject of this appendix. Besides these volumetric parameters, the ASMITA model requires parameters expressing the sediment exchange capacity between and inside elements. The significance of these parameters are treated at the end of this appendix.

With the Delft3D-FLOW computations, the ebb and flood volume through the inlets is obtained. According to Gerritsen (1990) the tidal prism equals half the tidal volume, thus:

$$P = 0.5 \cdot (FV + EV) \tag{D.1}$$

In which:
P: Tidal prism [m^3]
FV: Flood volume through the inlet per tide [m^3]
EV: Ebb volume through the inlet per tide [m^3]

With this relation, the modelled ebb and flood volumes can be translated in tidal prism.

Calculation of the volumetric values in Current Situation with values from Eysink (1993)
Because the tidal prism, obtained with the Delft3D-FLOW computations, does not correspond with the tidal prism published by Eysink (1993), new values of the basin's volumetric parameters are determined for the current situation. The latter is needed to calculate the change in volumetric parameters induced by the construction of the reservoir. The proportion between the tidal prism published by Eysink (1993) and the modelled tidal prism are used to determine the new values for the volumetric parameters.

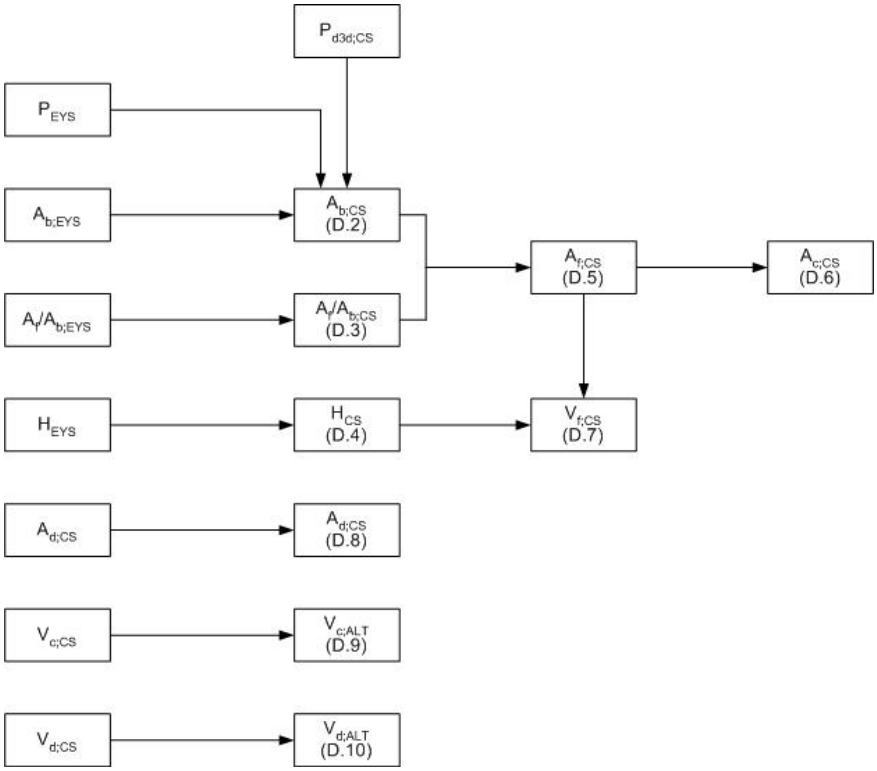

Figure D.1: Flow diagram for determination parameters basin in current situation with tidal prism Delft3D-FLOW

In Figure D.1 the follow relations are used:

For the area of the basin:

$$A_{b;CS} = A_{b;EYS} \cdot \left(\frac{P_{d3d;CS}}{P_{EYS}} \right) \tag{D.2}$$

For the relation between the area of the basin and the flat:

$$\left(\frac{A_f}{A_b} \right)_{CS} = \left(\frac{A_f}{A_b} \right)_{EYS} \tag{D.3}$$

For the tidal range:

$$H_{CS} = H_{EYS} \tag{D.4}$$

For the area of the flat-element:

$$A_{f;CS} = \left(\frac{A_f}{A_b} \right)_{CS} \cdot A_{b;CS} \tag{D.5}$$

For the area of the channel-element:

$$A_{c;CS} = A_{b;CS} - A_{f;CS} \tag{D.6}$$

For the volume of the flat-element:

$$V_{f;CS} = A_{b;CS} \cdot H_{CS} - P_{d3d;CS} \tag{D.7}$$

For the area of the delta-element:

$$A_{d;CS} = A_{d;EYS} \cdot \left(\frac{P_{d3d;CS}}{P_{EYS}} \right)^{1.23} \tag{D.8}$$

For the volume of the delta-element:

$$V_{d;CS} = V_{d;EYS} \cdot \left(\frac{P_{d3d;CS}}{P_{EYS}} \right)^{1.23} \tag{D.9}$$

For the volume of the channel-element:

$$V_{c;CS} = V_{c;EYS} \cdot \left(\frac{P_{d3d;CS}}{P_{EYS}} \right)^{1.55} \tag{D.10}$$

Calculation of the volumetric parameters in a certain alternative
Due to the construction of the reservoir, part of the tidal basin is excluded from the basin and both flat and channel areas diminish. However, the construction of a reservoir does not only influence the basin where the reservoir is constructed (basin p), but also the adjacent basins (basin n and basin m). Basin n and m are influenced by the reservoir due to the displacement of the tidal divides. When the displacements of the tidal divides are known, the volumetric parameters of are known for basin n, m and p.

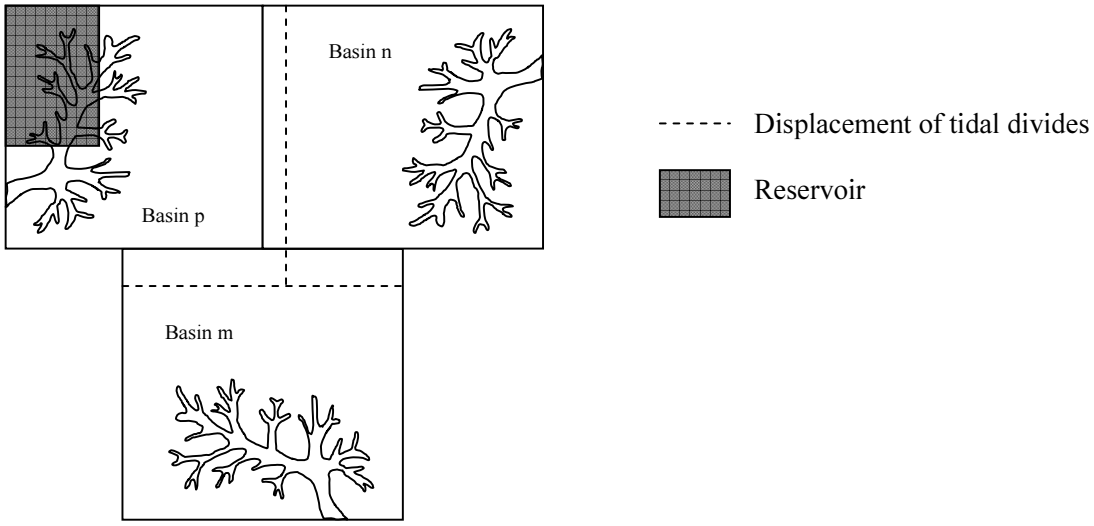

Figure D.2: Schematisation of basins, reservoir and shifts of tidal basins

Calculation of the elements in basin without reservoir (basin n/m)
By means of the values for the tidal inlet system (Eysink, 1993) and the modelled tidal prism, the new tidal basin area can be defined with the assumption that h_{mean_flat} and the tidal range are not affected by the reservoir.

With the general relation:

$$P = A_b \cdot H - V_f \tag{D.11}$$

and:

$$V_f = h_{mean\_flat} \cdot A_f \tag{D.12}$$

the new surface area of basin n or m is:

$$A_{b\_n,m;ALT} = \left(\frac{P_{d3d;ALT} - A_{c\_n,m;ALT} \cdot h_{mean\_flat}}{H - h_{mean\_flat}} \right) \tag{D.13}$$

where:
$A_{b\_n,m;ALT}$: surface area for basin n or m, after human intervention in basin p [m^2]

P_{ALT}: tidal prism for basin n or m, after human intervention in basin p [m^3]
$A_{c\_n,m;ALT}$: surface area channel in basin n or m, after human intervention in basin p [m2]
H: tidal range in basin n or m [m]
h_{mean_flat}: mean high of flats in basin n or m [m]

If assumed that the channel area does not immediately change with a displacement of the tidal divides, the new flats area can be defined:

$$A_{f\_n,m;ALT} = A_{b\_n,m;ALT} - A_{c\_CS} \tag{D.14}$$

For the area of the delta the initial area does not change whether an intervention has occurred or not.

$$A_{d;ALT} = A_{d;CS} \tag{D.15}$$

To determine the initial volume of the flat element the general relation D.11 is used. To determine the initial volume of the delta and the channel in basin n or m after the human intervention in basin p, a relation between channel volume and channel area is applied:

$$V_{c\_p;ALT} = V_{c\_p;CS} \cdot \left(\frac{A_{c\_p;ALT}}{A_{c\_p;CS}} \right) \tag{D.16}$$

Due to the assumption that the channel area does not change immediately, relation (D.16) reduces to:

$$V_{c;ALT} = V_{c;CS} \tag{D.17}$$

and

$$V_{d;ALT} = V_{d;CS} \tag{D.18}$$

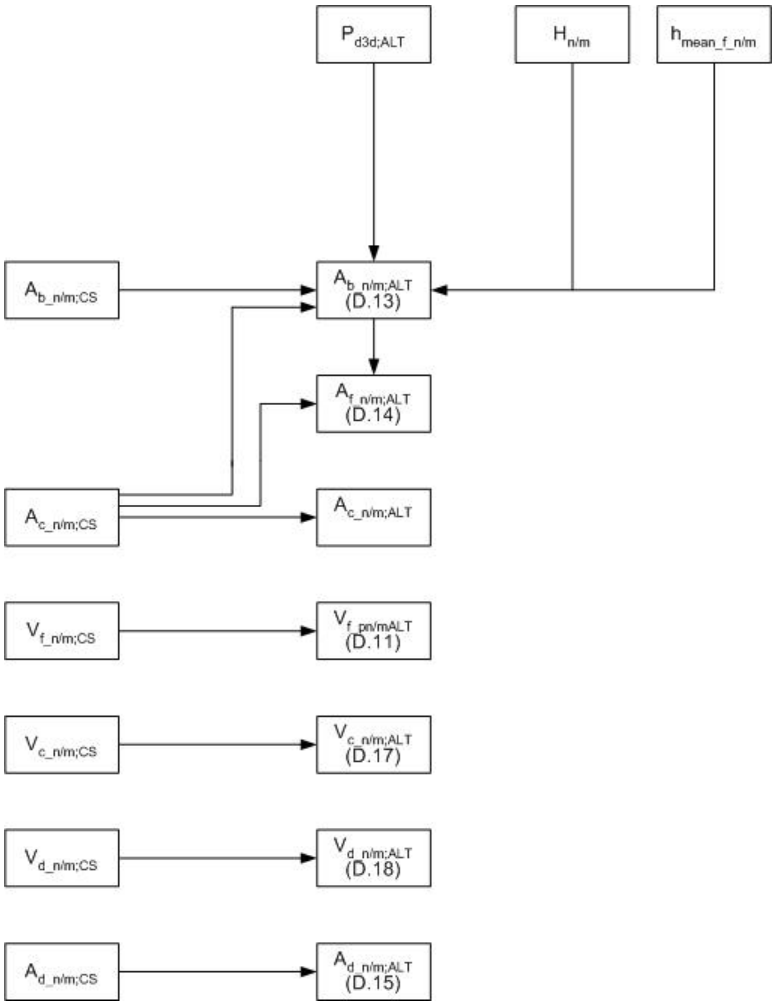

Figure D.3: Flow diagram for determination parameters in basin n or m

Calculation of elements in basin with reservoir (basin p)

If the new areas of the adjacent basins (basin n or m) are known, the area of basin p (basin with reservoir) can be determined as follow:

$$A_{b\_p;ALT} = A_{b\_p;CS} + (A_{b\_n;CS} - A_{b\_n;ALT}) + (A_{b\_m;CS} - A_{b\_m;ALT}) - A_{hi} \quad \text{(D.19)}$$

in which

$A_{b\_p;ALT}$: surface area basin p, after human intervention in basin [m^2]
$A_{b\_p;CS}$: surface area basin p, in current situation [m^2]
$A_{b\_n;ALT}$: surface area adjacent basin n, after human intervention in basin p [m^2]
$A_{b\_n;CS}$: surface area adjacent basin n, in current situation [m^2]
$A_{b\_m;ALT}$: surface area adjacent basin m, after human intervention in basin p [m^2]

$A_{b\_m;CS}$: surface area adjacent basin m, in current situation [m^2]
A_{hi}: surface area of human intervention (e.g. reservoir) [m^2]

To determine the flat area in basin p:

$$A_{f\_p;ALT} = A_{f\_p;CS} + (A_{f\_n;CS} - A_{f\_n;ALT}) + (A_{f\_m;CS} - A_{f\_m;ALT}) - A_{f\_hi} \quad \text{(D.20)}$$

where:

$A_{f\_p;ALT}$: surface area flat in basin p, after human intervention in basin [m^2]
$A_{f\_p;CS}$: surface area flat in basin p, in current situation [m^2]
$A_{f\_n;ALT}$: surface area flat in adjacent basin n, after human intervention in basin p [m^2]
$A_{f\_n;CS}$: surface area flat in adjacent basin n, in current situation [m^2]
$A_{f\_m;ALT}$: surface area flat in adjacent basin m, after human intervention in basin p [m^2]
$A_{f\_m;CS}$: surface area flat in adjacent basin m, in current situation [m^2]
A_{f_hi}: surface area flat in human intervention (e.g. reservoir) [m^2]

And channel area:

$$A_{c\_p;ALT} = A_{c\_p;CS} - A_{c\_p;hi} \quad \text{(D.21)}$$

in which:

$A_{c\_p;ALT}$: surface area channel in basin p, after human intervention in basin p [m^2]
$A_{c\_p;CS}$: surface area channel in basin p, in current situation [m^2]
$A_{c\_p;hi}$: surface area channel in human intervention (e.g. reservoir) [m^2]

The volume of the flat is determined with:

$$V_{f\_p;ALT} = V_{f\_p;CS} + (V_{f\_n;CS} - V_{f\_n;ALT}) + (V_{f\_m;CS} - V_{f\_m;ALT}) - A_{f\_hi} \cdot h_{mean\_flat} \quad \text{(D.22)}$$

where:

$V_{f\_p;ALT}$: volume of flats in basin p after human intervention [m^3]
$V_{f\_p;CS}$: volume of flats in basin p in the current situation [m^3]
$V_{f\_n;ALT}$: volume of flats in basin n after human intervention in basin p [m^3]

$V_{f\_n;CS}$: volume of flats in basin n for the current situation [m^3]
$V_{f\_m;ALT}$: volume of flats in basin m after human intervention in basin p [m^3]
$V_{f\_m;CS}$: volume of flats in basin m for the current situation [m^3]

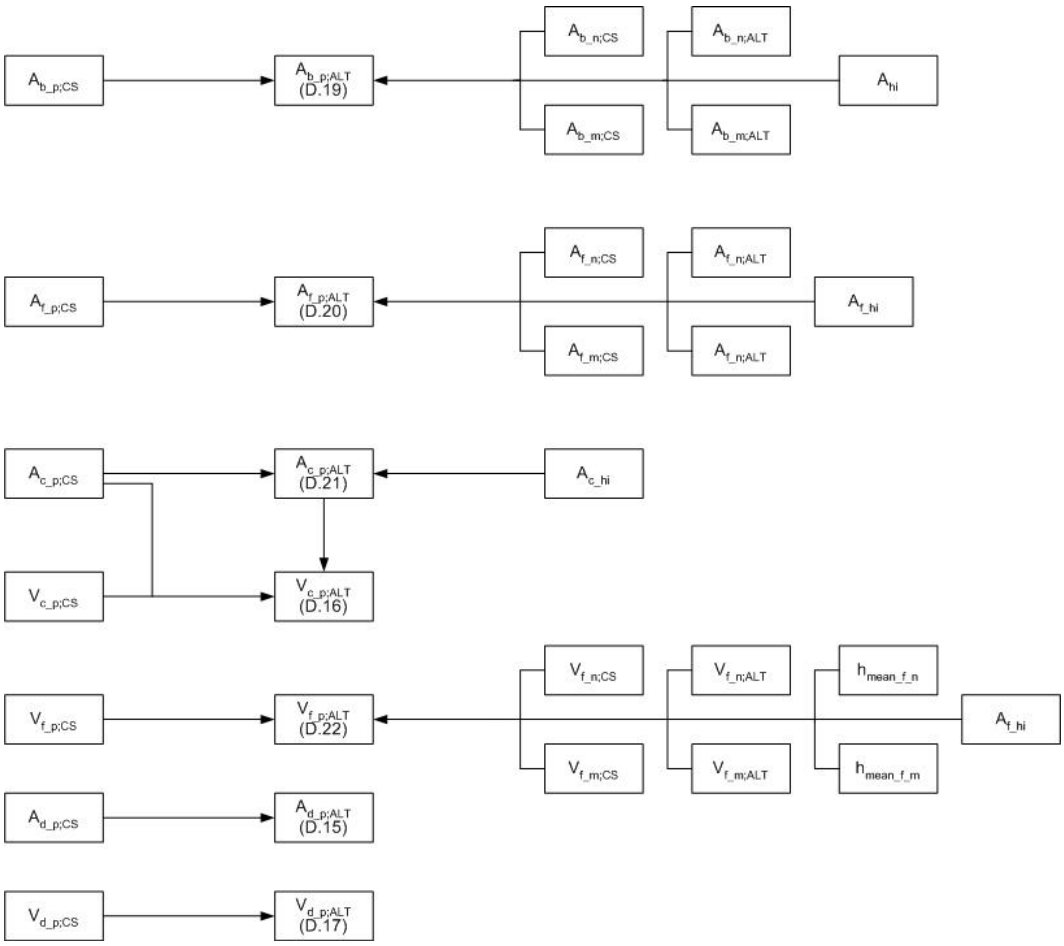

Figure D.4: Flow diagram for determination parameters in basin p

Besides the geometric parameters of the tidal inlet system other parameters are required for the ASMITA model. These parameters represent the capability of sediment transport within and between elements.

Vertical sediment exchange (w_{sf}, w_{sc}, w_{sd})
This parameter represents the net vertical exchange in the element per unit area, per second. Although this parameter seems to represent the fall velocity, (it has the same dimension) it is a sediment exchange between the bottom and the water volume. Buijsman (1997) used values between 1e-5 and 1e-4 m/s.

Horizontal sediment exchange (δ_{do}, δ_{dc}, δ_{fc})
If tide is dominating the system, tidal asymmetry leads to a non-zero tide-residual transport of sediment. At the aggregated scale in ASMITA, this net effect is described with a diffusion type of

sediment transport. The diffusion coefficient represents the sediment exchange capacity between two adjacent elements. Buijsman (1997) used values between 500 m^3/s and 1500 m^3/s for the Zoutkamperlaag.

n-parameter
This parameter is used in the definition of the local equilibrium concentration. Based on the non-linear relation between sediment transport and mean velocity, the value for this parameter is 2 (Buijsman, 1997; Van Goor, 2001), which is in correspondence with a third power for sediment transport formula.

Overall equilibrium concentration in the outside world (c_E)
The outside world is represented by the adjacent coast and offshore area. It is assumed that the concentration in the outside world is found in all elements of the tidal inlet system. The equilibrium concentration is mainly determined by longshore transport. By estimating the sediment transport caused by waves, the magnitude of the concentration can be derived. Along the Dutch coast, the sediment transport is about 1 to 2 million m^3. According to Van Goor (2001) this leads to a concentration between 1.2e-4 and 2.4e-4, Buijsman used 2e-4.

Appendix E

Results ASMITA

Input ASMITA for Current Situation

Input parameter		Marsdiep	Eierlandse Gat	Vlie
V_f	[$*10^6$ m^3]	70.42	59.46	128.75
V_c	[$*10^6$ m^3]	2426.13	107.65	830.81
V_d	[$*10^6$ m^3]	530.82	131.75	244.91
A_f	[$*10^6$ m^2]	133.64	97.07	236.55
A_c	[$*10^6$ m^2]	551.71	60.77	289.12
A_d	[$*10^6$ m^2]	138.25	36.89	155.65
H	[m]	1.65	1.65	1.9
Coefficient a for V_{fe}[3]	[-]	0.3	0.3	0.3
Coefficient a for V_c	[$m^{-1.55}$]	1.6e-5	1.6e-5	1.6e-5
Coefficient b for V_c	[-]	1.55	1.55	1.55
Coefficient a for V_d	[$m^{-1.23}$]	6.57e-3	6.57e-3	6.57e-3
Coefficient b for V_d	[-]	1.23	1.23	1.23
w_{sf}	[m/s]	1.0e-5	1.0e-5	1.0e-5
w_{sc}	[m/s]	1.0e-5	1.0e-5	1.0e-5
w_{sd}	[m/s]	1.0e-5	1.0e-5	1.0e-5
δ_{fc}	[m^3/s]	1.5e3	1.5e3	1.5e3
δ_{dc}	[m^3/s]	1.5e3	1.5e3	1.5e3
δ_{do}	[m^3/s]	1.5e3	1.5e3	1.5e3
c_E	[-]	2.0e-4	2.0e-4	2.0e-4
n	[-]	2	2	2

[3] Stive et al. (1997)

Results ASMITA for Marsdiep in current situation

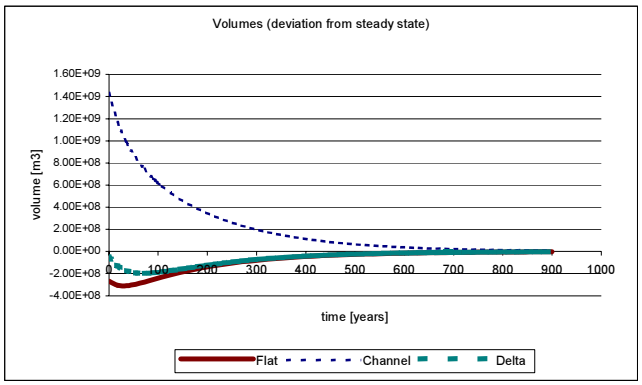

Figure E.1: Development of elements Marsdiep, current situation

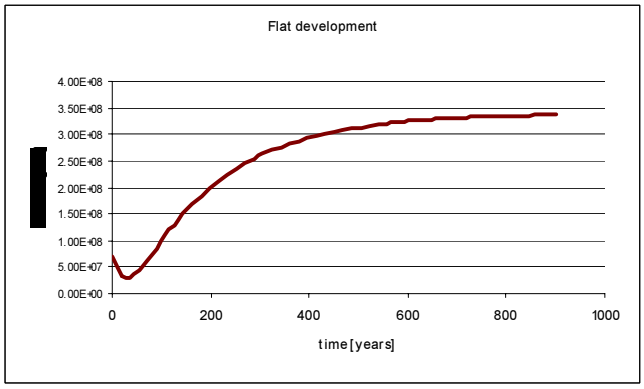

Figure E.2: Development of flats Marsdiep, current situation

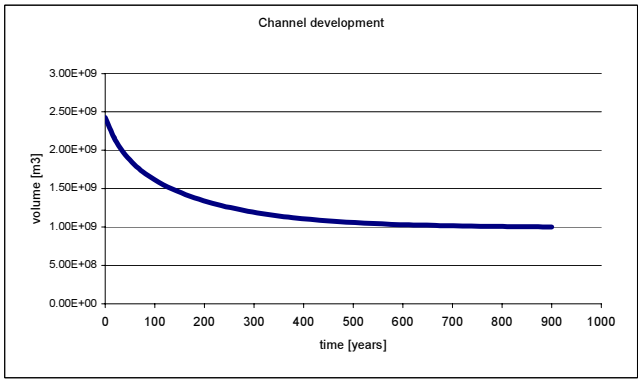

Figure E.3: Development of channels Marsdiep, current situation

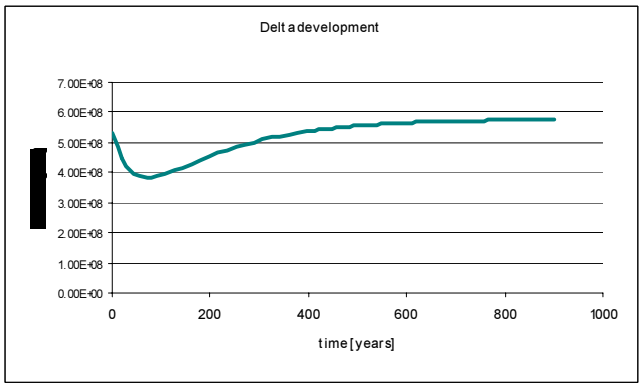

Figure E.4: Development of delta Marsdiep, current situation

Marsdiep System time scales:

180 years
30 years
46 years

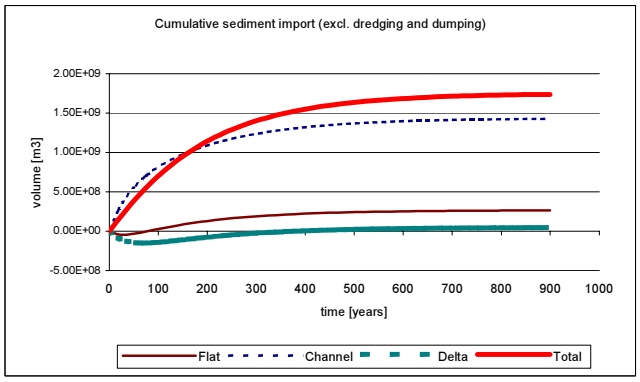

Figure E.5: Cumulative sediment import Marsdiep, current situation

Results ASMITA for Eierlandse Gat in current situation

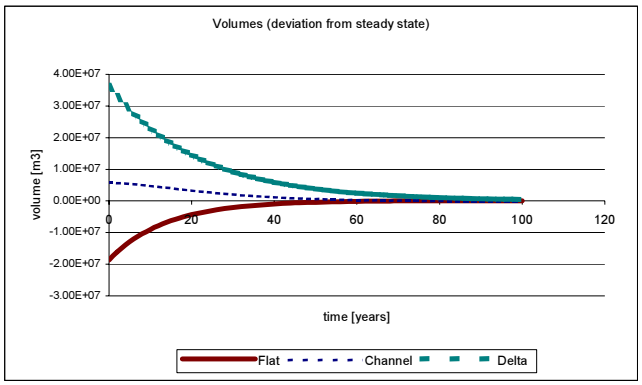

Figure E.6: Development of elements Eierlandse Gat, current situation

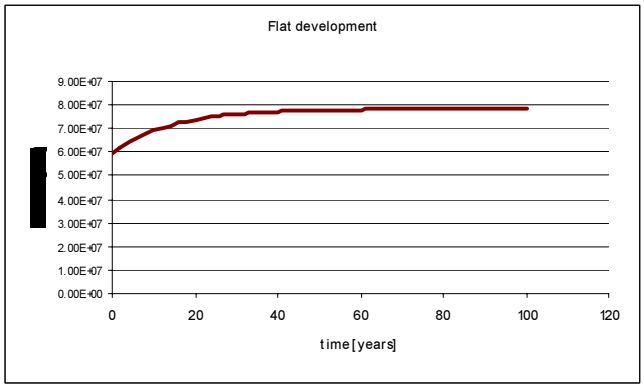

Figure E.7: Development of flats Eierlandse Gat, current situation

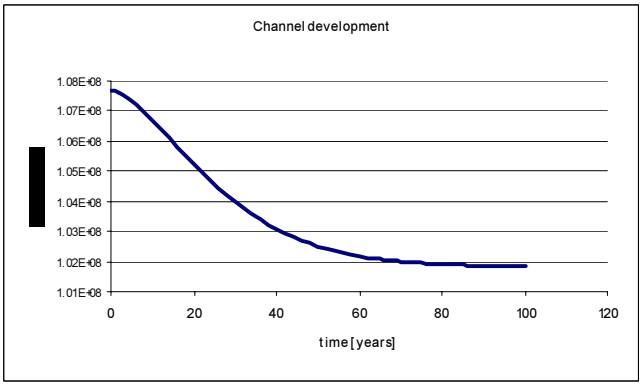

Figure E.8: Development of channels Eierlandse Gat, current situation

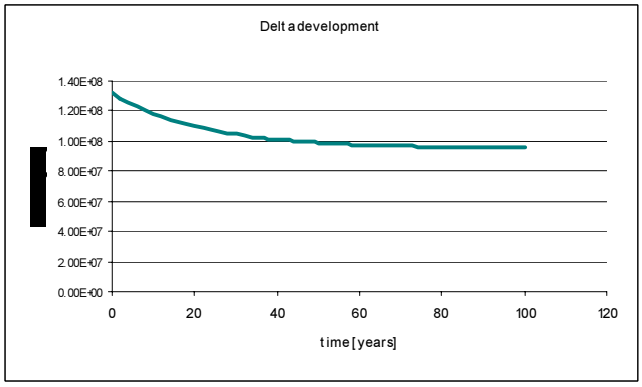

Figure E.9: Development of delta Eierlandse Gat, current situation

Eierlandse Gat system time scales:

36 years
12 years
21 years

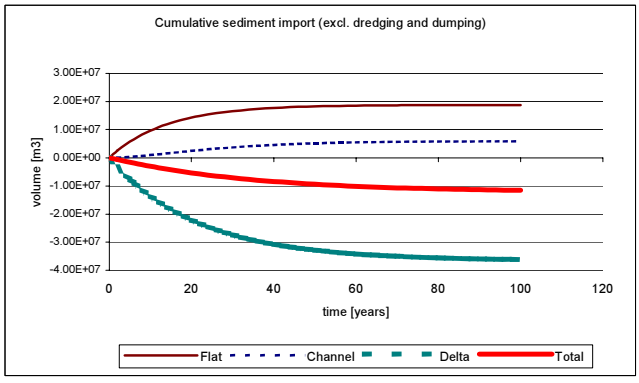

Figure E.10: Cumulative sediment transport Eierlandse Gat, current situation

Results ASMITA for Vlie in current situation

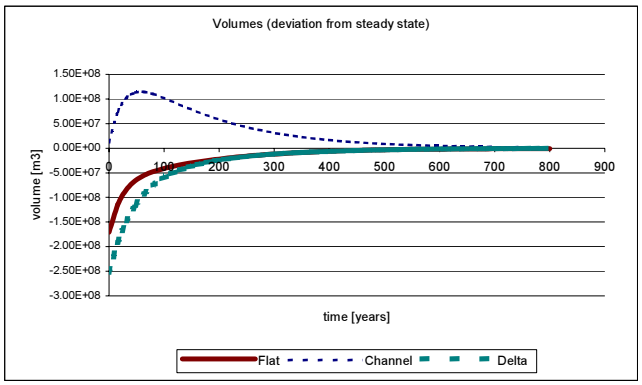

Figure E.11: Development of elements Vlie, current situation

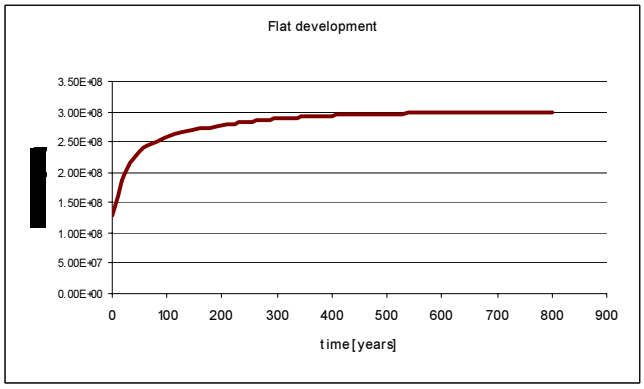

Figure E.12: Development of flats Vlie, current situation

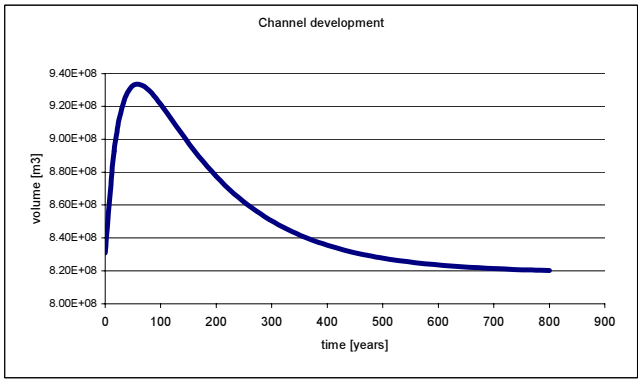

Figure E.13: Development of channels Vlie, current situation

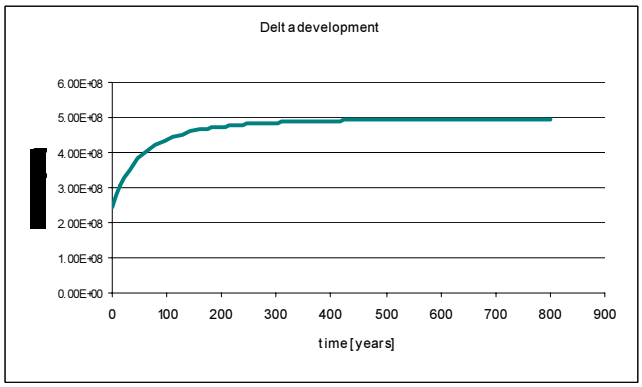

Figure E.14: Development of delta Vlie, current situation

Vlie system time scales

157 years
25 years
44 years

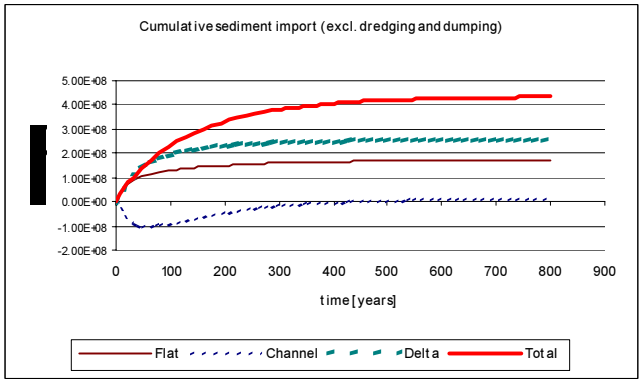

Figure E.15: Cumulative sediment import Vlie, current situation

Input ASMITA for alternative AD1

Input parameter		Marsdiep	Eierlandse Gat	Vlie
V_f	[$*10^6$ m^3]	87.65	47.63	116.07
V_c	[$*10^6$ m^3]	1725.04	107.65	830.81
V_d	[$*10^6$ m^3]	530.82	131.75	244.91
A_f	[$*10^6$ m^2]	162.45	77.76	213.25
A_c	[$*10^6$ m^2]	392.28	60.77	289.12
A_d	[$*10^6$ m^2]	138.25	36.89	115.65
H	[m]	1.65	1.65	1.9
Coefficient a for V_{fe}	[-]	0.3	0.3	0.3
Coefficient a for V_c	[$m^{-1.55}$]	1.6e-5	1.6e-5	1.6e-5
Coefficient b for V_c	[-]	1.55	1.55	1.55
Coefficient a for V_d	[$m^{-1.23}$]	6.57e-3	6.57e-3	6.57e-3
Coefficient b for V_d	[-]	1.23	1.23	1.23
w_{sf}	[m/s]	1.0e-5	1.0e-5	1.0e-5
w_{sc}	[m/s]	1.0e-5	1.0e-5	1.0e-5
w_{sd}	[m/s]	1.0e-5	1.0e-5	1.0e-5
δ_{fc}	[m^3/s]	1.5e3	1.5e3	1.5e3
δ_{dc}	[m^3/s]	1.5e3	1.5e3	1.5e3
δ_{do}	[m^3/s]	1.5e3	1.5e3	1.5e3
c_E	[-]	2.0e-4	2.0e-4	2.0e-4
n	[-]	2	2	2

Results ASMITA for Marsdiep with alternative AD1

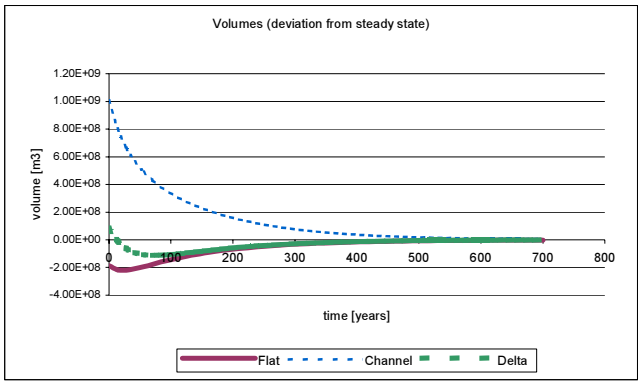

Figure E.16: Development of elements Marsdiep, alternative AD1

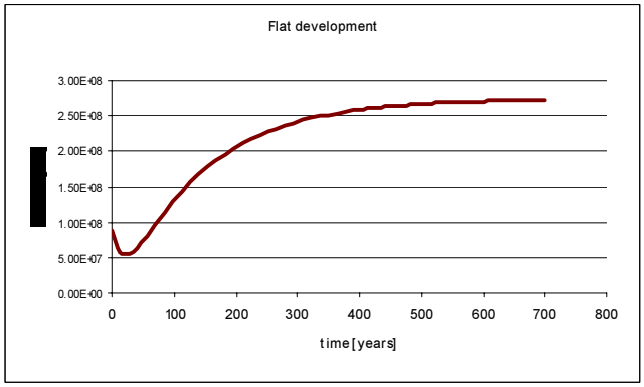

Figure E.17: Development of flats Marsdiep, alternative AD1

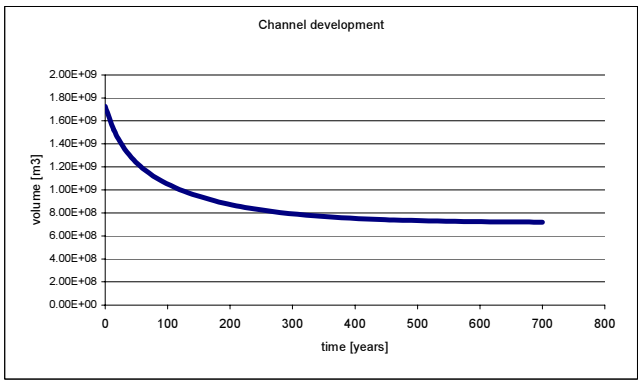

Figure E.18: Development of channels Marsdiep, alternative AD1

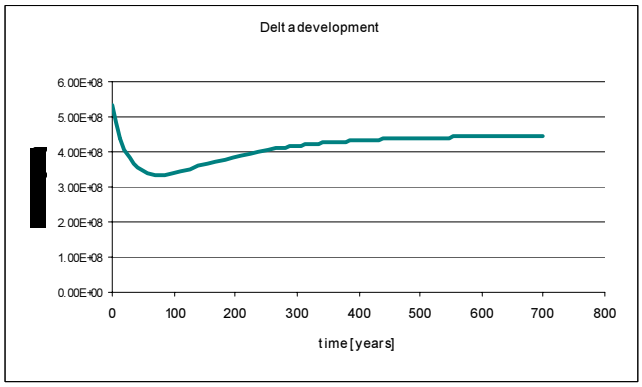

Figure E.19: Development of delta Marsdiep, alternative AD1

Marsdiep system time scales:
137 years
23 years
36 years

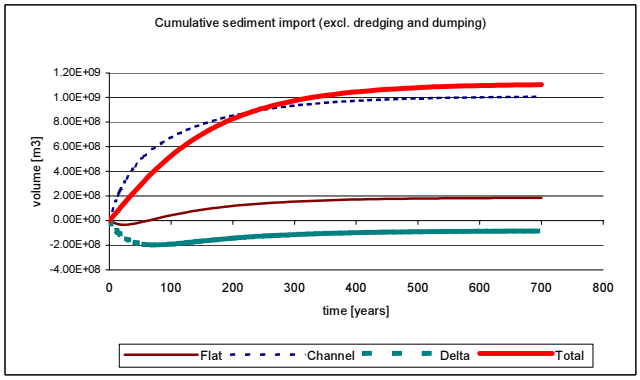

Figure E.20: Cumulative sediment import Marsdiep, alternative AD1

Results ASMITA for Eierlandse Gat with alternative AD1

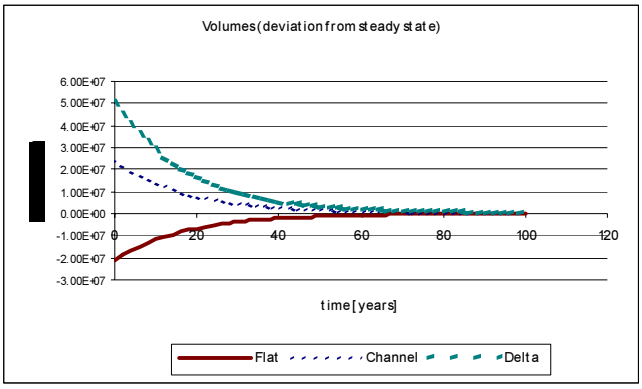

Figure E.21: Development of elements Eierlandse Gat, alternative AD1

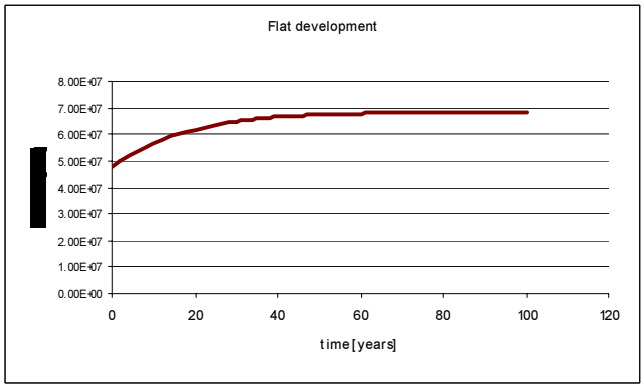

Figure E.22: Development of flats Eierlandse Gat, alternative AD1

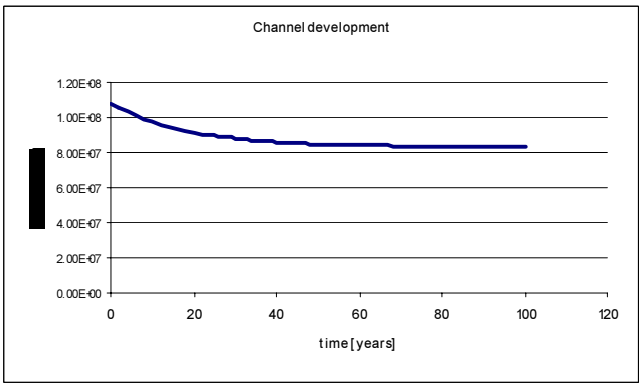

Figure E.23: Development of channels Eierlandse Gat, alternative AD1

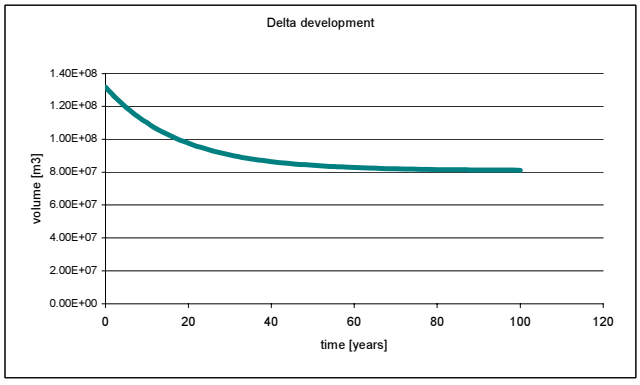

Figure E.24: Development of delta Eierlandse Gat, alternative AD1

Eierlandse Gat system time scales:
31 years
11 years
18 years

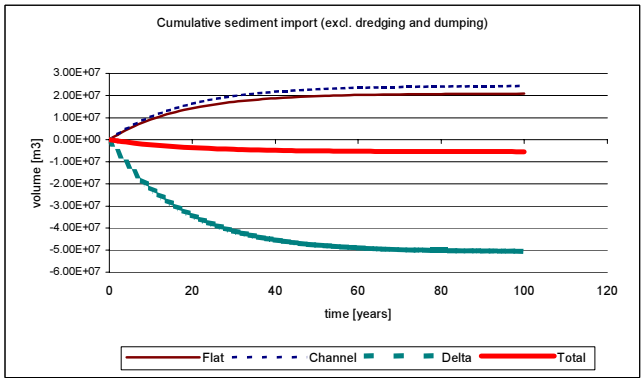

Figure E.25: Cumulative sediment import Eierlandse Gat, alternative AD1

Results ASMITA for Vlie with alternative AD1

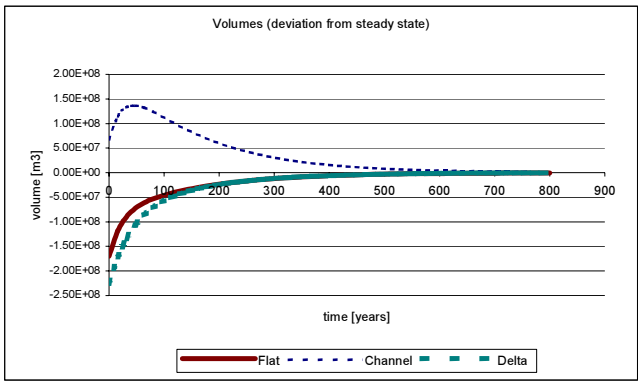

Figure E.26: Development of elements Vlie, alternative AD1

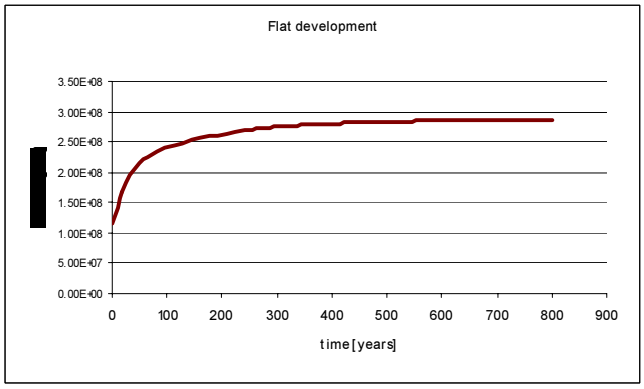

Figure E.27: Development of flats Vlie, alternative AD1

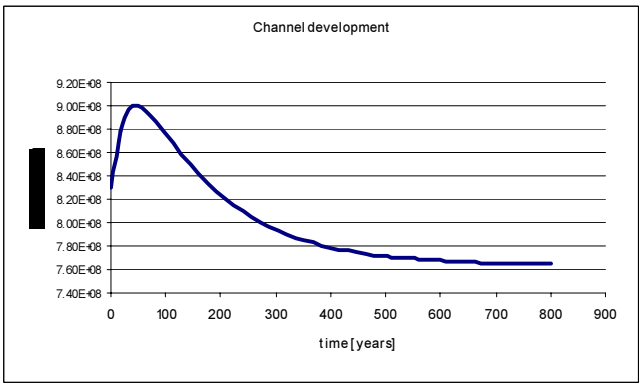

Figure E.28: Development of channels Vlie, alternative AD1

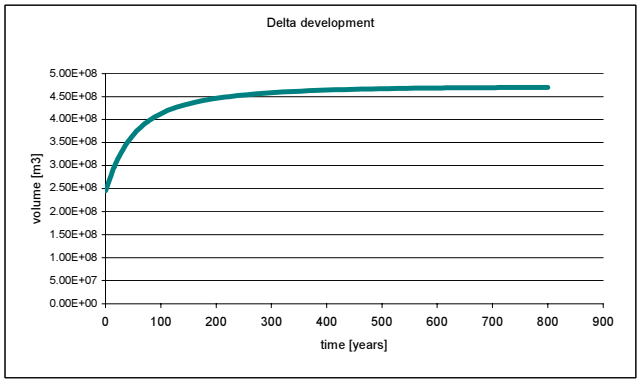

Figure E.29: Development of delta Vlie, alternative AD1

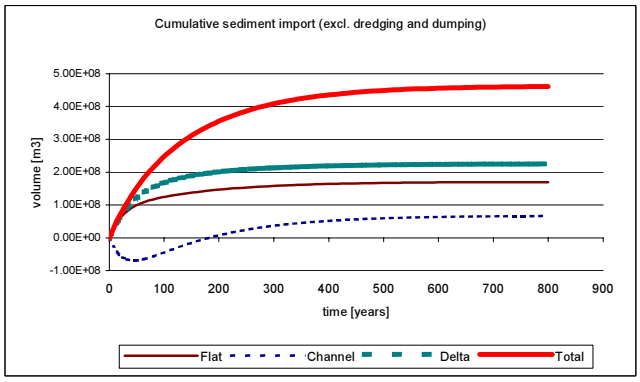

Figure E.30: Cumulative sediment import Vlie, alternative AD1

Vlie system time scales:
148 years
24 years
42 years

Input ASMITA for alternative AD2

Input parameter		Marsdiep	Eierlandse Gat	Vlie
V_f	[$*10^6$ m^3]	83.30	51.68	119.13
V_c	[$*10^6$ m^3]	1959.74	107.65	830.81
V_d	[$*10^6$ m^3]	530.82	131.75	244.91
A_f	[$*10^6$ m^2]	155.44	84.37	218.89
A_c	[$*10^6$ m^2]	445.65	60.77	289.12
A_d	[$*10^6$ m^2]	138.25	36.89	115.65
H	[m]	1.65	1.65	1.9
Coefficient a for V_{fe}	[-]	0.3	0.3	0.3
Coefficient a for V_c	[$m^{-1.55}$]	1.6e-5	1.6e-5	1.6e-5
Coefficient b for V_c	[-]	1.55	1.55	1.55
Coefficient a for V_d	[$m^{-1.23}$]	6.57e-3	6.57e-3	6.57e-3
Coefficient b for V_d	[-]	1.23	1.23	1.23
w_{sf}	[m/s]	1.0e-5	1.0e-5	1.0e-5
w_{sc}	[m/s]	1.0e-5	1.0e-5	1.0e-5
w_{sd}	[m/s]	1.0e-5	1.0e-5	1.0e-5
δ_{fc}	[m^3/s]	1.5e3	1.5e3	1.5e3
δ_{dc}	[m^3/s]	1.5e3	1.5e3	1.5e3
δ_{do}	[m^3/s]	1.5e3	1.5e3	1.5e3
c_E	[-]	2.0e-4	2.0e-4	2.0e-4
n	[-]	2	2	2

Results ASMITA for Marsdiep with alternative AD2

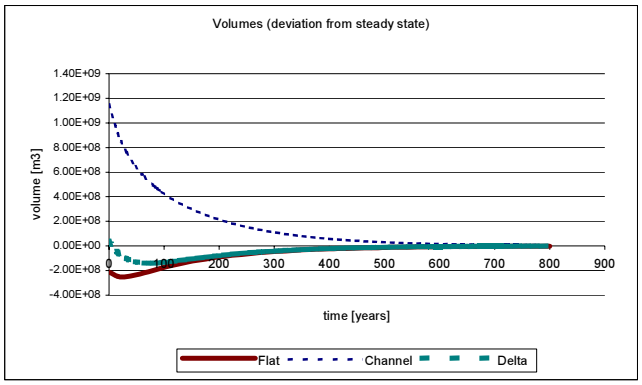

Figure E.31: Development of elements Marsdiep, alternative AD2

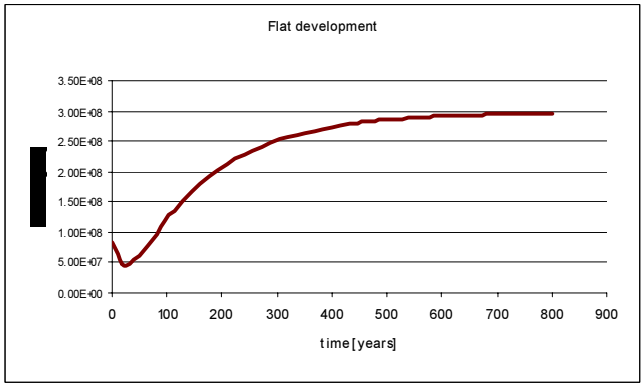

Figure E.32 Development of flats Marsdiep, alternative AD2

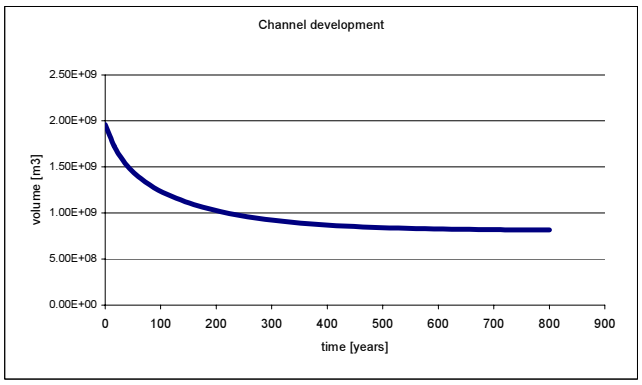

Figure E.33: Development of channels Marsdiep, alternative AD2

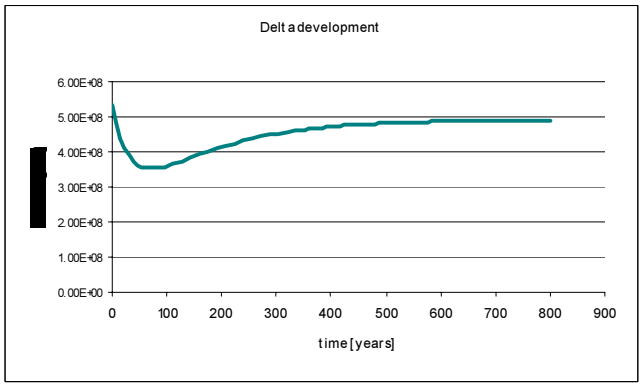

Figure E.34: Development of delta Marsdiep, alternative AD2

Marsdiep system time scales:
152 years
26 years
39 years

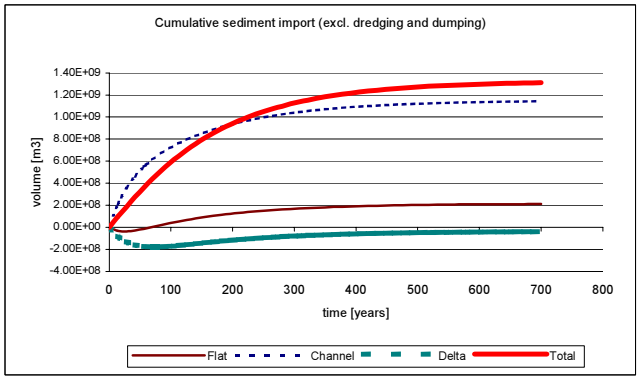

Figure E.35: Cumulative sediment import Marsdiep, alternative AD2

Results ASMITA for Eierlandse Gat with alternative AD2

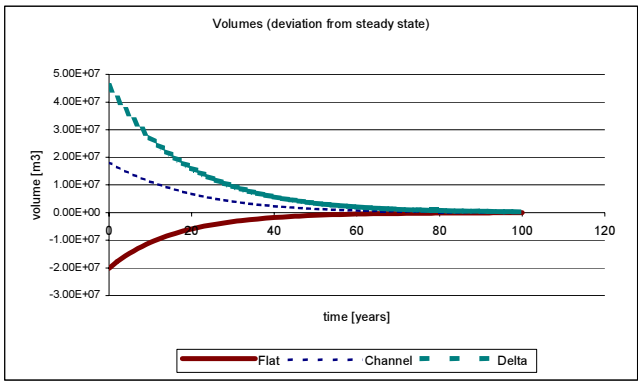

Figure E.36: Development of elements Eierlandse Gat, alternative AD2

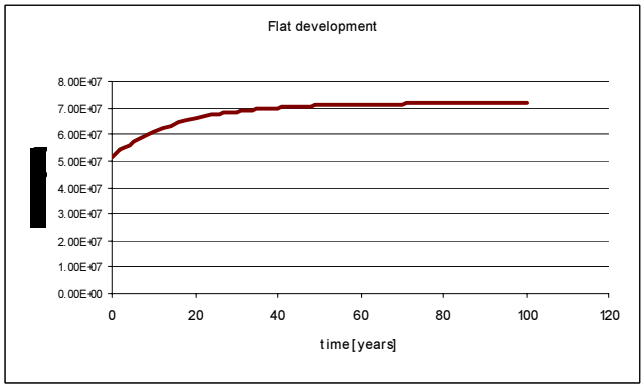

Figure E.37: Development of flats Eierlandse Gat, alternative AD2

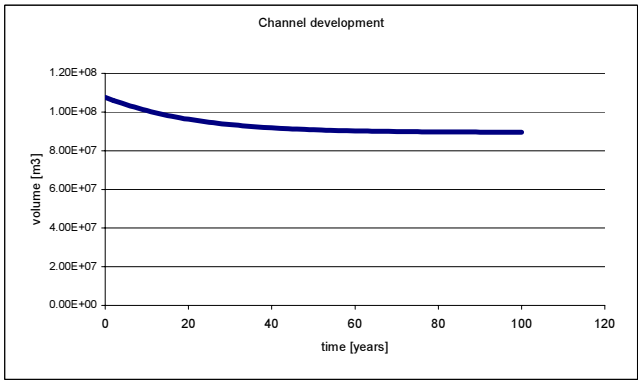

Figure E.38: Development of channels Eierlandse Gat, alternative AD2

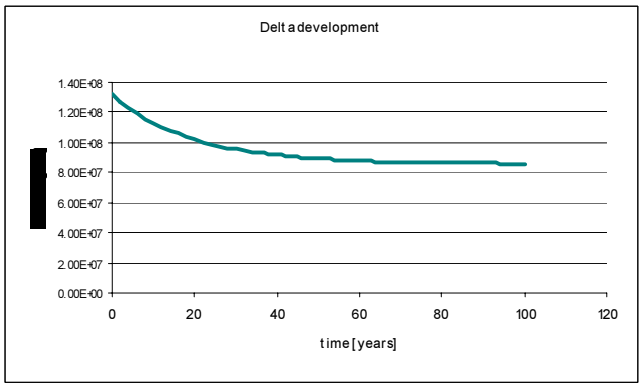

Figure E.39: Development of delta Eierlandse Gat, alternative AD2

Eierlandse Gat system time scales:

32 years
11 years
19 years

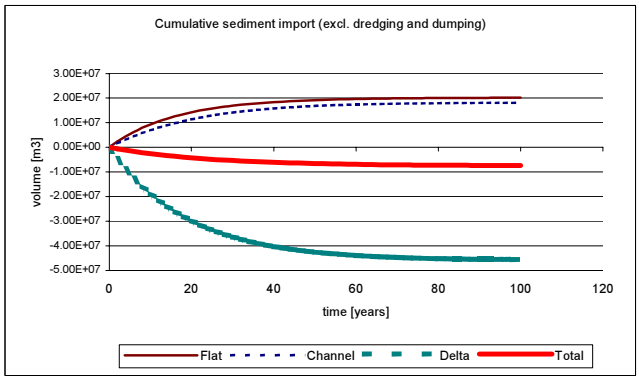

Figure E.40: Cumulative sediment transport Eierlandse Gat, alternative AD2

Results ASMITA for Vlie with alternative AD2

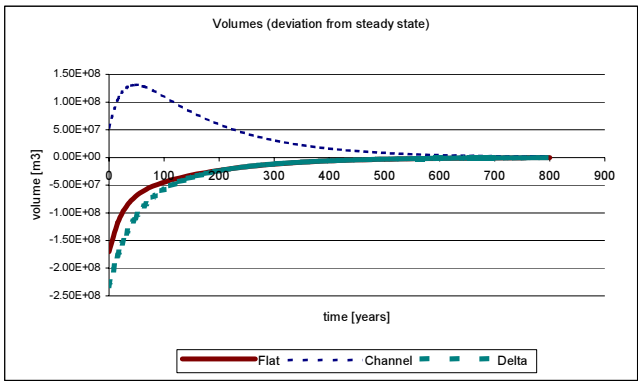

Figure E.41: Development of elements Vlie, alternative AD2

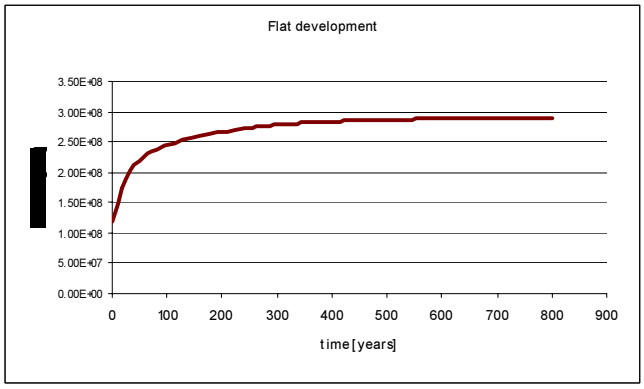

Figure E.42: Development of flats Vlie, alternative AD2

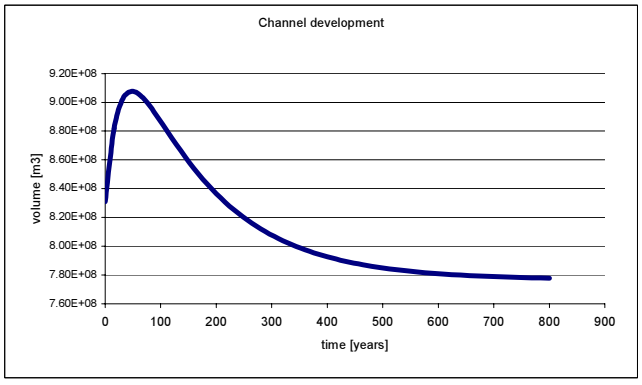

Figure E.43: Development of channels Vlie, alternative AD2

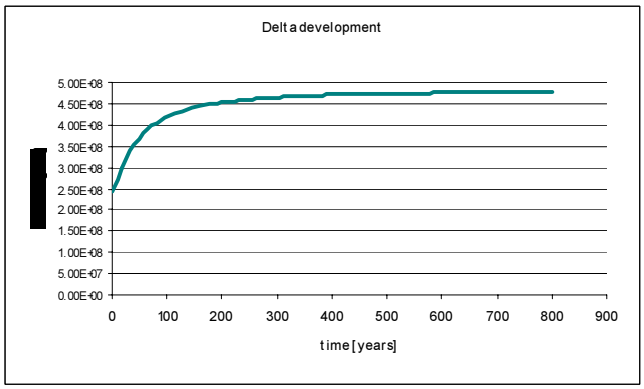

Figure E.44: Development of delta Vlie, alternative AD2

Vlie system time scales:

150 years
24 years
43 years

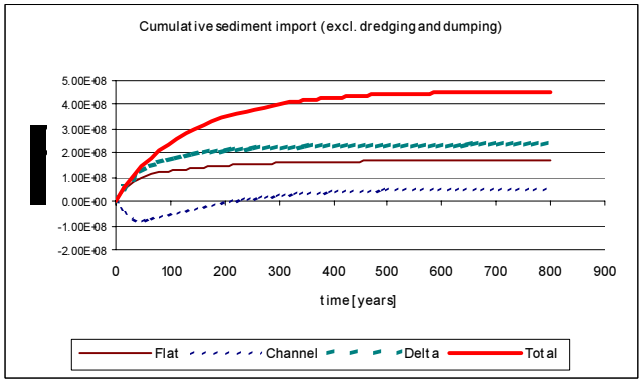

Figure E.45: Cumulative sediment import Vlie, alternative AD2

Input ASMITA for alternative AD3

Input parameter		Marsdiep	Eierlandse Gat	Vlie
V_f	[$*10^6$ m^3]	80.89	86.88	120.74
V_c	[$*10^6$ m^3]	2084.53	60.77	830.81
V_d	[$*10^6$ m^3]	530.82	36.89	244.91
A_f	[$*10^6$ m^2]	151.37	53.22	221.84
A_c	[$*10^6$ m^2]	474.03	107.65	289.12
A_d	[$*10^6$ m^2]	138.25	131.75	115.65
H	[m]	1.65	1.65	1.9
Coefficient a for V_{fe}	[-]	0.3	0.3	0.3
Coefficient a for V_c	[$m^{-1.55}$]	1.6e-5	1.6e-5	1.6e-5
Coefficient b for V_c	[-]	1.55	1.55	1.55
Coefficient a for V_d	[$m^{-1.23}$]	6.57e-3	6.57e-3	6.57e-3
Coefficient b for V_d	[-]	1.23	1.23	1.23
w_{sf}	[m/s]	1.0e-5	1.0e-5	1.0e-5
w_{sc}	[m/s]	1.0e-5	1.0e-5	1.0e-5
w_{sd}	[m/s]	1.0e-5	1.0e-5	1.0e-5
δ_{fc}	[m^3/s]	1.5e3	1.5e3	1.5e3
δ_{dc}	[m^3/s]	1.5e3	1.5e3	1.5e3
δ_{do}	[m^3/s]	1.5e3	1.5e3	1.5e3
c_E	[-]	2.0e-4	2.0e-4	2.0e-4
n	[-]	2	2	2

Results ASMITA for Marsdiep with alternative AD3

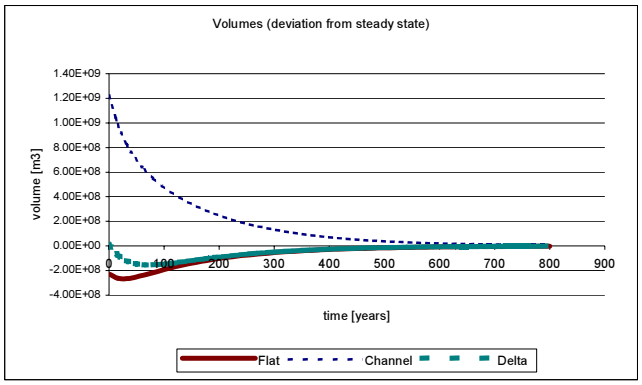

Figure E.46: Development of elements Marsdiep, alternative AD3

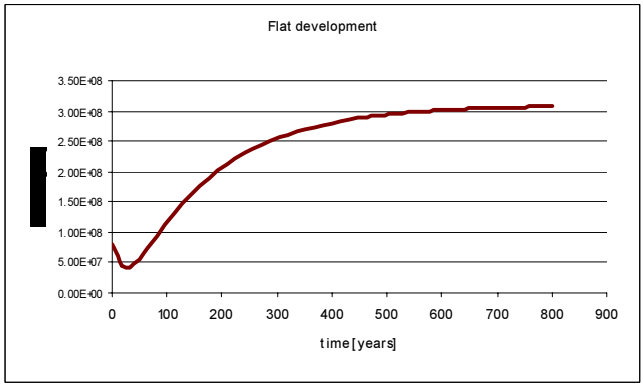

Figure E.47: Development of flats Marsdiep, alternative AD3

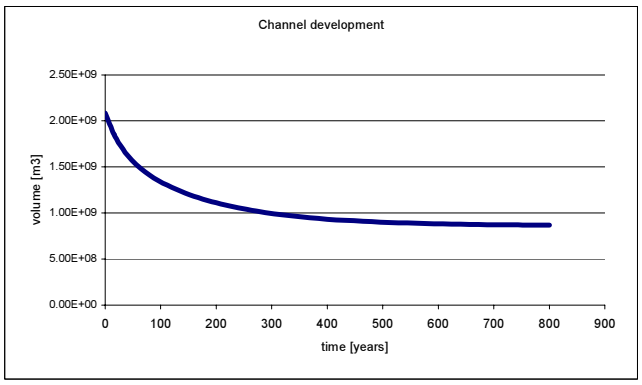

Figure E.48: Development of channels Marsdiep, alternative AD3

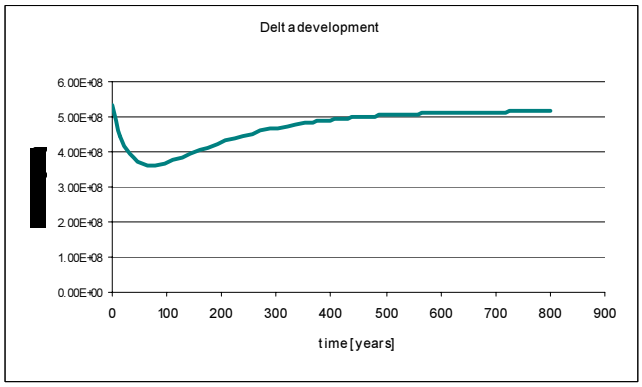

Figure E.49: Development of delta Marsdiep, alternative AD3

Marsdiep system time scales:

160 years
27 years
41 years

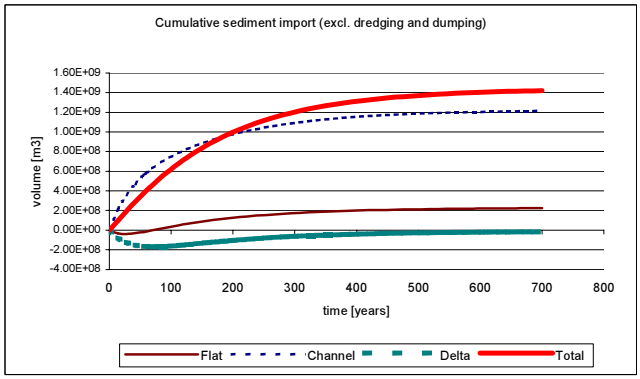

Figure E.50: Cumulative sediment import Marsdiep, alternative AD3

Results ASMITA for Eierlandse Gat with alternative AD3

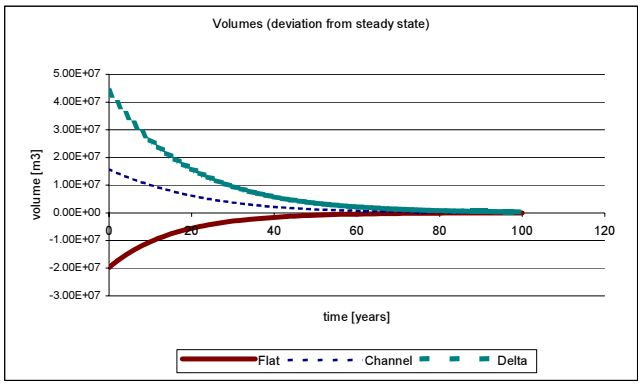

Figure E.51: Development of elements Eierlandse Gat, alternative AD3

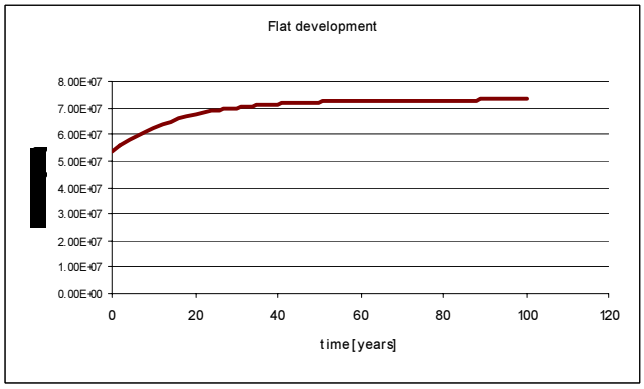

Figure E.52: Development of flats Eierlandse Gat, alternative AD3

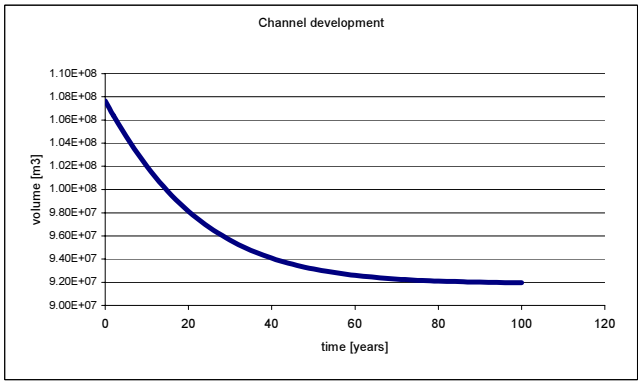

Figure E.53: Development of channels Eierlandse Gat, alternative AD3

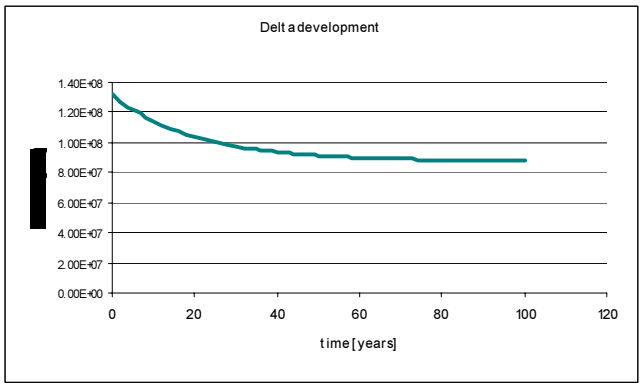

Figure E.54: Development of delta Eierlandse Gat, alternative AD3

Eierlandse Gat system time scales:

33 years
11 years
19 years

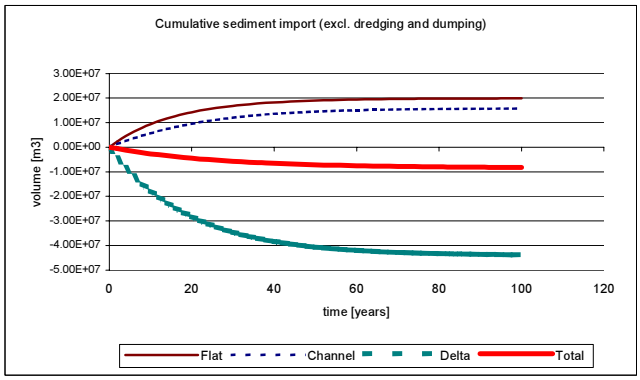

Figure E.55: Cumulative sediment import Eierlandse Gat, alternative AD3

Results ASMITA for Vlie with alternative AD3

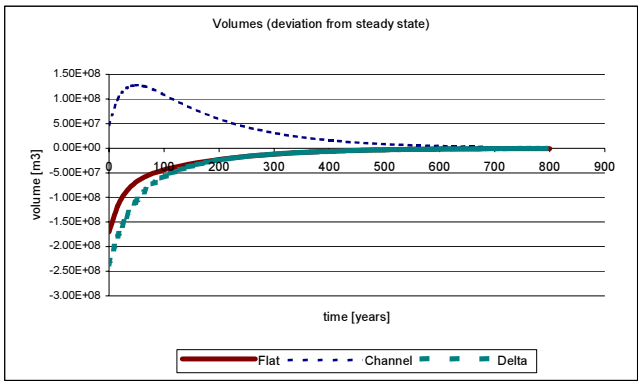

Figure E.56: Development of elements Vlie, alternative AD3

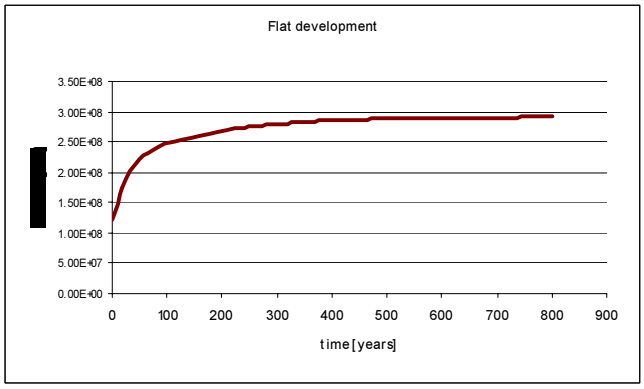

Figure E.57: Development of flats Vlie, alternative AD3

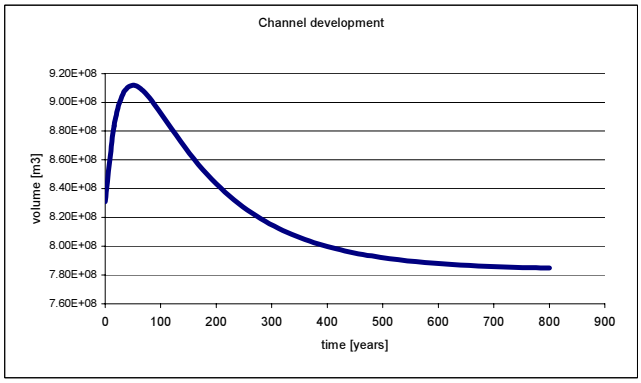

Figure E.58: Development of channels Vlie, alternative AD3

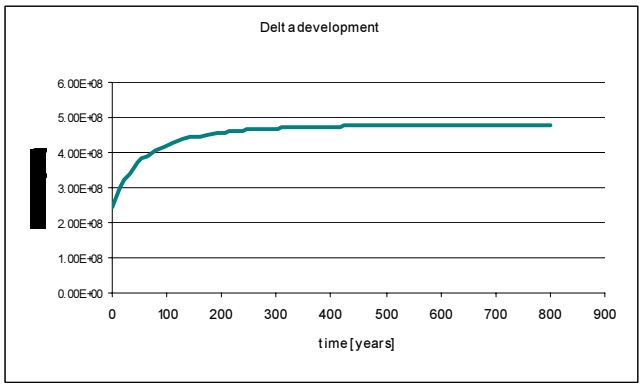

Figure E.59: Development of delta Vlie, alternative AD3

Vlie system time scales:

152 years
25 years
43 years

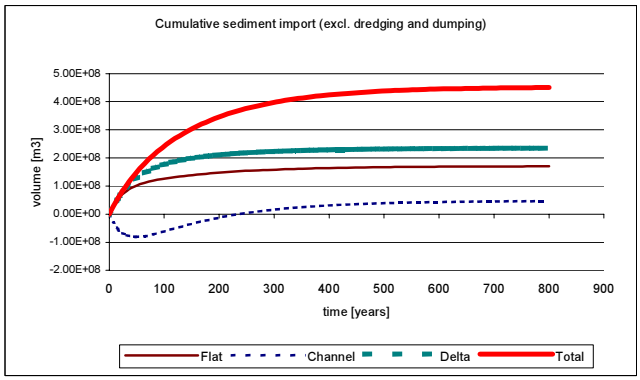

Figure E.60: Cumulative sediment import Vlie, alternative AD3

Input ASMITA for alternative KZ1

Input parameter		Marsdiep	Eierlandse Gat	Vlie
V_f	[$*10^6$ m^3]	77.42	58.93	108.48
V_c	[$*10^6$ m^3]	2426.13	107.65	580.92
V_d	[$*10^6$ m^3]	530.82	131.75	244.91
A_f	[$*10^6$ m^2]	146.93	95.66	198.35
A_c	[$*10^6$ m^2]	551.71	60.77	202.15
A_d	[$*10^6$ m^2]	138.25	36.89	115.65
H	[m]	1.65	1.65	1.9
Coefficient a for V_{fe}	[-]	0.3	0.3	0.3
Coefficient a for V_c	[$m^{-1.55}$]	1.6e-5	1.6e-5	1.6e-5
Coefficient b for V_c	[-]	1.55	1.55	1.55
Coefficient a for V_d	[$m^{-1.23}$]	6.57e-3	6.57e-3	6.57e-3
Coefficient b for V_d	[-]	1.23	1.23	1.23
w_{sf}	[m/s]	1.0e-5	1.0e-5	1.0e-5
w_{sc}	[m/s]	1.0e-5	1.0e-5	1.0e-5
w_{sd}	[m/s]	1.0e-5	1.0e-5	1.0e-5
δ_{fc}	[m^3/s]	1.5e3	1.5e3	1.5e3
δ_{dc}	[m^3/s]	1.5e3	1.5e3	1.5e3
δ_{do}	[m^3/s]	1.5e3	1.5e3	1.5e3
c_E	[-]	2.0e-4	2.0e-4	2.0e-4
n	[-]	2	2	2

Results ASMITA for Marsdiep with alternative KZ1

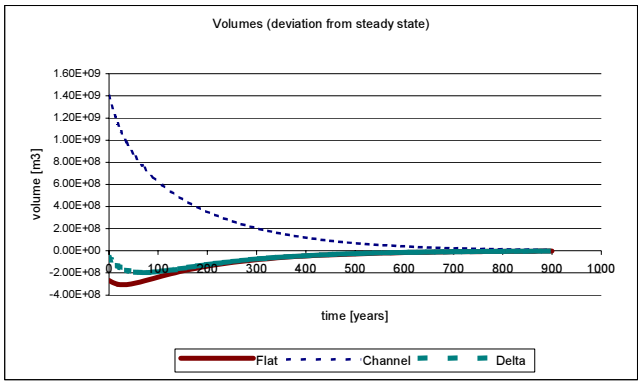

Figure E.61: Development of elements Marsdiep, alternative KZ1

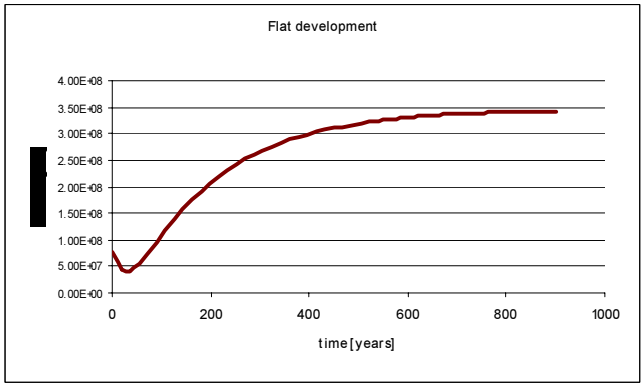

Figure E.62: Development of flats Marsdiep, alternative KZ1

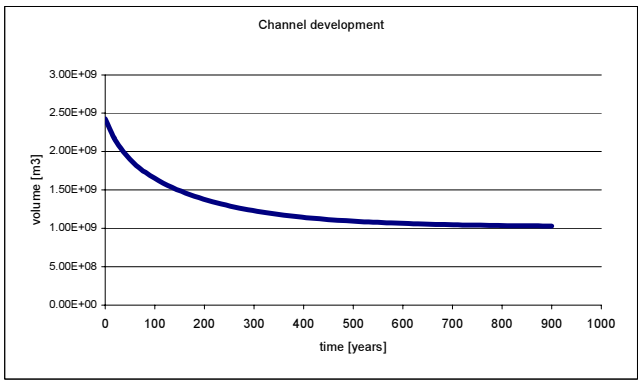

Figure E.63: Development of channels Marsdiep, alternative KZ1

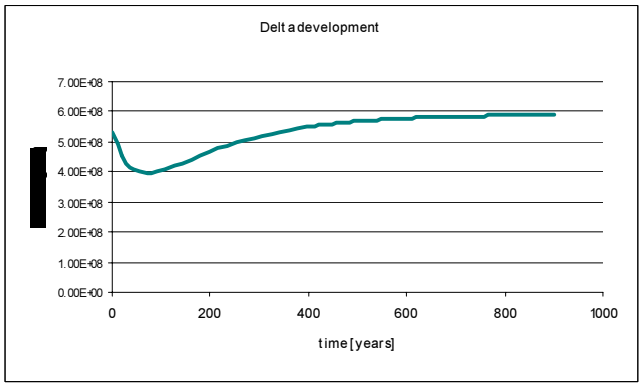

Figure E.64: Development of delta Marsdiep, alternative KZ1

Marsdiep system time scales:

184 years
30 years
47 years

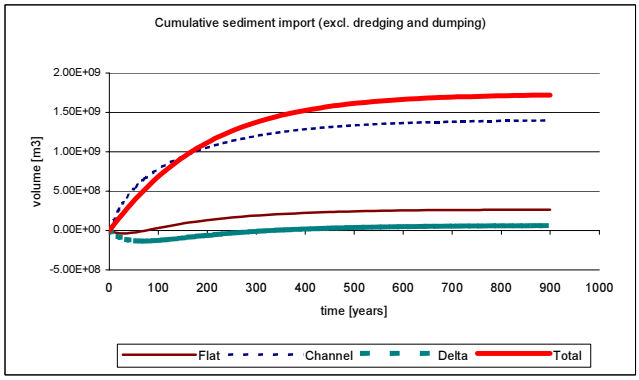

Figure E.65: Cumulative sediment import Marsdiep, alternative KZ1

Results ASMITA for Eierlandse Gat with alternative KZ1

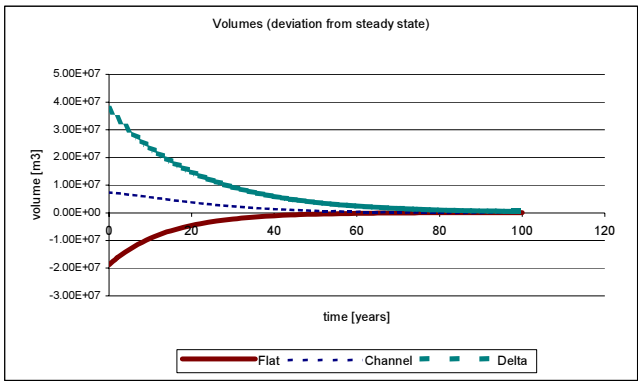

Figure E.66: Development of elements Eierlandse Gat, alternative KZ1

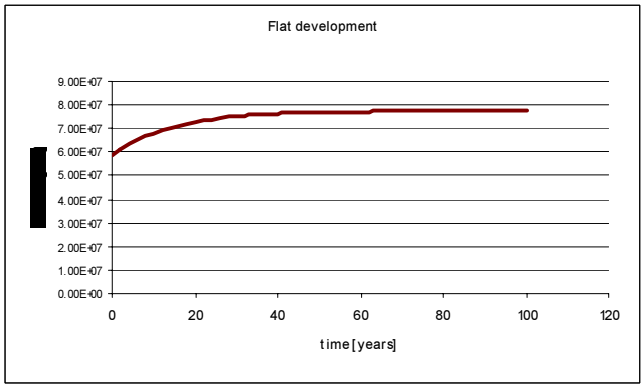

Figure E.67: Development of flats Eierlandse Gat, alternative KZ1

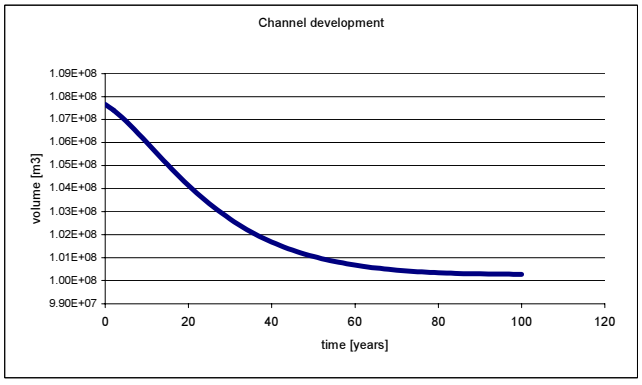

Figure E.68: Development of channels Eierlandse Gat, alternative KZ1

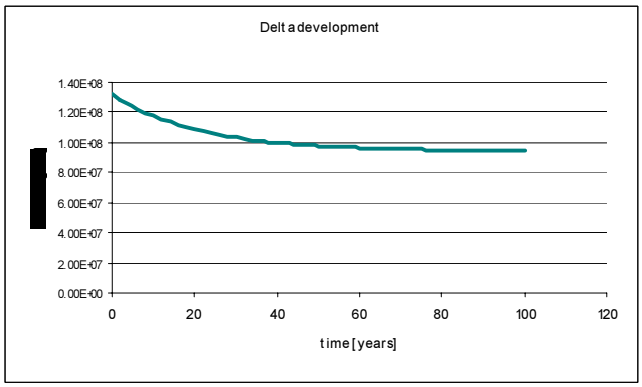

Figure E.69: Development of delta Eierlandse Gat, alternative KZ1

Eierlandse Gat system time scales:

35 years
12 years
21 years

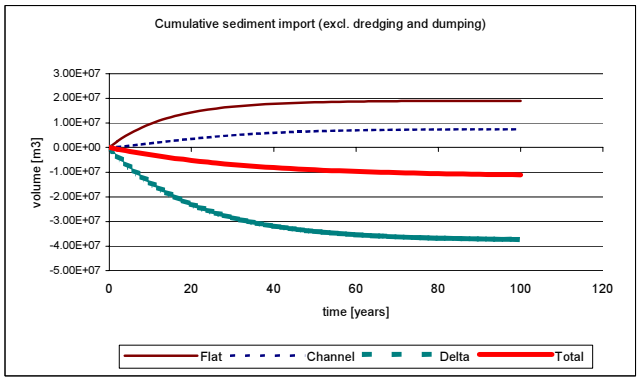

Figure E.70: Cumulative sediment import Eierlandse Gat, alternative KZ1

Results ASMITA for Vlie with alternative KZ1

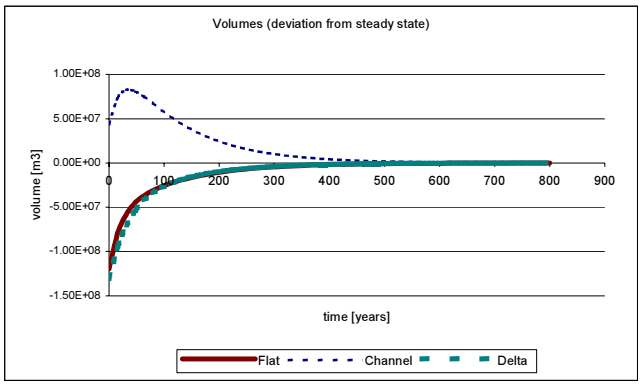

Figure E.71: Development of elements Vlie, alternative KZ1

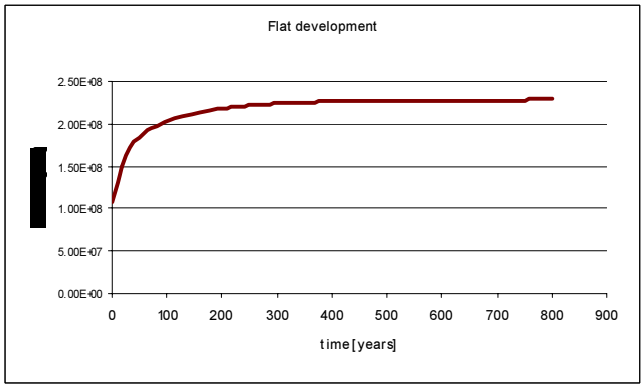

Figure E.72: Development of flats Vlie, alternative KZ1

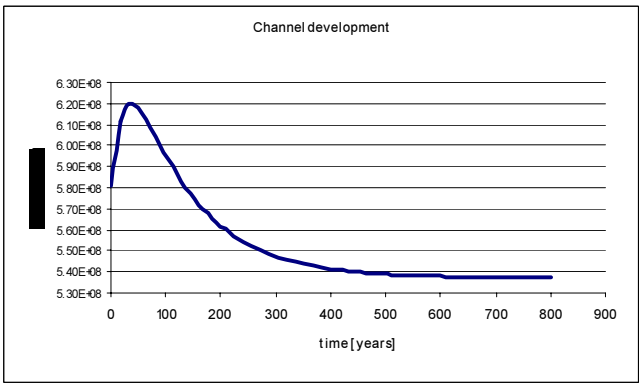

Figure E.73: Development of channels Vlie, alternative KZ1

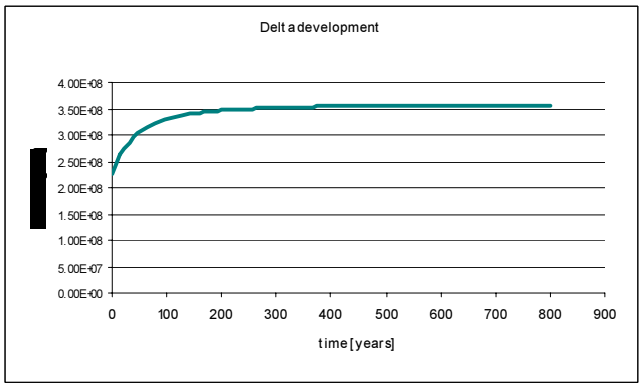

Figure E.74: Development of delta Vlie, alternative KZ1

Vlie system time scales:

113 years
21 years
32 years

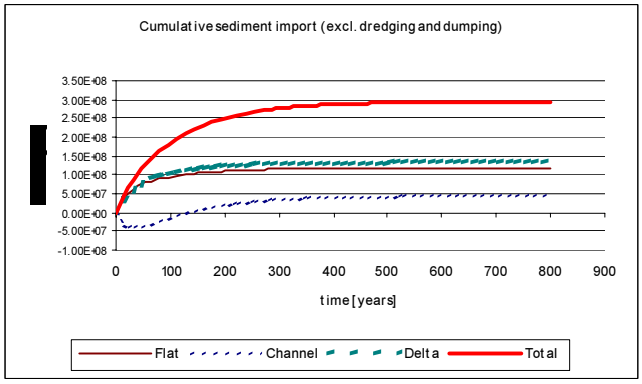

Figure E.75: Cumulative sediment import Vlie, alternative KZ1

Input ASMITA for alternative KZ2

Input parameter		Marsdiep	Eierlandse Gat	Vlie
V_f	[$*10^6$ m^3]	76.85	58.74	114.12
V_c	[$*10^6$ m^3]	2426.13	107.65	599.01
V_d	[$*10^6$ m^3]	530.82	131.75	244.91
A_f	[$*10^6$ m^2]	145.86	95.89	209.13
A_c	[$*10^6$ m^2]	551.71	60.77	208.45
A_d	[$*10^6$ m^2]	138.25	36.89	115.65
H	[m]	1.65	1.65	1.9
Coefficient a for V_{fe}	[-]	0.3	0.3	0.3
Coefficient a for V_c	[$m^{-1.55}$]	1.6e-5	1.6e-5	1.6e-5
Coefficient b for V_c	[-]	1.55	1.55	1.55
Coefficient a for V_d	[$m^{-1.23}$]	6.57e-3	6.57e-3	6.57e-3
Coefficient b for V_d	[-]	1.23	1.23	1.23
w_{sf}	[m/s]	1.0e-5	1.0e-5	1.0e-5
w_{sc}	[m/s]	1.0e-5	1.0e-5	1.0e-5
w_{sd}	[m/s]	1.0e-5	1.0e-5	1.0e-5
δ_{fc}	[m^3/s]	1.5e3	1.5e3	1.5e3
δ_{dc}	[m^3/s]	1.5e3	1.5e3	1.5e3
δ_{do}	[m^3/s]	1.5e3	1.5e3	1.5e3
c_E	[-]	2.0e-4	2.0e-4	2.0e-4
n	[-]	2	2	2

Results ASMITA for Marsdiep with alternative KZ2

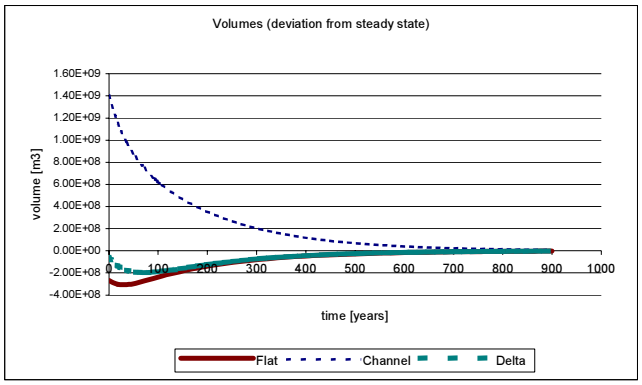

Figure E.76: Development of elements Marsdiep, alternative KZ2

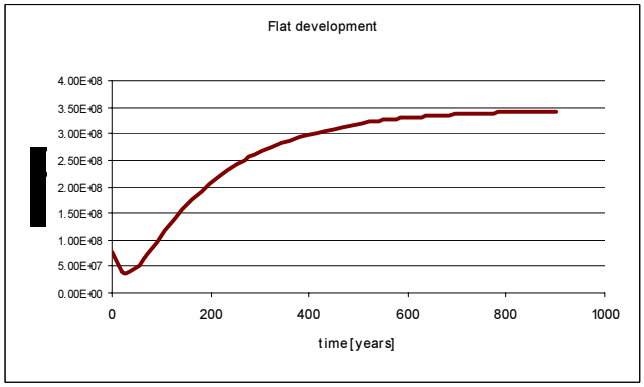

Figure E.77: Development of flats Marsdiep, alternative KZ2

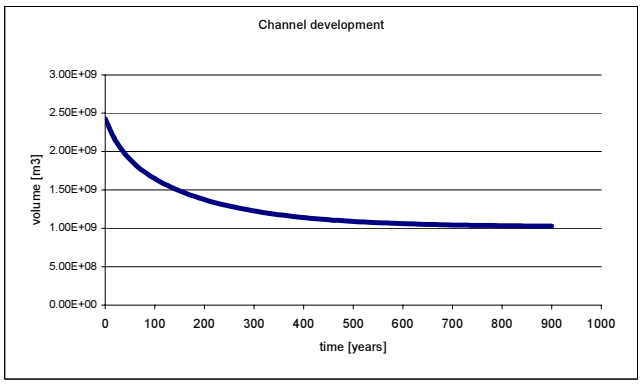

Figure E.78: Development of channels Marsdiep, alternative KZ2

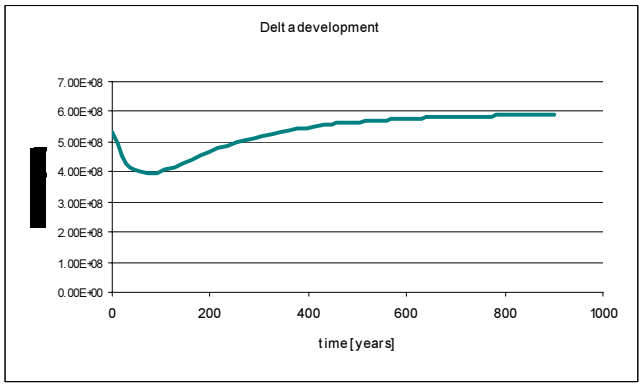

Figure E.79: Development of delta Marsdiep, alternative KZ2

Marsdiep system time scales:

184 years
30 years
47 years

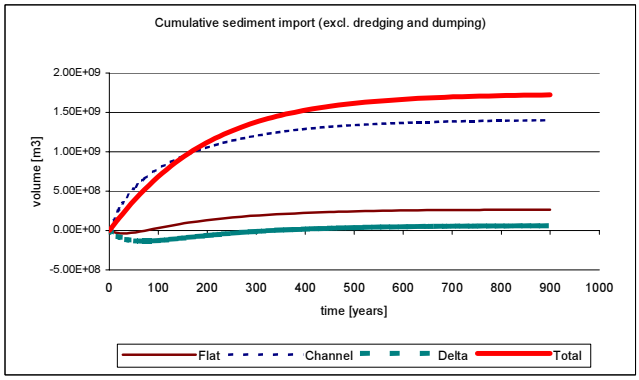

Figure E.80: Cumulative sediment import Marsdiep, alternative KZ2

Results ASMITA for Eierlandse Gat with alternative KZ2

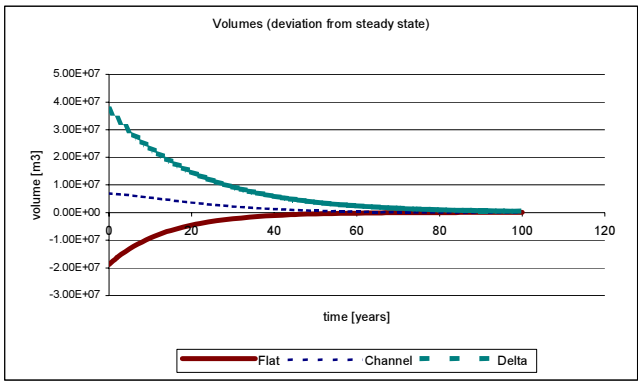

Figure E.81 Development of elements Eierlandse Gat, alternative KZ2

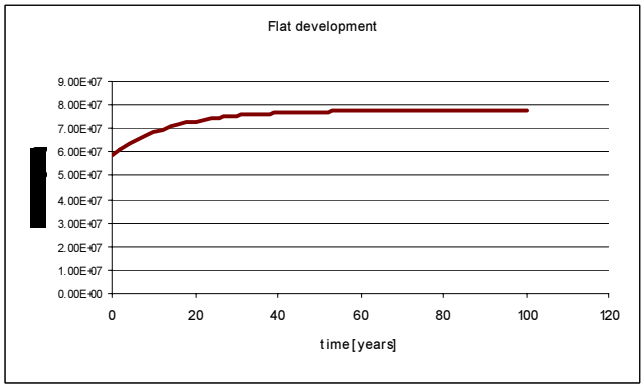

Figure E.82: Development of flats Eierlandse Gat, alternative KZ2

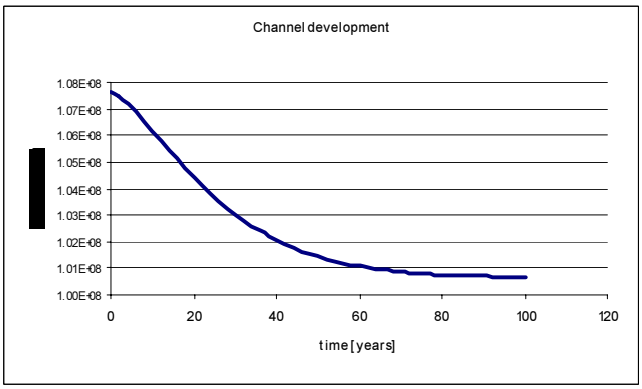

Figure E.83: Development of channels Eierlandse Gat, alternative KZ2

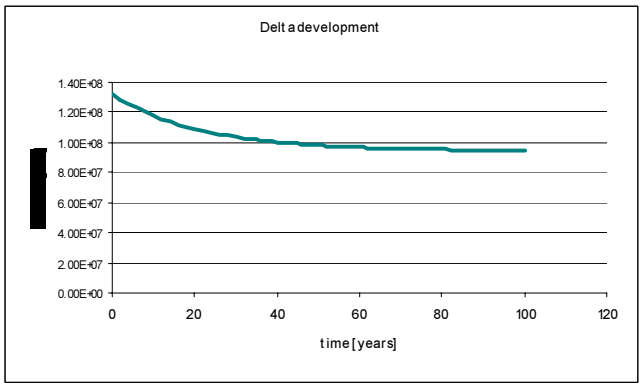

Figure E.84: Development of delta Eierlandse Gat, alternative KZ2

Eierlandse Gat system time scales:

35 years
12 years
21 years

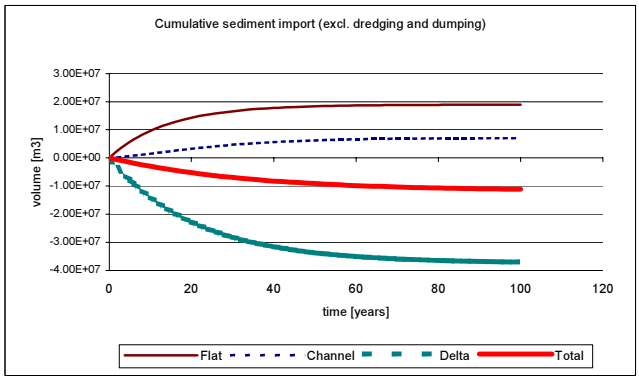

Figure E.85: Cumulative sediment import Eierlandse Gat, alternative KZ2

Results ASMITA for Vlie with alternative KZ2

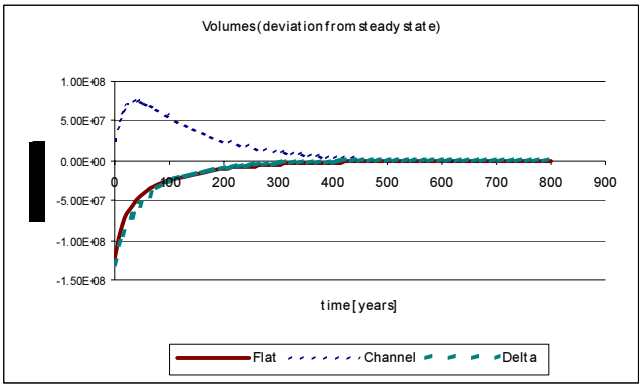

Figure E.86: Development of elements Vlie, alternative KZ2

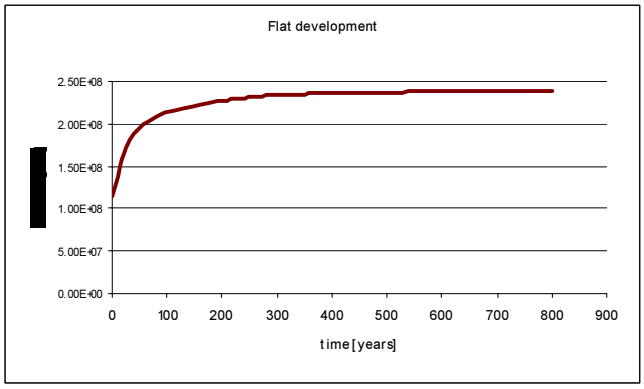

Figure E.87: Development of flats Vlie, alternative KZ2

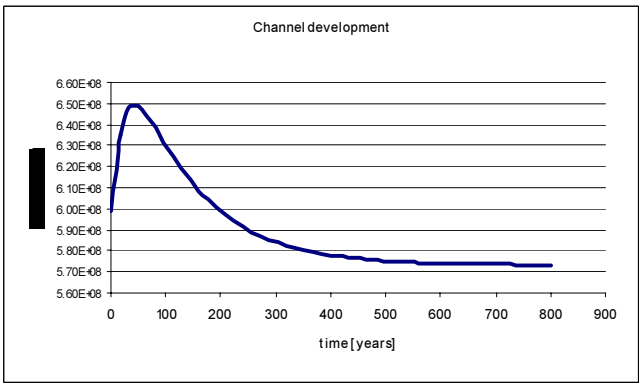

Figure E.88: Development of channels Vlie, alternative KZ2

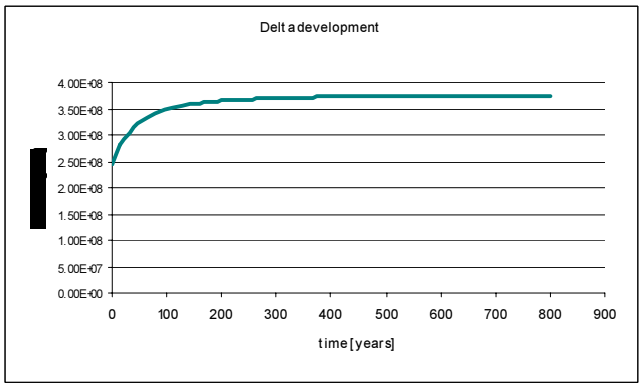

Figure E.89: Development of delta Vlie, alternative KZ2

Vlie system time scales:

119 years
22 years
34 years

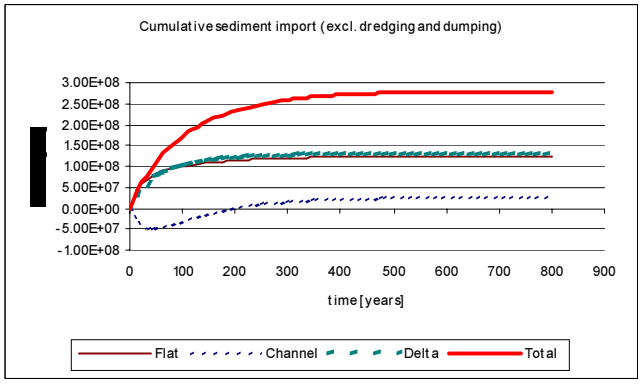

Figure E.90: Cumulative sediment import Vlie, alternative KZ2

Input ASMITA for alternative LW1

Input parameter		Marsdiep	Eierlandse Gat	Vlie
V_f	[$*10^6$ m^3]	67.07	58.19	127.50
V_c	[$*10^6$ m^3]	1937.62	107.65	830.81
V_d	[$*10^6$ m^3]	530.82	131.75	244.91
A_f	[$*10^6$ m^2]	126.89	95.00	234.25
A_c	[$*10^6$ m^2]	440.62	60.77	289.12
A_d	[$*10^6$ m^2]	138.25	36.89	115.65
H	[m]	1.65	1.65	1.9
Coefficient a for V_{fe}	[-]	0.3	0.3	0.3
Coefficient a for V_c	[$m^{-1.55}$]	1.6e-5	1.6e-5	1.6e-5
Coefficient b for V_c	[-]	1.55	1.55	1.55
Coefficient a for V_d	[$m^{-1.23}$]	6.57e-3	6.57e-3	6.57e-3
Coefficient b for V_d	[-]	1.23	1.23	1.23
w_{sf}	[m/s]	1.0e-5	1.0e-5	1.0e-5
w_{sc}	[m/s]	1.0e-5	1.0e-5	1.0e-5
w_{sd}	[m/s]	1.0e-5	1.0e-5	1.0e-5
δ_{fc}	[m^3/s]	1.5e3	1.5e3	1.5e3
δ_{dc}	[m^3/s]	1.5e3	1.5e3	1.5e3
δ_{do}	[m^3/s]	1.5e3	1.5e3	1.5e3
c_E	[-]	2.0e-4	2.0e-4	2.0e-4
n	[-]	2	2	2

Results ASMITA for Marsdiep with alternative LW1

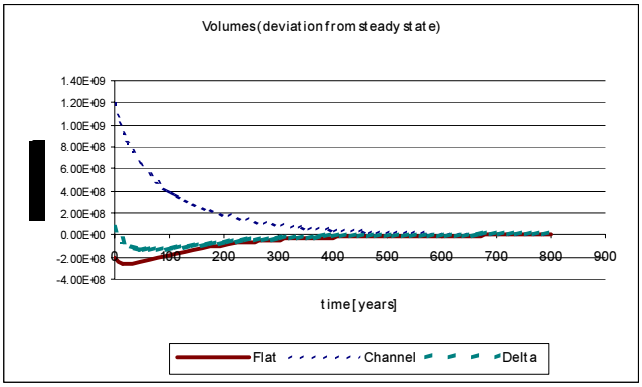

Figure E.91: Development of elements Marsdiep, alternative LW1

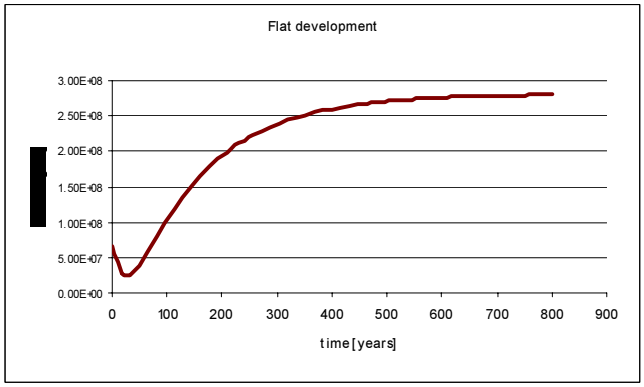

Figure E.92: Development of flats Marsdiep, alternative LW1

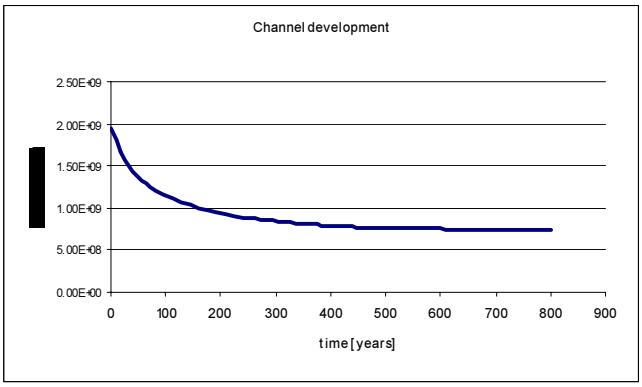

Figure E.93: Development of channels Marsdiep, alternative LW1

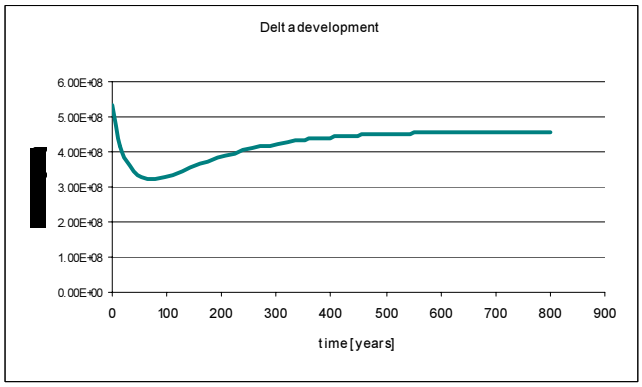

Figure E.94: Development of delta Marsdiep, alternative LW1

Marsdiep system time scales:

142 years
26 years
37 years

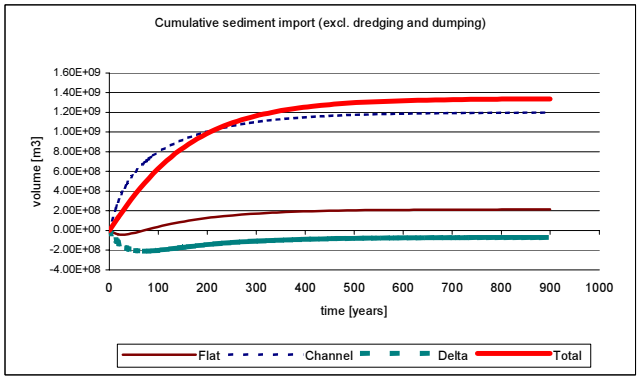

Figure E.95: Cumulative sediment import Marsdiep, alternative LW1

Results ASMITA for Eierlandse Gat with alternative LW1

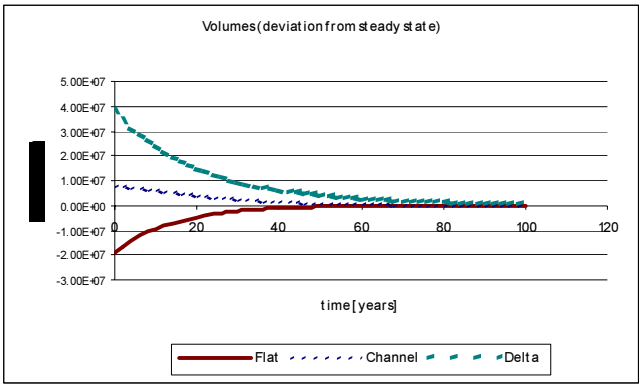

Figure E.96: Development of elements Eierlandse Gat, alternative LW1

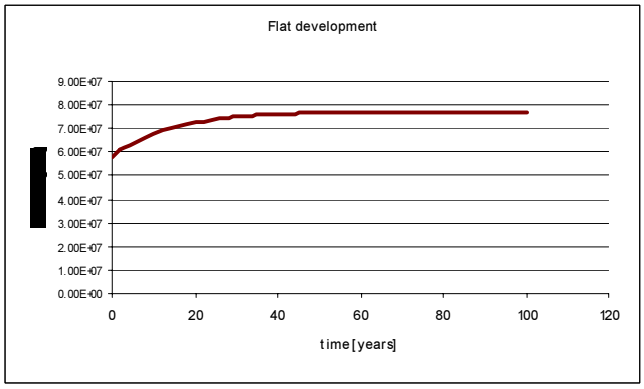

Figure E.97: Development of flats Eierlandse Gat, alternative LW1

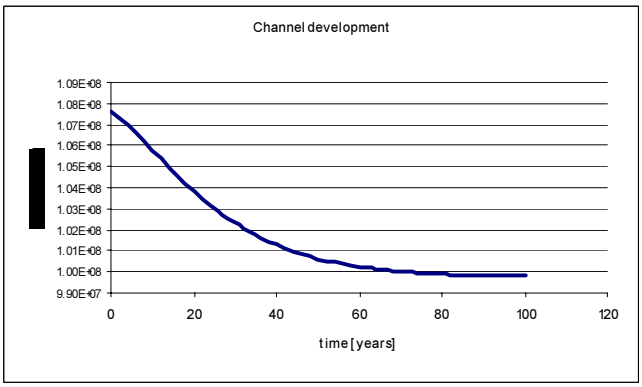

Figure E.98: Development of channels Eierlandse Gat, alternative LW1

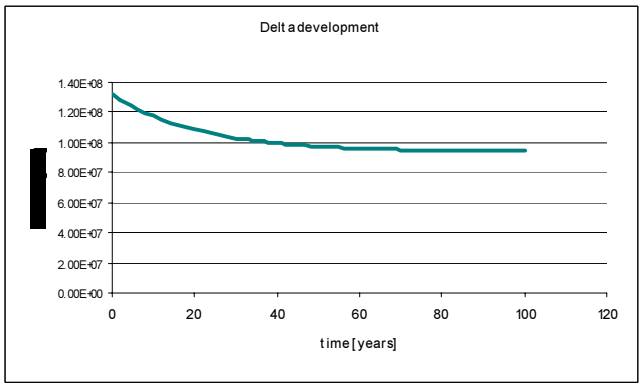

Figure E.99: Development of delta Eierlandse Gat, alternative LW1

Eierlandse Gat system time scales:

35 years
12 years
21 years

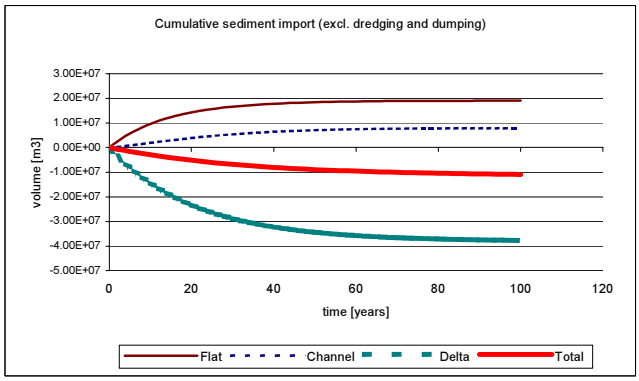

Figure E.100: Cumulative sediment import Eierlandse Gat, alternative LW1

Results ASMITA for Vlie with alternative LW1

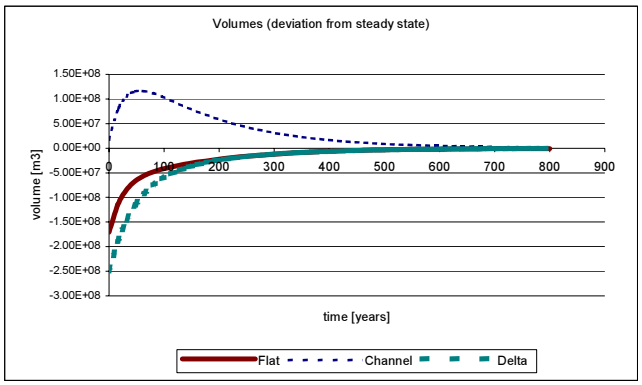

Figure E.101: Development of elements Vlie, alternative LW1

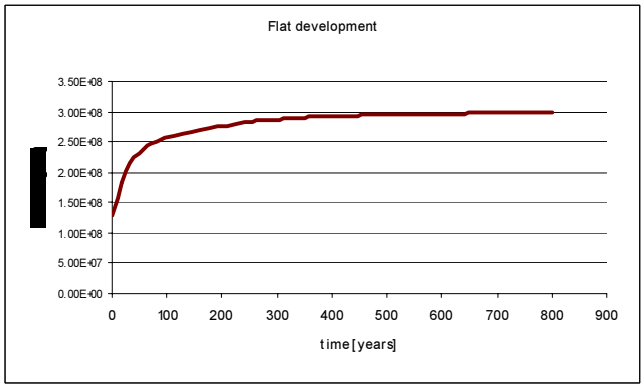

Figure E.102: Development of flats Vlie, alternative LW1

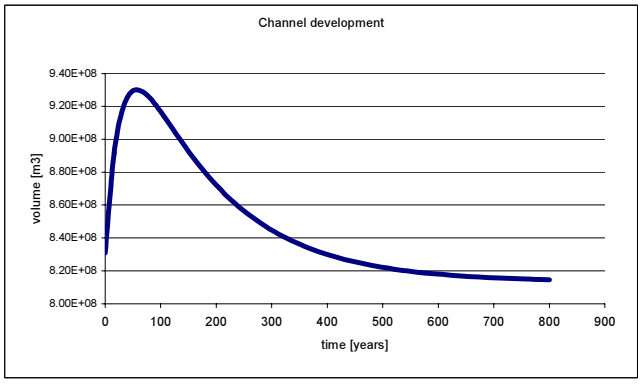

Figure E.103: Development of channels Vlie, alternative LW1

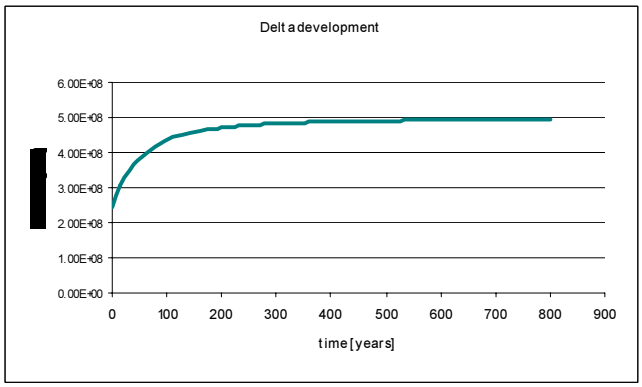

Figure E.104: Development of delta Vlie, alternative LW1

Vlie system time scales:

157 years
25 years
44 years

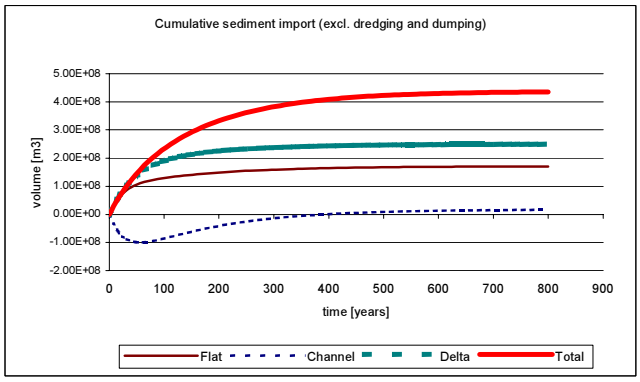

Figure E.105: Cumulative sediment import Vlie, alternative LW1

Input ASMITA for alternative LW2

Input parameter		Marsdiep	Eierlandse Gat	Vlie
V_f	[$*10^6$ m^3]	69.28	57.92	126.26
V_c	[$*10^6$ m^3]	2056.20	107.65	830.81
V_d	[$*10^6$ m^3]	530.82	131.75	244.91
A_f	[$*10^6$ m^2]	130.92	94.56	231.97
A_c	[$*10^6$ m^2]	467.58	60.77	289.12
A_d	[$*10^6$ m^2]	138.25	36.89	115.65
H	[m]	1.65	1.65	1.9
Coefficient a for V_{fe}	[-]	0.3	0.3	0.3
Coefficient a for V_c	[$m^{-1.55}$]	1.6e-5	1.6e-5	1.6e-5
Coefficient b for V_c	[-]	1.55	1.55	1.55
Coefficient a for V_d	[$m^{-1.23}$]	6.57e-3	6.57e-3	6.57e-3
Coefficient b for V_d	[-]	1.23	1.23	1.23
w_{sf}	[m/s]	1.0e-5	1.0e-5	1.0e-5
w_{sc}	[m/s]	1.0e-5	1.0e-5	1.0e-5
w_{sd}	[m/s]	1.0e-5	1.0e-5	1.0e-5
δ_{fc}	[m^3/s]	1.5e3	1.5e3	1.5e3
δ_{dc}	[m^3/s]	1.5e3	1.5e3	1.5e3
δ_{do}	[m^3/s]	1.5e3	1.5e3	1.5e3
c_E	[-]	2.0e-4	2.0e-4	2.0e-4
n	[-]	2	2	2

Results ASMITA for Marsdiep with alternative LW2

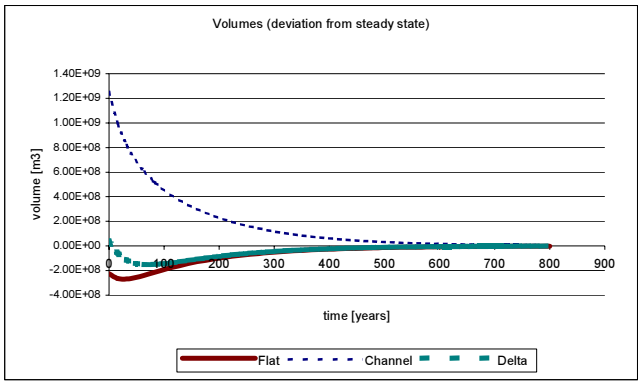

Figure E.106: Development of elements Marsdiep, alternative LW2

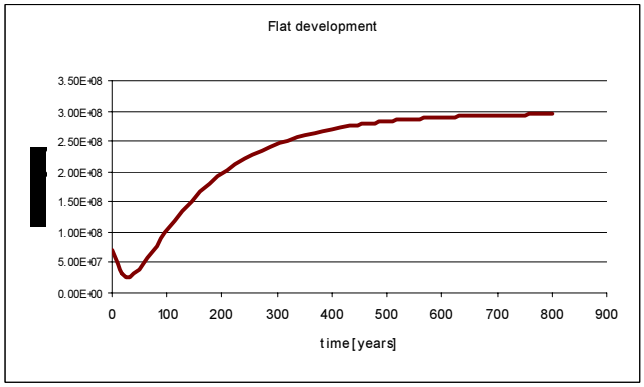

Figure E.107: Development of flats Marsdiep, alternative LW2

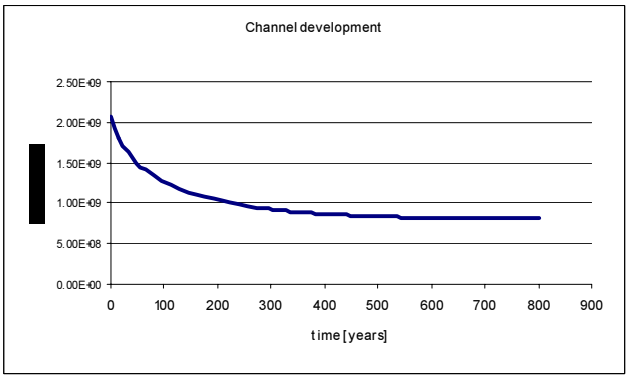

Figure E.108: Development of channels Marsdiep, alternative LW2

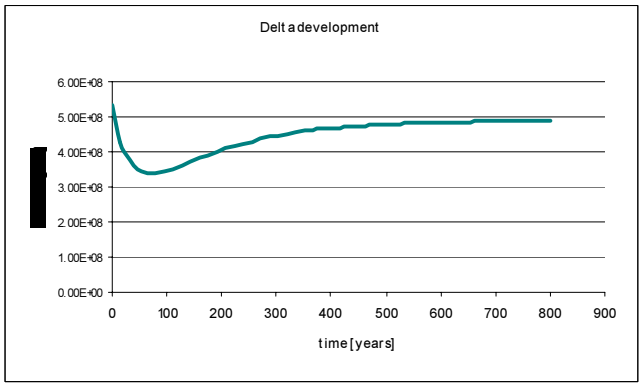

Figure E.109: Development of delta Marsdiep, alternative LW2

Marsdiep system time scales:

151 years
27 years
39 years

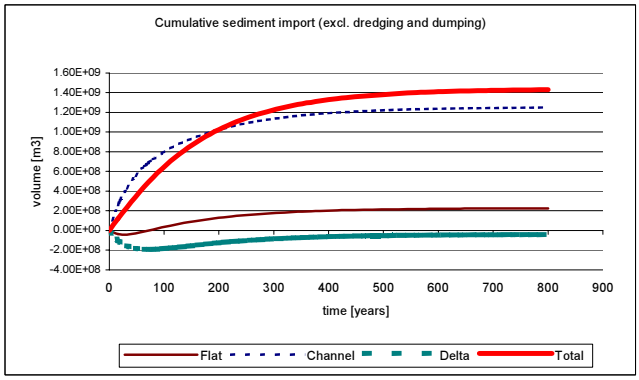

Figure E.110: Cumulative sediment import Marsdiep, alternative LW2

Results ASMITA for Eierlandse Gat with alternative LW2

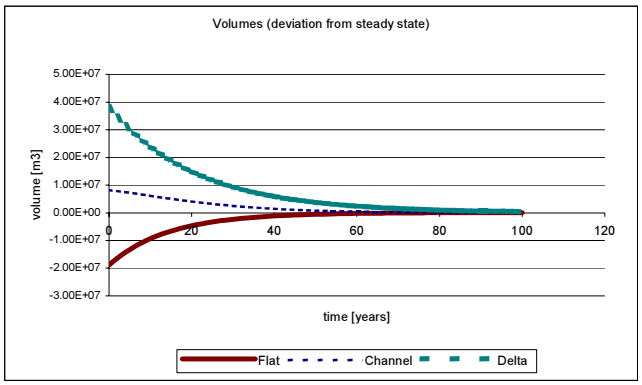

Figure E.111: Development of elements Eierlandse Gat, alternative LW2

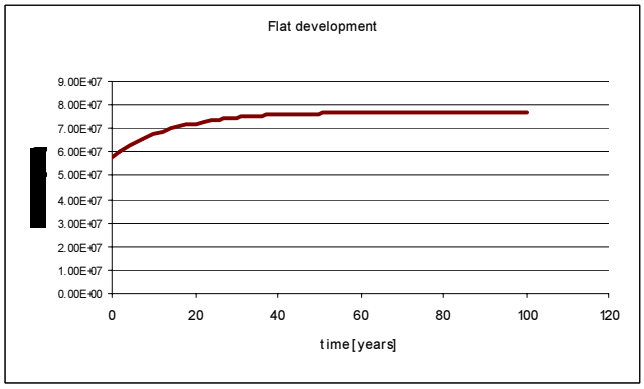

Figure E.112: Development of flats Eierlandse Gat, alternative LW2

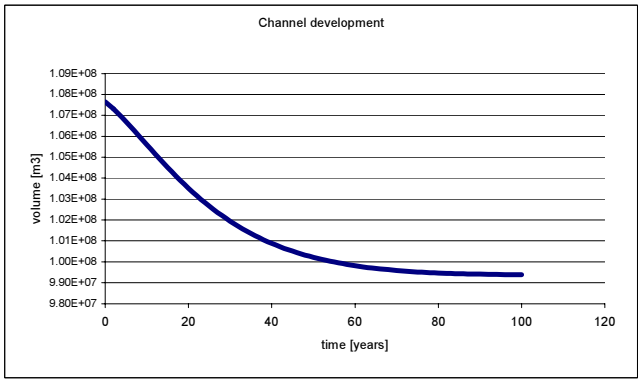

Figure E.113: Development of channels Eierlandse Gat, alternative LW2

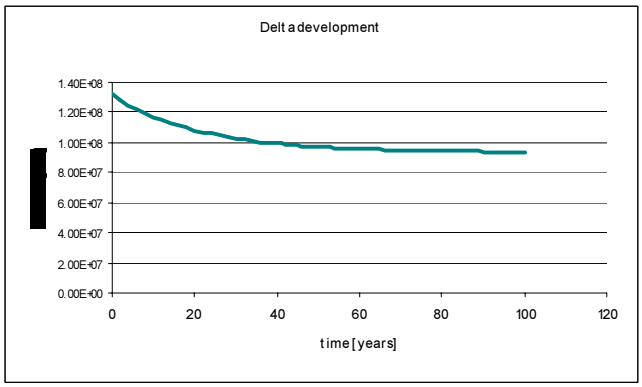

Figure E.114: Development of delta Eierlandse Gat, alternative LW2

Eierlandse Gat system time scales:

35 years
11 years
20 years

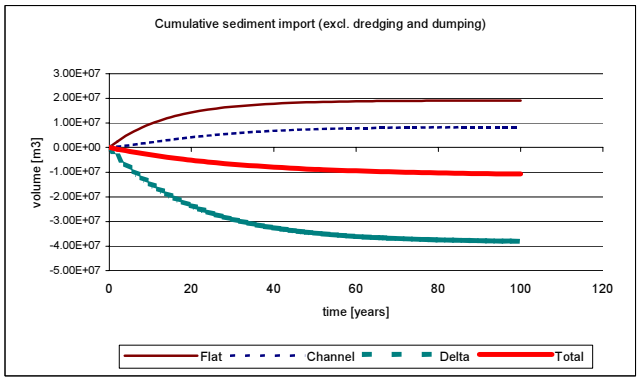

Figure E.115: Cumulative sediment import Eierlandse Gat, alternative LW2

Results ASMITA for Vlie with alternative LW2

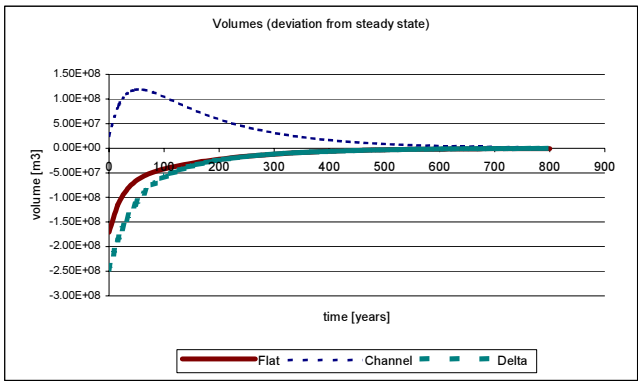

Figure E.116: Development of elements Vlie, alternative LW2

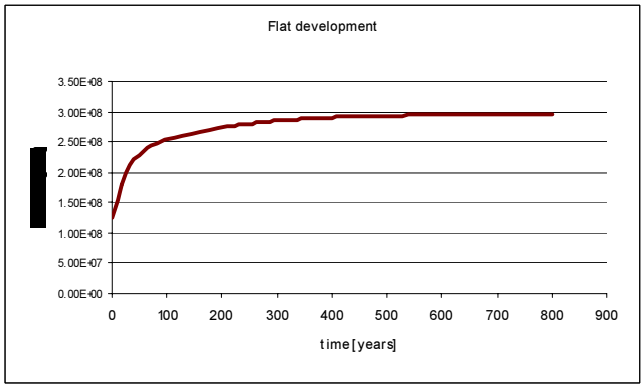

Figure E.117: Development of flats Vlie, alternative LW2

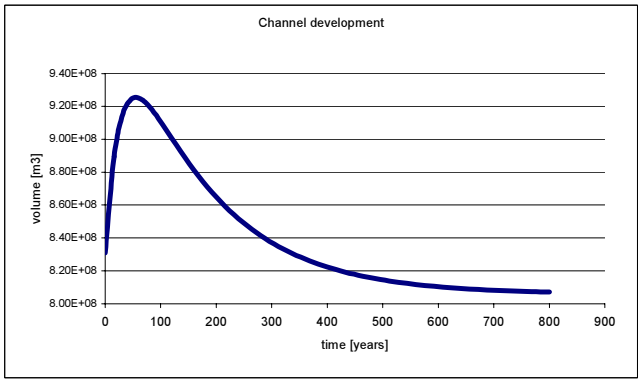

Figure E.118: Development of channels Vlie, alternative LW2

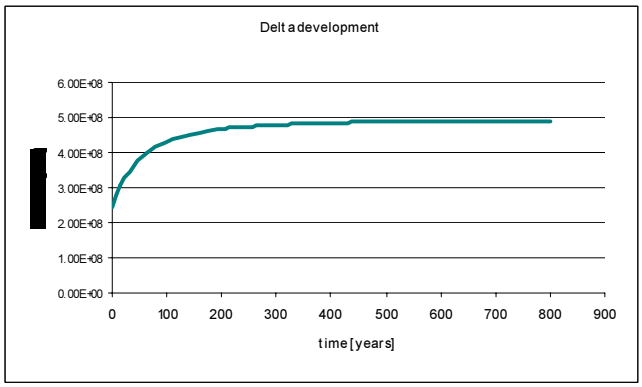

Figure E.119: Development of delta Vlie, alternative LW2

Vlie system time scales:

155 years
25 years
44 years

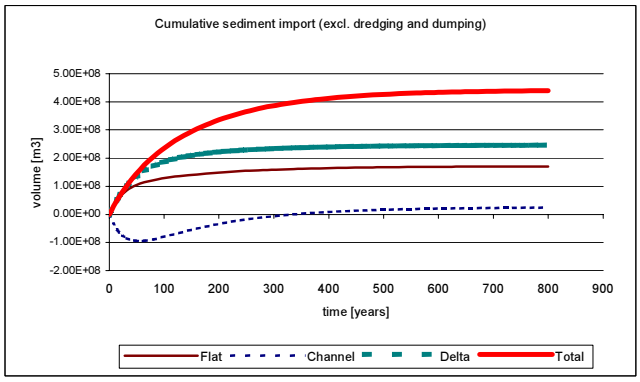

Figure E.120: Cumulative sediment transport Vlie, alternative LW2

Input ASMITA for Current Situation + Sea Level Rise (17 cm/century)

Input parameter		Marsdiep	Eierlandse Gat	Vlie
V_f	[$*10^6$ m^3]	70.42	59.46	128.75
V_c	[$*10^6$ m^3]	2426.13	107.65	830.81
V_d	[$*10^6$ m^3]	530.82	131.75	244.91
A_f	[$*10^6$ m^2]	133.64	97.07	236.55
A_c	[$*10^6$ m^2]	551.71	60.77	289.12
A_d	[$*10^6$ m^2]	138.25	36.89	155.65
H	[m]	1.65	1.65	1.9
Coefficient a for V_{fe}	[-]	0.3	0.3	0.3
Coefficient a for V_c	[$m^{-1.55}$]	1.6e-5	1.6e-5	1.6e-5
Coefficient b for V_c	[-]	1.55	1.55	1.55
Coefficient a for V_d	[$m^{-1.23}$]	6.57e-3	6.57e-3	6.57e-3
Coefficient b for V_d	[-]	1.23	1.23	1.23
w_{sf}	[m/s]	1.0e-5	1.0e-5	1.0e-5
w_{sc}	[m/s]	1.0e-5	1.0e-5	1.0e-5
w_{sd}	[m/s]	1.0e-5	1.0e-5	1.0e-5
δ_{fc}	[m^3/s]	1.5e3	1.5e3	1.5e3
δ_{dc}	[m^3/s]	1.5e3	1.5e3	1.5e3
δ_{do}	[m^3/s]	1.5e3	1.5e3	1.5e3
c_E	[-]	2.0e-4	2.0e-4	2.0e-4
n	[-]	2	2	2

Results ASMITA for Marsdiep in Current Situation + SLR

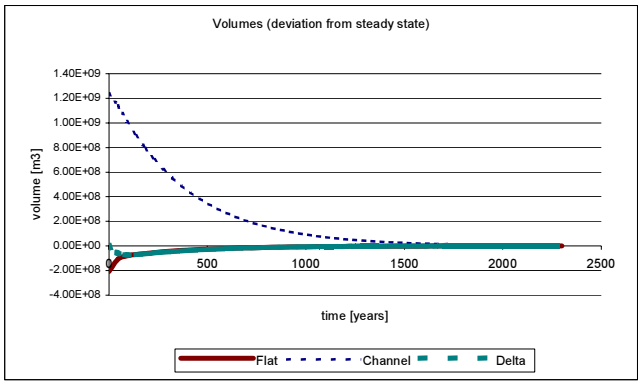

Figure E.121: Development of elements Marsdiep, CS + SLR

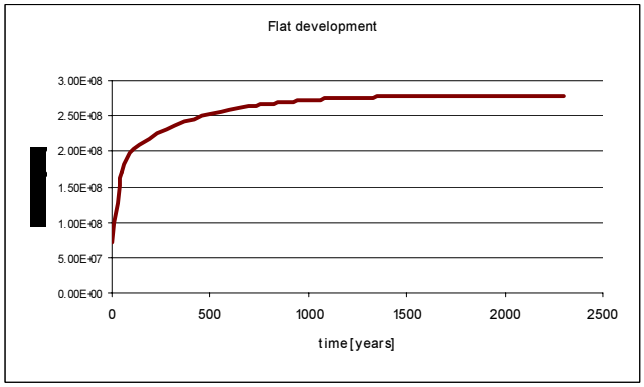

Figure E.122: Development of flats Marsdiep, CS + SLR

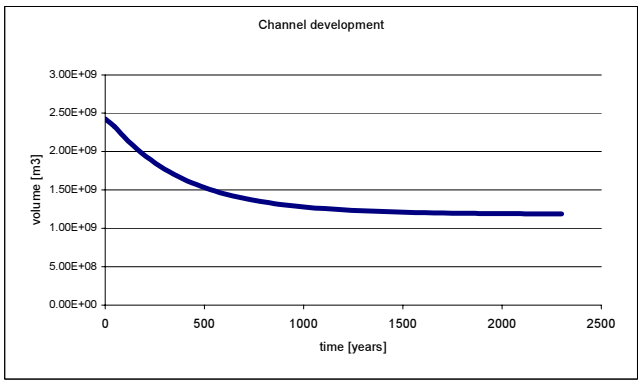

Figure E.123 Development of channels Marsdiep, CS + SLR

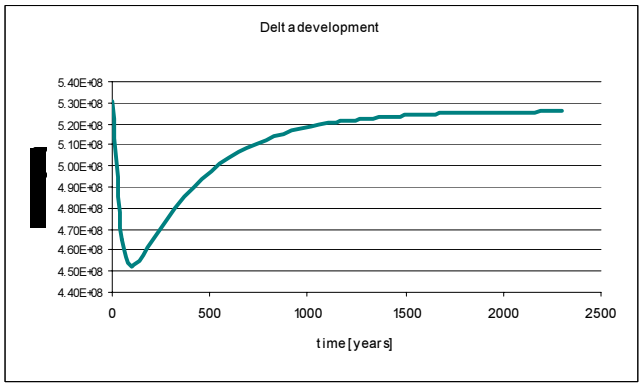

Figure E.124: Development of delta Marsdiep, CS + SLR

Marsdiep system time scales:

380 years
27 years
40 years

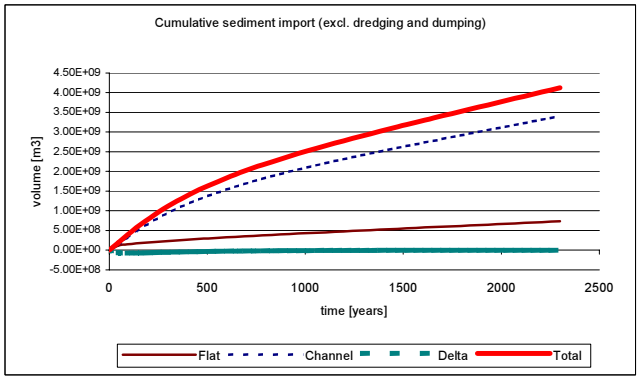

Figure E.125: Cumulative sediment import Marsdiep, CS + SLR

Results ASMITA for Eierlandse Gat in Current Situation + SLR

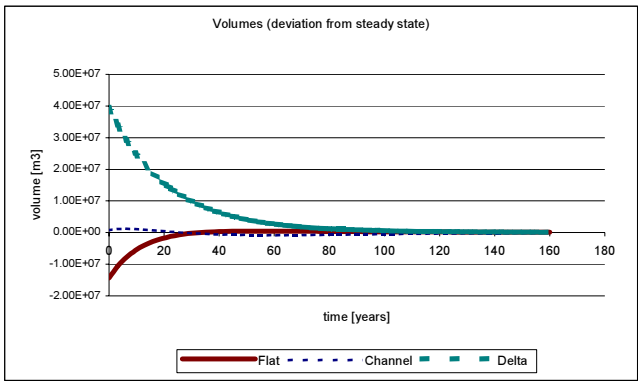

Figure E.126: Development of elements Eierlandse Gat, CS + SLR

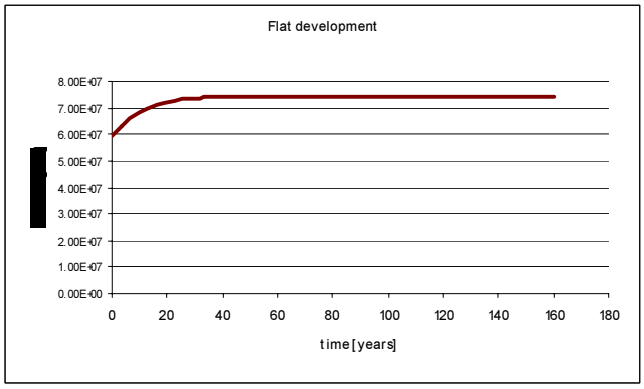

Figure E.127: Development of flats Eierlandse Gat, CS + SLR

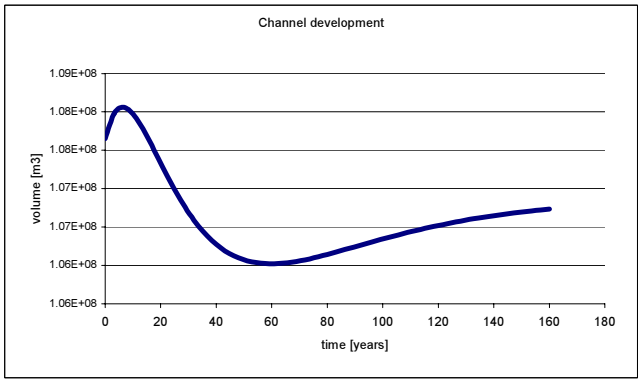

Figure E.128: Development of channels Eierlandse Gat, CS + SLR

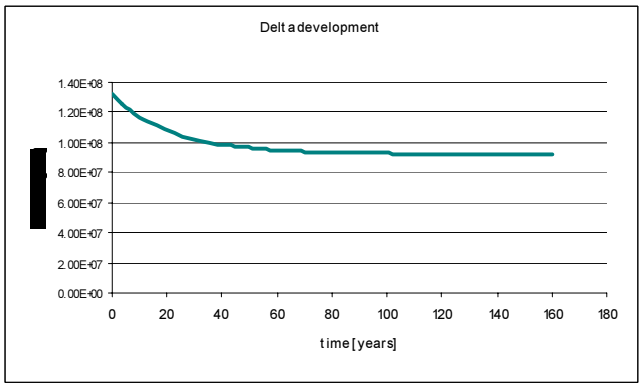

Figure E.129: Development of delta Eierlandse Gat, CS + SLR

Eierlandse Gat system time scales:

40 years
11 years
21 years

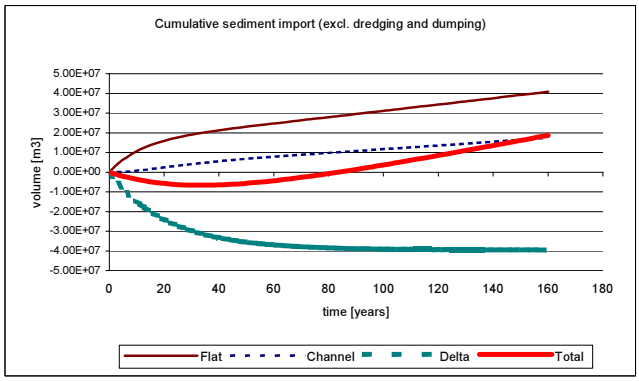

Figure E.130: Cumulative sediment import Eierlandse Gat, CS + SLR

Results ASMITA for Vlie in Current Situation + SLR

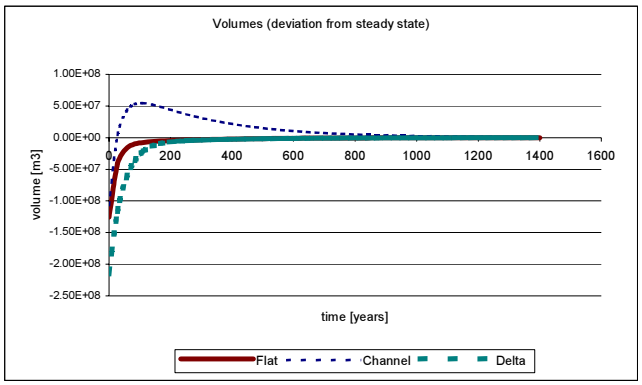

Figure E.131: Development of elements Vlie, CS + SLR

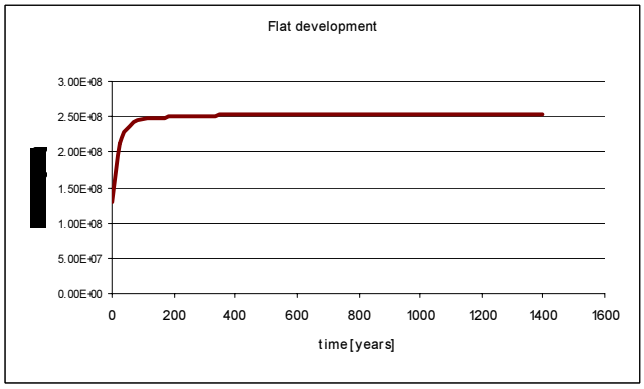

Figure E.132: Development of flats Vlie, CS + SLR

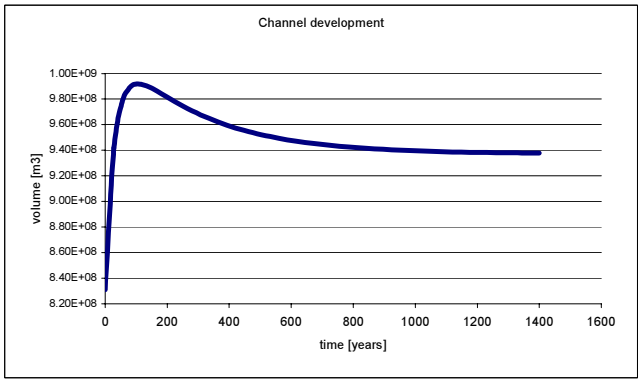

Figure E.133: Development of channels Vlie, CS + SLR

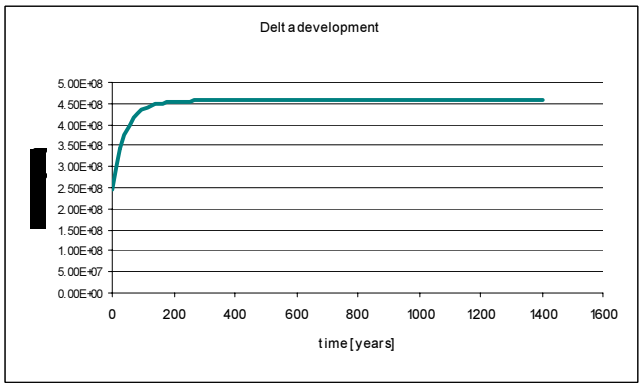

Figure E.134: Development of delta Vlie, CS + SLR

Vlie system time scales:

276 years
21 years
41 years

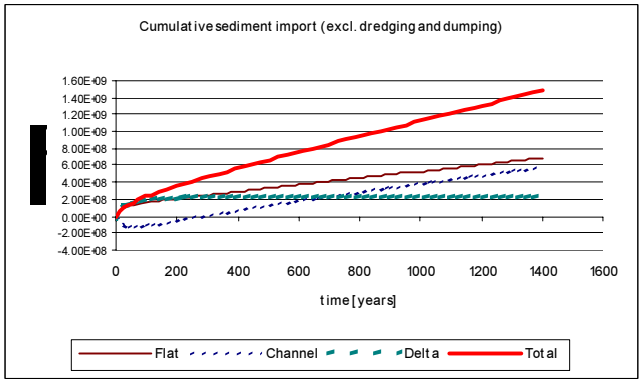

Figure E.135: Cumulative sediment import Vlie, CS + SLR